MECHANISMS OF OCEAN HEAT UPTAKE

by

Oluwayemi Garuba
A Dissertation
Submitted to the
Graduate Faculty
of
George Mason University
In Partial fulfillment of
The Requirements for the Degree
of
Doctor of Philosophy
Climate Dynamics

Committee:

_____ Dr. Barry Klinger, Dissertation Director

_____ Dr. James Kinter, Committee Member

_____ Dr. Bohua Huang, Committee Member

_____ Dr. Jian Lu, Committee Member

_____ Dr. Edwin Schneider, Department Chair

_____ Dr. Donna M. Fox, Associate Dean, Office of Student Affairs & Special Programs College of Science

_____ Dr. Peggy Agouris, Dean, College of Science

Date: _____ Fall 2015
George Mason University
Fairfax, VA

Mechanisms of Ocean Heat Uptake

A dissertation submitted in partial fulfillment of the requirements for the degree of Doctor of Philosophy at George Mason University

By

Oluwayemi Garuba
Pre- Phd Diploma
Abdus Salam International centre for theoretical Physics Trieste, Italy, 2010
Bachelor of Technology
Federal University of Technology Akure, Nigeria, 2007

Director: Dr. Barry Klinger, Professor
Department of (AOES)

Fall 2015
George Mason University
Fairfax, VA

Dedication

I dedicate this dissertation to first to Jehovah God, the source of all knowledge, and to my parents Mr and Mrs Garuba for being there always

Acknowledgments

My greatest gratitude first goes to Jehovah, the source of life and knowledge, especially for giving me the strength to go through this experience despite the challenges that I could not have faced on my own.

I would like to show my heartfelt gratitude my advisor Dr. Barry Klinger for his support and guidance both in academic and research work and also on general issues, during the entire course of the doctoral program, also for his patience and making time for regular discussions during research work and helping me to think more like a scientist. This dissertation would not have been possible without his support. Special thanks also to my dissertation committee members, Dr Kinter, Dr Huang and Dr. Lu for making time to meet when necessary and reading the dissertation work, and for their invaluable and insightful suggestions that moved this research work forward in the right direction.

And to the entire GMU/COLA staff and professors who worked to provide funding that supported students that afforded me the opportunity to be part of the Ph.D program and for generously sharing their knowledge. And to my colleagues Ioana Colfescu and Abheera Hazra, Erool Palipane, Abhishek Scrivastava, Yan Xiaoqin and Sara Amini who have helped in so many ways during my stay at GMU

I would also like to acknowledge funding source supported by NSF Grant 1249156 and the high-performance computing support from Yellowstone (ark:/85065/d7wd3xhc) provided by NCAR's Computational and Information Systems Laboratory, sponsored by the National Science Foundation.

My heartfelt gratitude and love also goes to my family, my parents and sister Joy for their unwavering love and support. My deep gratitude goes to my friends, who have become my family also in these five years, Jennifer and Richmond Osei Kufour, Sherry and Enoch Asomaning, Mr and Mrs Atakora, Grace Mogida, Letisia Robinson and Sonya Williams and Frank Matthews, for your unselfish love, support and encouragement, you all really made me feel at home!

Table of Contents

List of Tables

List of Figures

Abstract

MECHANISMS OF OCEAN HEAT UPTAKE

Oluwayemi Garuba, PhD

George Mason University, 2015

Dissertation Director: Dr. Barry Klinger

An important parameter for the climate response to increased greenhouse gases or other radiative forcing is the speed at which heat anomalies propagate downward in the ocean. Ocean heat uptake occurs through passive advection/diffusion of surface heat anomalies and through the redistribution of existing temperature gradients due to circulation changes. Atlantic meridional overturning circulation (AMOC) weakens in a warming climate and this should slow the downward heat advection (compared to a case in which the circulation is unchanged). However, weakening AMOC also causes a deep warming through the redistributive effect, thus increasing the downward rate of heat propagation compared to unchanging circulation. Total heat uptake depends on the combined effect of these two mechanisms.

Passive tracers in a perturbed CO_2 quadrupling experiments are used to investigate the effect of passive advection and redistribution of temperature anomalies. A new passive tracer formulation is used to separate ocean heat uptake into contributions due to redistribution and passive advection-diffusion of surface heating during an ocean model experiment with abrupt increase in surface temperature. The spatial pattern and mechanisms of each component are examined. With further experiments, the effects of surface wind, salinity and temperature changes in changing circulation and the resulting effect on redistribution

in the individual basins are isolated.

Analysis of the passive advection and propagation path of the tracer show that the Southern ocean dominates heat uptake, largely through vertical and horizontal diffusion. Vertical diffusion transports the tracer across isopycnals down to about 1000m in 100 years in the Southern ocean. Advection is more important in the subtropical cells and in the Atlantic high latitudes, both with a short time scale of about 20 years. The shallow subtropical cells transport the tracer down to about 500m along isopycnal surfaces, below this vertical diffusion takes over transport in the tropics; in the Atlantic, the MOC transports heat as deep 2000m in about 30 years.

Redistributive surface heat uptake alters the total amount surface heat uptake among the basins. Compared to the passive-only heat uptake, which is about the same among the basins, redistribution nearly doubles the surface heat input into the Atlantic but makes smaller increases in the Indian and Pacific oceans for a net global increase of about 25%, in the perturbation experiment with winds unchanged. The passive and redistributive heat uptake components are further distributed among the basins through the global conveyor belt. The Pacific gains twice the surface heat input into it through lateral transport from the other two basins, as a result, the Atlantic and Pacific gain similar amounts of heat even though surface heat input is in the Atlantic is much bigger. Of this heat transport, most of the passive component comes from the Indian and the redistributive component comes from the Atlantic.

Different surface forcing perturbation gives different circulation change pattern and as a result yield different redistributive uptake. Ocean heat uptake is more sensitive to wind forcing perturbation than to thermohaline forcing perturbation. About 2% reduction in subtropical cells transport and southern ocean transport, in the wind-change perturbation experiment, resulted in about 10% reduction in the global ocean heat uptake of wind-unchanged experiment. The AMOC weakened by about 35% and resulted in a 25% increase in passive heat uptake in the wind-unchanged experiment. Surface winds weakening reduces heat uptake by warming the reservoir surface temperatures, while MOC weakening increases heat input by a cooling reservoir surface temperatures. Thermohaline forcing

perturbation is combination of salinity and temperature perturbations, both weaken the AMOC, however, they have opposite redistributive effects. Ocean surface freshening gives positive redistributive effect, while surface temperature increase gives negative redistributive effect on heat uptake. The salinity effect dominates the redistributive effect for thermohaline perturbation.

Chapter 1: Introduction

1.1 Introduction

The large heat capacity of the Ocean makes it an immense reservoir of heat and thus an important influence on the rate of global warming. Ocean heat uptake not only influences the rate of climate change but also the sea level rise due to thermal expansion of the ocean and the pattern of surface warming. Ocean heat uptake may be defined as the change in ocean heat content under anomalous surface temperature changes. In a steady state, the net surface heat flux is zero, however due to anthropogenic forcing, there is additional downward heat flux from the atmosphere resulting in surface temperature anomalies which are propagated into deep ocean. Ocean heat content changes when a temperature layer warms or depth of a temperature layer changes. Hence, ocean heat uptake can be measured as the difference in heat content between one climate state and another. It can also be measured in terms of the depth to which temperature anomalies have been transported (effective depth).

1.2 Steady state ocean heat transports and mechanisms

The temperature - depth profile or stratification of the ocean determines its heat content. In steady state, ocean circulation and associated heat transports determine its stable stratification and hence heat content. Ocean temperature layers consist of a warm constant temperature upper layer (mixed layer) that interacts with the atmosphere and deep cold layers. These layers are seperated by the thermocline, a region where temperature changes rapidly with depth. Cold deep layers outcrop at the high latitudes, hence temperature layers are horizontal in the equator and midlatitudes and and sloped at high latitudes where

deep layers outcrop. Ocean heat content changes with depth of the thermocline in the mid-latitudes. The deeper the thermocline, the more the ocean heat content because a deeper thermocline means deeper warm upper layer and reduced thickness of the cold deep layer. The strength of ocean circulation and heat transport in these different regions together determine the depth of the thermocline and thus its heat content. In steady state ocean heat transports balance out one another to maintain a stable stratification.

Ocean heat transports occur mainly through advective and diffusive processes. Other processes such as convection and turbulent mixing are important as well. Together these processes determine the deep stratification of the ocean and thus the heat content. Diffusion smooths out temperature gradients. Vertical diffusion transports surface heat downward from the warm upper layers to deep cold layer, this is especially true in the midlatitudes where isopycnals are horizontal and there is a strong vertical temperature gradient. Lateral diffusion can also occur along sloped isopycnals due to baroclinic instability. Lateral diffusion occurs through mesoscale eddies, these flatten steep isopycnals by mixing and results in heat transfer especially when a temperature gradient exists along an isopycnal. Heat can be transferred upward or downward depending on the direction of the temperature gradient along the isopycnal. This process is especially important in the Southern Ocean where isopycnals are sloped and there is surface cooling. Heat transfer is upward in this case because the surface temperatures are cooler than those in the deep end of the isopycnals.

Advective processes depend on the ocean circulation driven by pressure gradient forces from the ocean temperature and density distribution and surface wind. Surface pressure gradient due to differences in high latitude cooling and low latitude warming results in a deep meridional overturning circulation, MOC. This circulation is present in the Atlantic and the in the southern ocean. In the northern hemisphere, the MOC brings warm water from low latitudes where there is net heat gain to the high latitudes where it sinks into the deep ocean. This transport keeps the high latitude from getting too cold. The pressure gradient is sustained by continous differential heating at the surface. At the surface, winds also cause upwelling deep waters and downwelling of surface through Ekman pumping resulting

in shallow overturning cells at the surface around the equator and in the subtropics. Wind driven cells are more prominent in the Pacific in the tropical and subtropical gyres and in the Southern ocean. In the Southern ocean, the wind driven cell goes into the deep ocean. Since there are no land boundaries, upwelling goes all the way to the deep ocean and hence intense vertical mixing. Convection also brings cools the deep ocean by bringing surface denser water to the deep and warmer deep water to the surface.

1.2.1 Ocean heat transport and stratification

The advective - diffusive model have long been used to model ocean stratification. In this model, heat diffuses downward from the warm surface layer and it is balanced by advection (upwelling) of cold deep water through thermocline in equilibrium. However, this model requires very high diffusivities to produce the observed ocean stratification and diapycnal diffusion occurs very on long timescales. Gnanadesikan (1999) and later Nikurashin and Vallis (2012), proposed a theory of how ocean circulation determines its stratification. Vallis and Nikurashin extended his model to a two dimensional model using equations of motion which is able to predict the latitude-depth variation of the fields. They showed how vertical diffusion, upwelling in the pycnocline, North Atlantic deep water formation, Southern ocean wind and Southern ocean eddies are connected. Pressure gradients produces a surface northward meridional flow that sinks in the Northern high latitudes where it is converted to dense deep water forming the North Atlantic deep water (NADW). Here isopycnals are pulled up to the surface by surface buoyancy flux and mixing. The sinking waters, return southward at middepth.

In the Southern ocean, pressure gradient and the Southern ocean wind stress drive another meridional southward flow. Strong westerly winds in the Southern Ocean induce an upwelliing poleward of the surface wind maximum and a downwelling equatorwards of the maximum, known as the Deacon cell. Eddy diffusion, tend to flatten isopycnals, resulting in a southward flow at the surface, balancing the overturning of the density surface by the wind driven flow, the balance of the two opposite flow results in tilted isopycnals.

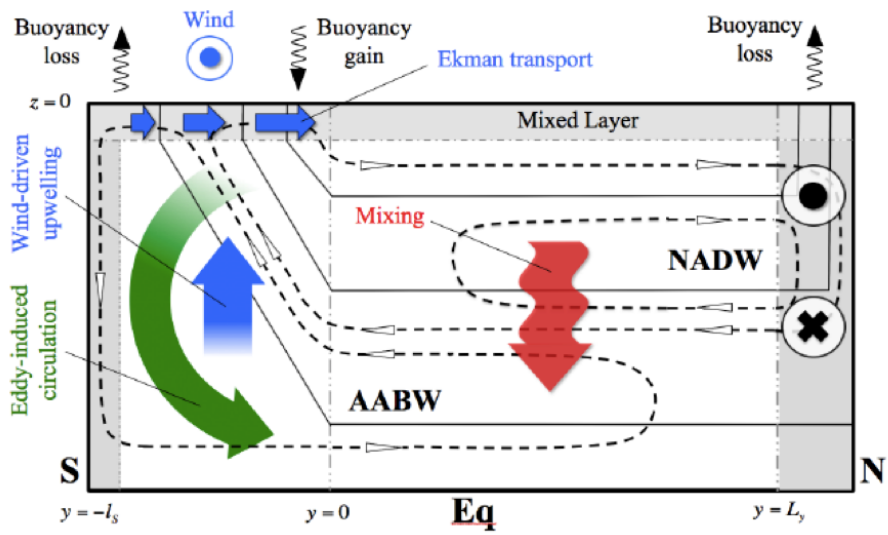

Figure 1.1: Schematic of meridional overturning circulation. Thin solid black lines are the isopycnal, thicker dashed black lines with arrows are the overturning streamlines of the residual circulation, dashed vertical lines are the boundares between adjacent regions, shaded gray areas are the convective regions at high latitudes and the surface mixed layer (Nikurashin and Vallis, 2012)

The residual flow is an abyssal cell moving southward at the surface and sinking around Antartica, returning northward in the abyssal ocean and upwelling to the surface. This gives to two inter-hemispheric meridional cells, flowing in opposite direction, one at mid depth and the other in the abyssal ocean, pictured in Figure 1.1. The difference between the rate of flow in the two cells, upwells in the midlatitudes, where it is balanced by the downward vertical diffusion of heat through pycnocline. The depth of the pycnocline can be calculated from the balance of the transports in these three regions. This balance gives a more realistic diapycnal diffusivity than would be required if all the water from the high latitudes upwells in the midlatitudes. These results essentially show that the rate of flow in the MOC cells is controlled by Southern Ocean wind and eddies and less by diapycnal mixing.

Gregory (2000) analysed heat transports in a control and perturbed (warming) experiments in a general circulation model under these processes. He grouped heat transport into: Advective, horizontal diffusion, vertical diffusion and vertical mixing. In the control

experiment, he showed that the direction of ocean heat transport in steady state is different from previous understanding of downward diffusion of heat balanced by upwelling or advection of cold deep water(upweling-diffusive model). He showed instead that, on a global average, upward diffusion of heat is balanced by downward advection of heat, though, the upwelling-diffusive model still works in the low latitudes, it does not work in the high latitudes. He showed that the high latitudes dominate heat transport, hence the global balance of heat transport is that of the upward diffusion of heat and downward advection of heat, (Figure 1.2). He explained the mechanisms by which this occurs, MOC transport (advection) brings warm water from the tropics to the high latitudes where it sinks to the deep ocean, while horizontal diffusion and convection (vertical mixing) transport heat upward from the deep ocean. At high latitudes, the surface continously loses heat, hence, it is cooler than the deep ocean. This unstable state results in convection, which mixes deeper warm water upward and the cooler surface water downward, as a result, convection cools deep waters without any volume transport. In steady state, this continual cooling of the deep layer is balanced by northward moving warm water from the tropics at the surface, sinking at high latitudes to replace the convectively cooled deep ocean as it moves southward in the deep ocean. In the southern high latitudes, surface temperature is also colder but density depends more on salinity. Convection is less important here because there is less vertical temperature and density gradient here, thus the warm deep water have roughly the same density as the cold surface water. However, isopycnals are tilted here, isopycnal slope upward to the south because of salinity, there is an isopycnal temperature gradient that is warmer downwards. Hence, isopycnal diffusion results in upward diffusion of heat. The continous cooling of the Southern deep ocean by upward diffusion of heat is also balanced by the downward advection of warm surface water in the Deacon cell described above.

1.3 Mechanisms of ocean heat uptake

Observations and numerical simulations show that the oceans have warmed in the last century under anthropogenic forcing. Globally, temperature anomalies have reached as deep

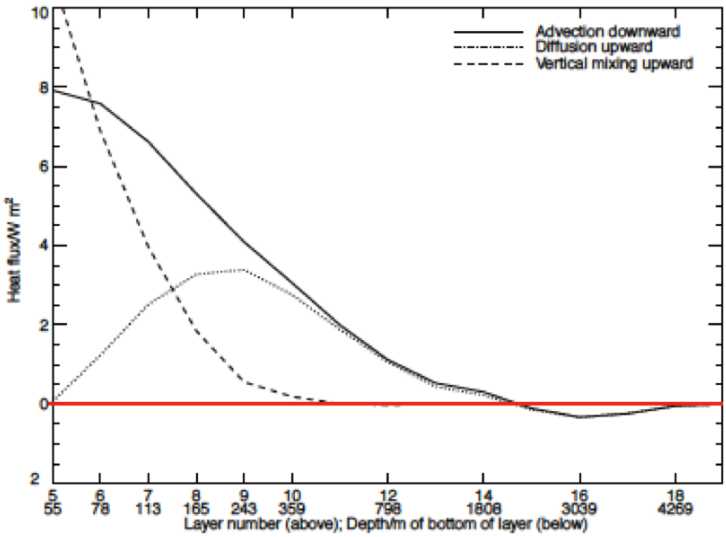

Figure 1.2: Global average vertical heat fluxes in a control climate (Gregory, 2000)

as 2000m in the last century. Figure 1.3 shows the observed ocean warming in the last 50 years. The spatial pattern of ocean warming at the surface and in deep ocean warming anomalies is not uniform in all the basins. The Atlantic have the largest and deepest heat uptake trend as shown in Figure 1.4. There is a midlatitude band of fast and deep warming in the southern hemisphere between 35^oS and 50^oS (Levitus et al., 2012). Southward of this band there is cooling. At the surface, the southern hemisphere intense warming band extends eastward from the Argentine Basin all the way to Australian continent. The Atlantic has the smallest surface temperatures anomalies, even though, it has the deepest subsurface anomalies. At the high latitudes between 50^oN to 60^oN Atlantic surface temperature actually reduced under anthropogenic forcing. While the Pacific has the largest surface temperature anomalies. The same pattern of ocean heat uptake have also been observed to be significant among CMIP3 and CMIP5 coupled ocean runs, Figure 1.5 (Kuhlbrodt and Gregory, 2012). Bryan et al. (1988) using a model with idealized geometry showed there is interhemispheric asymmetry in ocean heat uptake. The southern hemisphere have delayed response to surface warming. They cited land - ocean differences in both hemisphere as the

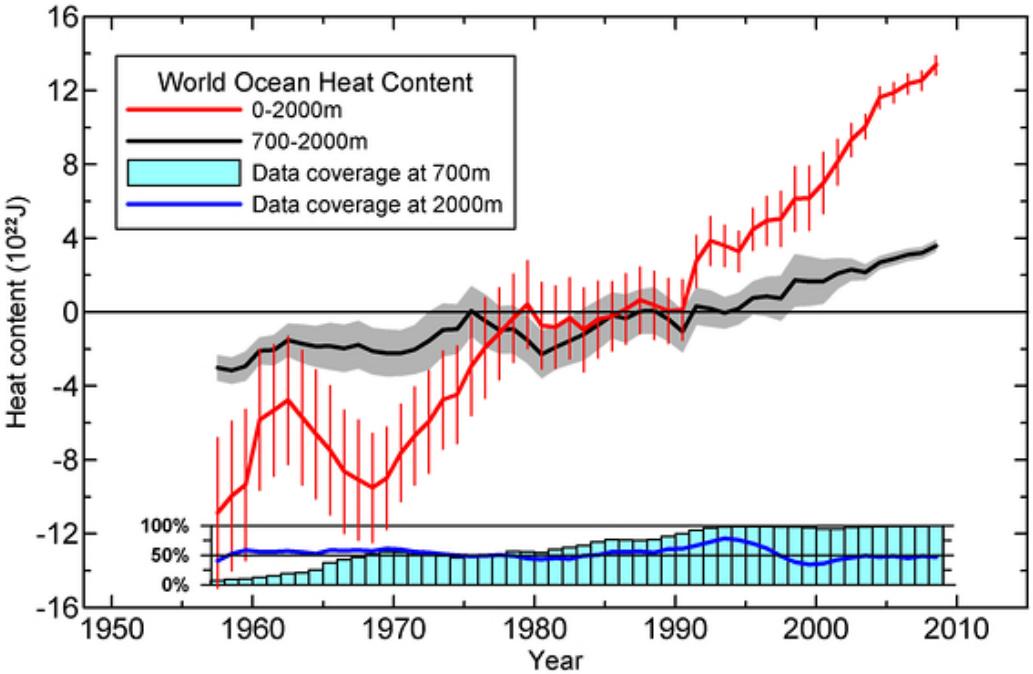

Figure 1.3: Time series for the World Ocean of ocean heat content (1022 J) for the 02000 m (red) and 7002000 m (black) layers based on running pentadal (five-year) analyses. Reference period is 19552006. Each pentadal estimate is plotted at the midpoint of the 5-year period. The vertical bars represent +/ 2 S.E. about the pentadal estimate for the 02000 m estimates and the grey-shaded area represent +/ 2S.E. about the pentadal estimate for the 0700 m estimates. The blue bar chart at the bottom represents the percentage of one-degree squares (globally) that have at least four pentadal one-degree square anomaly values used in their computation at 700 m depth. Blue line is the same as for the bar chart but for 2000 m depth. (Levitus et al., 2012)

reason, though their simulation has no significant overturning cell. Manabe and Spelman (1991) also showed that asymetry between warming and cooling experiments. Temperature anomalies reached deeper in the cooling experiment than in the warming experiment. Temperature anomalies reached deeper in cooling experiments because convection is enhanced hence anomalies reached deeper and faster than in warming experiment. This suggests the importance of convection.

The timescales of ocean heat uptake was studied by Stouffer (2004), Yang and Zhu (2011). They studied the equilibrum timescales for the ocean under increased and reduced CO_2 experiments. They found that the top 1km of the ocean reaches equilibrum in about

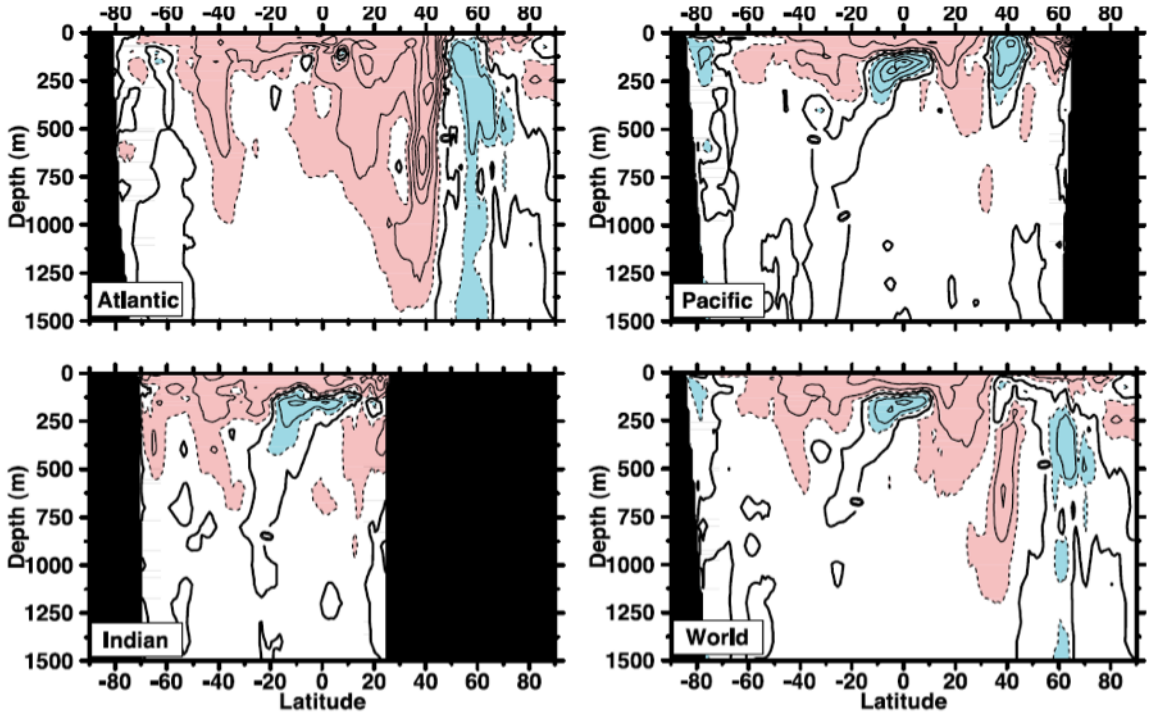

Figure 1.4: Linear trend (1955 − 2003) of zonally averaged temperature in the upper 1,500 m of the water column of the Atlantic, Pacific, Indian and World Oceans. The contour interval is 0.05C per decade, and the dark solid line is the zero contour. Red shading indicates values equal to or greater than 0.025C per decade and blue shading indicates values equal to or less than 0.025C per decade. Based on the work of Levitus et al. (2005a).(Solomon et al., 2007)

300yrs, while depths at 2km to 3km takes much longer time between 800 to 1500 years to reach equilibrium. Vertical profile of equilibrium timescale is comparable to the temperature profile, though the timescale layers are much deeper than the temperature layers. The short equilibrium timescale in the upper 1km is roughly constant and comparable to the temperature mixed layer. There is also a region of rapid change in time scale called the temporacline comparable to the thermocline, separating the fast timescale upper 1km layer from the lower 2km to 3km long timescale layer (Figure 1.6). The timescales are a good indicator of the mechanism of ocean heat uptake. The fast time scale top layer above the temporacline suggest it is wind driven while the long time scale deep layer below temporacline suggest overturning-driven uptake. The timescales also show interhemispheric

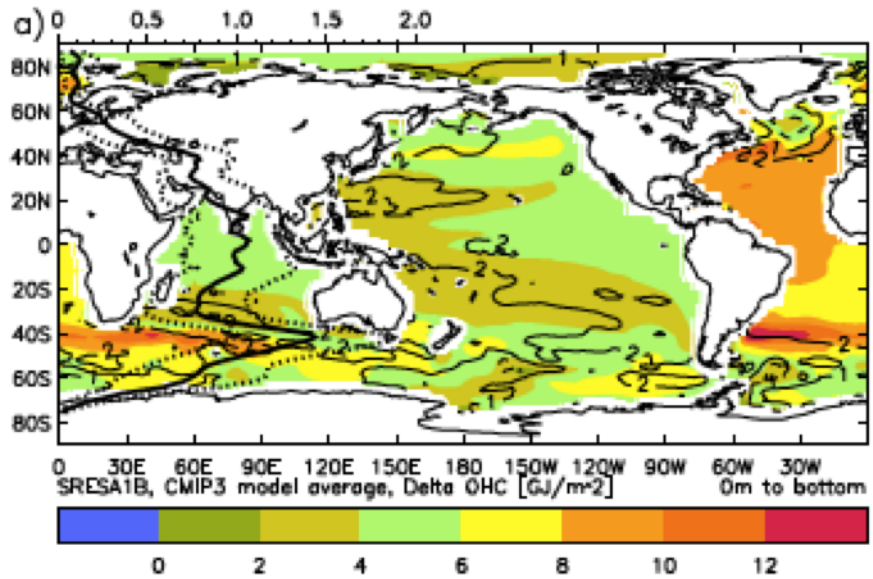

Figure 1.5: Vertically integrated ocean heat uptake (color shading ; in GJm $^{-2}$). SRES A1B scenerio of 17 CMIP3 models Ensemble average Ocean heat content. Thick black line: Zonal total in 10^{15} Jm^{-1}, (scale in the upper left corner), with 1 std dev (Kuhlbrodt and Gregory, 2012)

asymmetry in the Atlantic unlike that of the Pacific which is more symmetric. The Atlantic in the northern hemisphere has a deeper constant 200-year timescale layer and more defined temporacline than in the southern hemisphere. In the southern hemisphere, the constant 200-year layer gets shallower and the temporacline widens as one goes southward. This means that heat gets deep in a shorter time in the northern hemisphere than in the south. This may represent the effect of the overturning circulation present in the Atlantic northern hemisphere and absent in the Pacific

The importance of wind driven heat uptake was shown in the study of Church et al. (1991). Using non-mixing seven isopycnal layers Church et al. (1991) modeled heat uptake based on the subduction of the surface water in the subtropical gyre. They assumed that the subduction of surface water takes place on sloping isopycnals and vertical mixing across isopycnals is neglected thus treating heat uptake as a passive tracer. Using ocean surface density map, and the location of Ekman convergence in the subtropical gyres, they

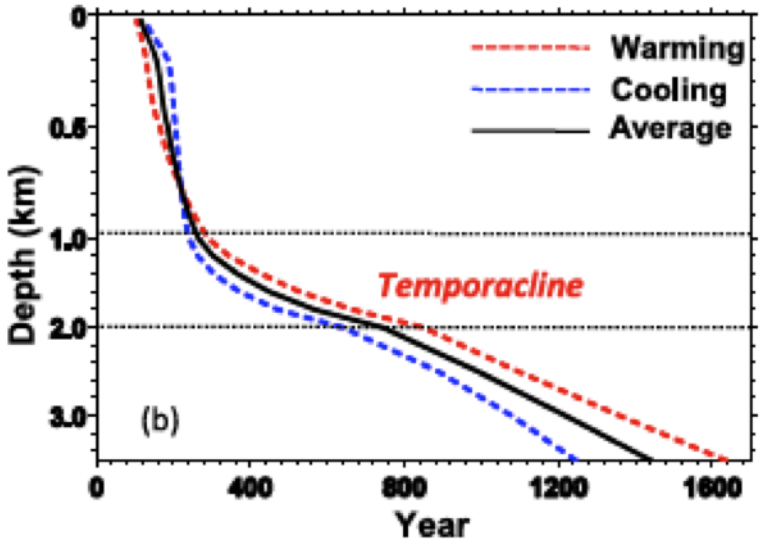

Figure 1.6: Vertical profile of equilibirum response time of global mean ocean temperature. The red dashed, blue dashed and black solid lines are for warming, cooling experiments and their average, respectively (Yang and Zhu, 2011)

determined the depth to which surface temperature warming can penetrate. Since they assumed no diapycnal mixing, surface heat is only transported within the density layers that outcrops in the subduction region, hence can penetrate only as deep as these density layers. They found the densities lower than 26.87 and densities higher than these are not considered since they are found poleward of the line of maximum wind stress. The renewal rate for each density layer is used, which depends on the volume of the density layer and the subduction rate at the surface. Hence the deeper layers have longer renewal times. The renewal rate also determines the rate at which green house warming is transported into the deep ocean. Using Ekman transport estimate in the subtropical gyre, and the volume of the density layers, they estimated the renewal time of about 20yrs for the surface layers within the subtropical gyre and about a 100 years for the intermediate waters. They thus estimated the rate of sea level rise.

Other studies have focused the importance of overturnning circulation in heat uptake. Studies have shown the link between the strength of ocean circulation to the amount of ocean heat uptake. Kostov Y. and Marshall (2014) analyzed the AMOC and heat uptake

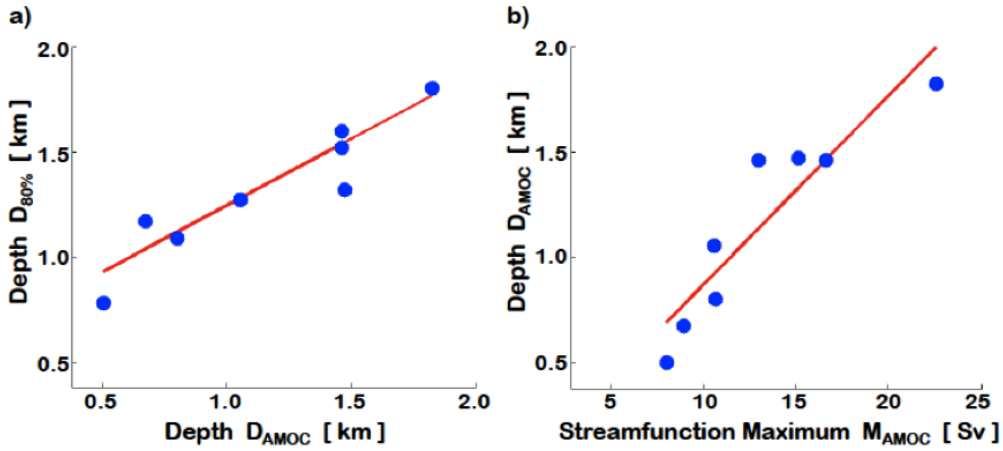

Figure 1.7: (a) Correlation between $D_{80\%}$ and D_{AMOC} (R=0.93, p-value p<0.01), (b.) Correlation between D_{AMOC} and M_{AMOC} (R=0.92, p-value p<0.01) (Kostov Y. and Marshall, 2014)

among CMIP5 models. They showed that heat uptake in the models correlate with strength and depth of the AMOC in the models. The stronger and deeper the MOC, the greater and deeper the temperature anomalies transported into the ocean among the models. Also the pattern of temperature anomalies is consistent with AMOC path. Temperature anomalies are concentrated in the north Atlantic and along western boundaries. They fitted an idealized two - layer Energy balance model, EBM to the SST and seas surface heat flux anomalies for each of the CMIP5 model. They found that EBM depth scale and q, the rate of heat exchange between the two layers, correlates well with the depth and strength of the AMOC (Figure 1.7). A feedback factor sets the SST damping rate due to the applied forcing. While the feedback factor is the major source of spread among the models, the rate of heat exchange and effective depth (which is set by the strength and depth of the AMOC) is also another source of spread among the climate response of the models. This relationship suggests that stronger AMOC should have more heat uptake. This is consistent with heat uptake mechanisms mentioned above, a stronger ocean circulation should give more volume transport and hence more heat transport.

More recently, studies have shown that heat uptake by ocean circulation cannot be

modelled only as passive process as suggested in the Church et al. (1991) paper. Banks and Gregory (2006) showed that heat transfer of anomalous surface temperature treated like a passive tracer is inadequate to measure ocean heat uptake. Rather it involves change in heat content due to redistribution of the ocean's existing heat reservoir due to circulation changes. They showed that the pattern of the uptake of a passive tracer forced from the anomlous heat flux from a climate change experiment is different from the pattern of heat uptake itself. The pattern of heat uptake itself includes the effect of weakening of the overturning circulation, weakening of convection and isopycnal diffusion. The difference in the passive tracer pattern and the heat uptake pattern mattered especially at the high latitudes. The total global uptake, however is the same for both the passive tracer and temperature anomalies. The high latitude pattern difference cancel out in the global average. Winton et al. (2012) also showed with experiments one in which ocean currents were fixed and another where ocean currents are allowed to change under anthropogenic climate forcing. The ocean surface warmed more when currents were fixed but heat anomaly reached deeper when currents were allowed to change. The surface pattern of warming was also different. The northern high latitude Atlantic cooling was not present when ocean currents were fixed and more warming was observed in the southern ocean

Xie and Vallis. (2012) focused more on the comparison of heat uptake through passive advection and redistribution on existing temperature reservoir. With a number of experiments showed that the redistribution of existing heat reservoir plays a more important in amount of heat uptake. Xie and Vallis. (2012), varied parameters known to control the strength of the MOC such as surface salinity and temperature forcing, Eddy diffusivity and southern ocean wind stress. They varied diffusivity and southern ocean wind stress in the background state (control), this results in control runs with different MOC strengths. These were then forced with the same same surface temperature and salinity anomalies in the perturbed experiment. All experiments showed a weakening of the MOC strength in the perturbed experiments, runs with stronger background MOC, have more weakening and but more heat uptake i.e the fractional change in the MOC in the warming experiment is

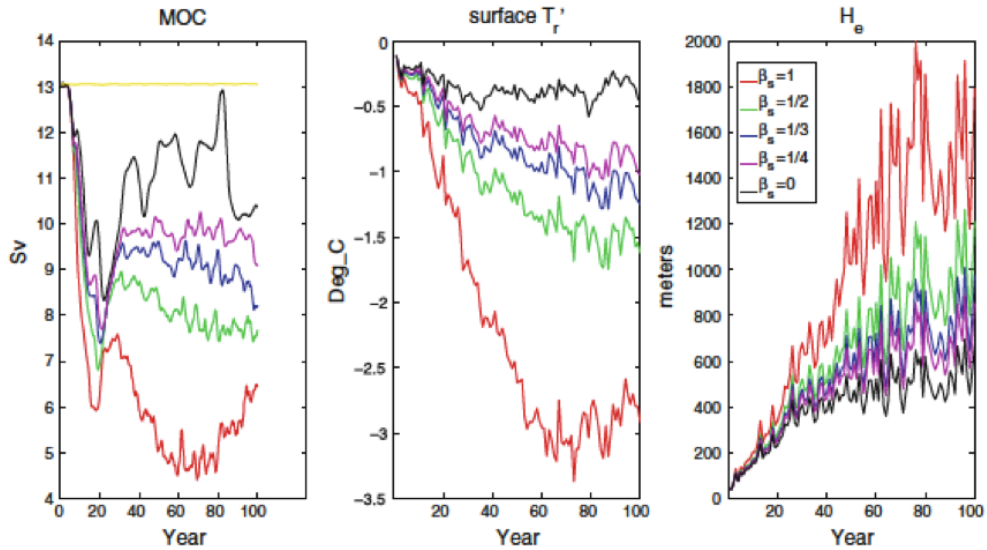

Figure 1.8: Integration with $\Delta T^{\star}$ and $\Delta S^{\star}$ and varied β_s runs. (Left) MOC strength, yellow line is the CTL run MOC strength. (Middle) the existing heat reservoir distribution T'$_r$ average through the surface layer. (Right) ocean effective depth H$_e$ (Xie and Vallis., 2012)

constant for the different background state. The greater change (weakening) in the MOC leads to more heat uptake and that this is a robust feature in all warming experiments. In another set of experiments, starting with the same control state, the surface salinity anomalies and idealized-latitude independent temperatute anomalies were varied in the perturbed experiments. All the perturbed runs have different strengths of the MOC. Runs with cooler temperature anomalies, have stronger MOC strength, while runs with stronger salinity anomalies have stronger MOC strength. However, the heat uptake in these experiments were different. The salinity-variation runs showed more heat uptake for weaker MOC strength, while the temperature-variation runs have more heat uptake for stronger MOCs (Figure 1.8 and Figure 1.9).

Xie and Vallis. (2012) explained the mechanism by which a weaker overturning yield more heat uptake. They showed that runs with weaker MOCs have cooler of existing reservoir surface temperature anomalies (Figure 1.8 *middle panel*). More surface anomalous heat is absorbed when existing reservoir temperatures cool, hence more heat uptake. This

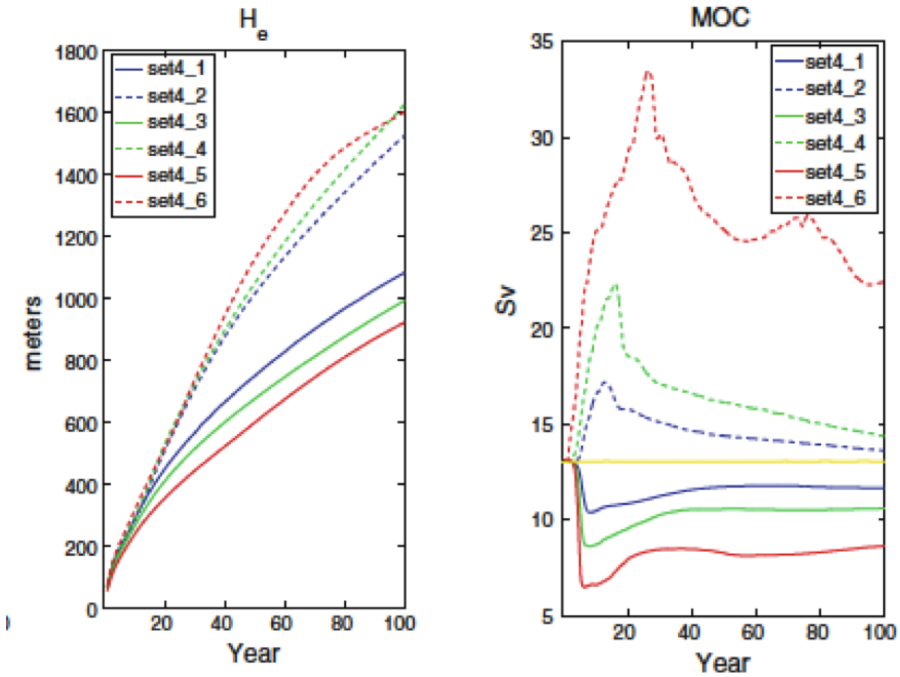

Figure 1.9: Time series of MOC strength and ocean effective depth H_e, in temperature perturbation experiments. Warming experiment have solid lines; Cooling experiments have dashed lines; Red to Blue line: high to low perturbation strength, Yellow line is the CTL run, (Xie and Vallis., 2012)

occurs especially in high latitudes, where anomalous heat is able to penetrate even deeper. They also showed that the increase in surface temperature in the tropics does not influence the MOC like it does for the high latitudes because of the buffering effect the thermocline has in the tropics.

Gregory (2000), showed a different mechanism through which a weaker overturning could lead to more heat uptake. In the warming experiment, reducing convection leads to weakened MOC and thus results in high latitude surface warming. Since convection brings heat up from the deep ocean, this leads to accumulation of heat in the deep ocean. In the midlatitudes too, the weakened MOC leads to weaker upwelling in the midlatitudes and hence deeper thermocline and as a result more heat uptake. In the Southern high latitude, surface warming reduces the isopycnal temperature gradient, thus a reduction upward heat transport through horizontal Eddy diffusion and more heat uptake.

Huang et al. (2003) made the same observation of the 'unexpected' increased deep ocean heat uptake with MOC weakening. They also explained the reason for increase in heat uptake when the MOC weakens to be due to reduction of convection in northern high latitude and reduction of Eddy diffusion in southern high latitudes. Zanna and Marshall (2013) presents a conceptual model of ocean heat uptake. A major component is the NADW formation rate. It also shows that a lower formation rate gives higher heat uptake. The mechanism proposed for this is that the weaker MOC rate deepens the temperature stratification and hence the heat content.

1.4 Unanswered Questions

Several questions about the mechanism of ocean heat uptake still remain. Heat uptake goes much deeper in the Atlantic than in other basins and this has been assumed to be due to the deep overturning cell in the Alantic. Studies mentioned in the previous section have linked the strength of the overturning in models to speed at which heat propagates downwards. The reduction in convection and isopycnal diffusion were also highlighted in the study of Gregory (2000) and Huang et al. (2003) as reasons for heat uptake in the southern and northern hemisphere high latitudes. These are also closely linked to redistribution of existing reservoir due to changes in overturning circulation. We use our analysis of CESM - CMIP5 abrupt $4xCO_2$ increase experiments shown in Figures 1.10, 1.11 and 1.12 to highlight these lingering questions. The pattern of heat uptake in this experiment is similar to observations and numerical experiments results mentioned in the previous section, hence it represents the mechanism of heat uptake. Compared to observations, however, temperature anomalies are much higher in this abrupt $4xCO_2$ increase experiment, giving a clear temperature anomaly gradient so that propagation is much obvious.

The figures show there is significant heat uptake around latitudes 30^oS to 60^oS up to a depth of 1km on short timescales 10, 20 years in all the basins. In the low latitudes (30^oS to 30^oN), the warming is much slower, reaching less than 500m in the Indian and Pacific oceans in the first 20 years. The Pacific northern hemisphere, between 30^oN to 60^oN, has

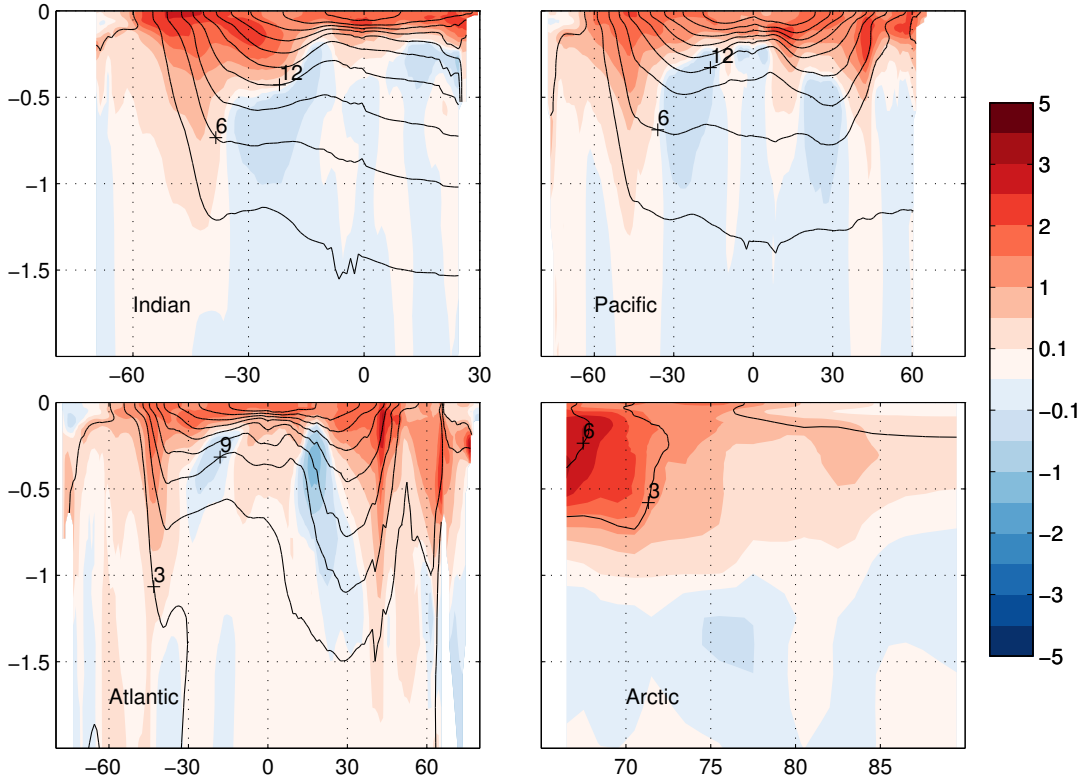

Figure 1.10: Basin zonal average temperature anomalies in $4XCO_2$ abrupt increase run for year 10 minus year 1 (Shading). $4xCO_2$ abrupt run basin zonal average temperature at year 10 (Line contours c.i=3^oC)

deeper warming (>500m) than the low latitudes but less deep than southern hemisphere warming in the same latitude band. The Atlantic warmed much faster both in the low latitudes and in 30^oN to 60^oN band. The low latitude warming reached a little deeper than 500m in 20 years and 30^oN to 60^oN band warmed even faster deeper than 1500m in 20 years. Though there is a near surface cooling around 50^oN to 65^oN, the warming is still noticed below this surface cooling. Within 20 to 50 years, the Southern hemisphere warming reaches 1500m in all the basins and the low latitude warming reached close to 1000m in the Indian and Pacific oceans. The Atlantic, however reached deeper, close to 2000m in the low latitudes and northern hemisphere within this time period.

The fast downward propagation of heat within 20 years, centered around 45^oS in all

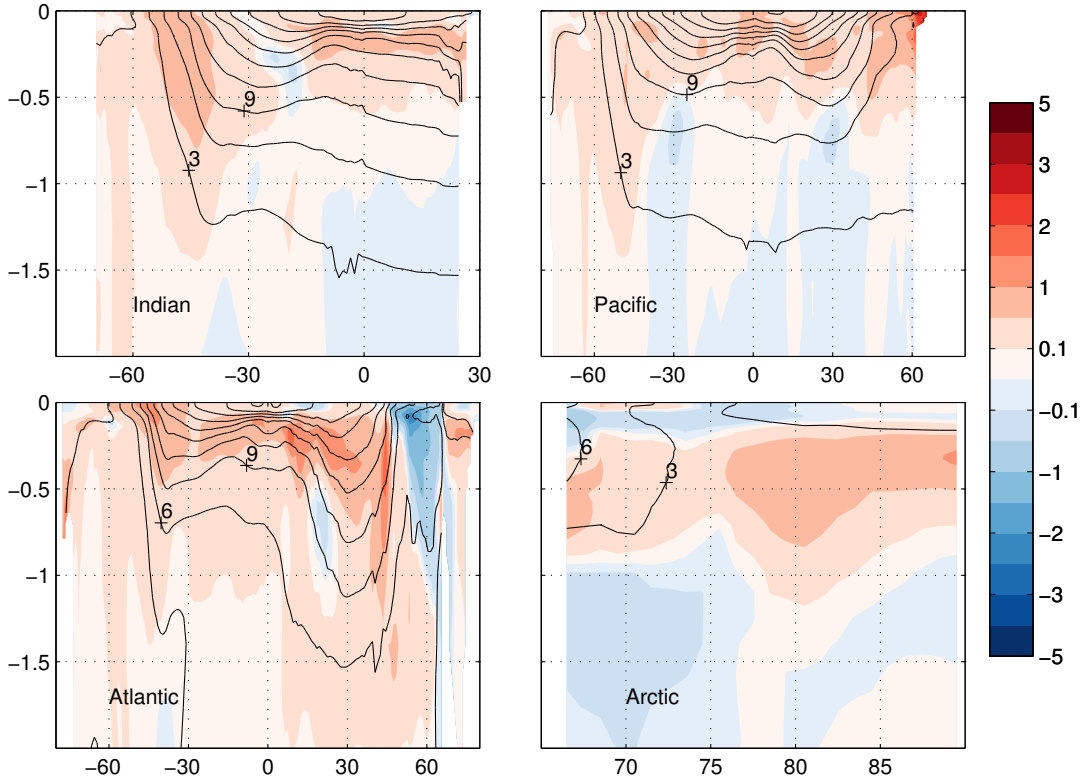

Figure 1.11: Basin zonal average temperature anomalies in $4XCO_2$ abrupt increase run for year 20 minus year 10 (Shading). $4xCO_2$ abrupt run zonal average temperature at year 20 (Line contours c.i=3^oC)

the basins and even faster in the Atlantic around 45^oN suggest a mechanism other than the deep overturning circulation. This is especially true for the Indian and Pacific oceans where there is no deep overturning cell. We propose another mechanism for this pattern of heat upake as wind or changes in it. The timescale and location of the heat uptake suggest it is wind driven. The latitude of deeper and faster heat uptake in the southern hemisphere centered around 45^oS and around 45^oN in the northern hemisphere. This is the edge of the subtropical gyre and there is downward Ekman transport here. We can estimate the time to advect water down to 1000km through Ekman transport at this latitude. Ekman vertical velocity can be obtained from the expression $\tau/\rho F$, where τ is the wind stress, ρ is the density and F, the coriolis force. Using $\tau = 0.2Nm^{-2}$ and $\rho = 1000Kgm^3$ and

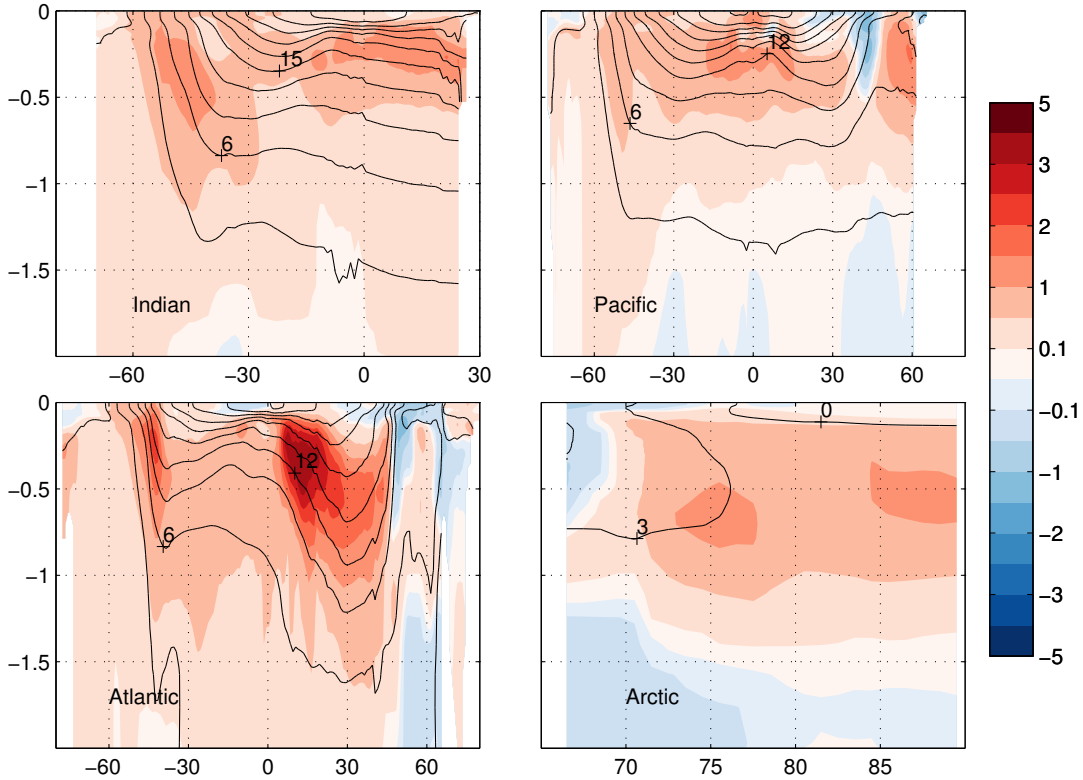

Figure 1.12: Basin zonal averaged temperature anomalies in $4XCO_2$ abrupt increase run, year 50 minus year 20 (Shading). $4xCO_2$ abrupt run basin zonal average temperature at year 50 (Line contours c.i=3^oC).

$F = 10^{-4}s^{-1}$, we obtain a time of 20 years. This is close to the 10-year time scale observed to reach this depth around 45^oS. Anomalies seem to go as far as the base of the isotherms that outcrop at the surface here. A change in wind could also be another mechanism, more likely on a shorter timescale. This can be seen in a comparison of figures 1.10 and 1.11 with 1.13. The region of with the greater change in barotropic streamfunction seem to be the around these latitudes of greater heat uptake. Similar studies, showing heat uptake due to subduction in the subtropical gyre was done by Church et al. (1991) as highlighted in the previous section. However, theirs is a conceptual model and heat uptake was modeled only as a passive process which have been shown to be an inadequate treatment of heat uptake. It also does not include the effect of change in wind on heat uptake.

If there is a different mechanism, however, there remains the question of what gets

the heat down even faster and deeper in the Atlantic than in the Indo-Pacific. A few explanations other than the deep overturning circulation for the deeper Atlantic have been given from previous studies. Xie and Vallis. (2012), using the effective depth measure, showed that redistribution of existing heat reservoir due to change in strength of ocean circulation, increases the speed and depth of penetration of surface temperature anomalies, compared with that due to passive advection. However their experiments used an Atlantic-like basin with idealized geometry, hence the effect of the redistributive mechanism across all basins was not studied. Another possibility is that the gyres advect warm water along the deeper and colder isotherms in the Atlantic (perhaps helped by convection), since the Atlantic has deeper convection and deeper isotherm depth than other oceans. Lee et al. (2011), gave another explanation of flow of warm water from the Indian ocean into the Atlantic due to strengthening of winds stress curl. This doesn't explain the deep warming in the north Atlantic that precedes deep warming in the south Atlantic. Lozier et al. (2008) also showed the deep heat uptake in the Atlantic might be due to the variability wind and bouyancy measured from the NAO index, their study couldn't distinguish warming due to the variablility and due to anthropogenic forcing.

In view of the highlighted points, it will be beneficial to be able to separate ocean heat uptake into its passive advective and redistributive components. The passive component should allow us to isolate the transport processes and timescales associated with the ocean circulation strength alone without redistributive effect, in the different basins. For example, we can determine if the fast uptake in the Atlantic is due to the AMOC in it or because of the redistributive effect of the AMOC changes, or why heat uptake reaches as deep as 1000m in the Indo-Pacific even though, the circulation in these basins do not reach that deep. The redistributive component allows us to study how changes to different circulation patterns and strength will increase or reduce the speed and depth of heat penetration and amount of heat uptake, in different basins. Hence, we hope to be able to answer the following questions:

- What mechanisms are responsible for heat uptake in short time scales of less than 20

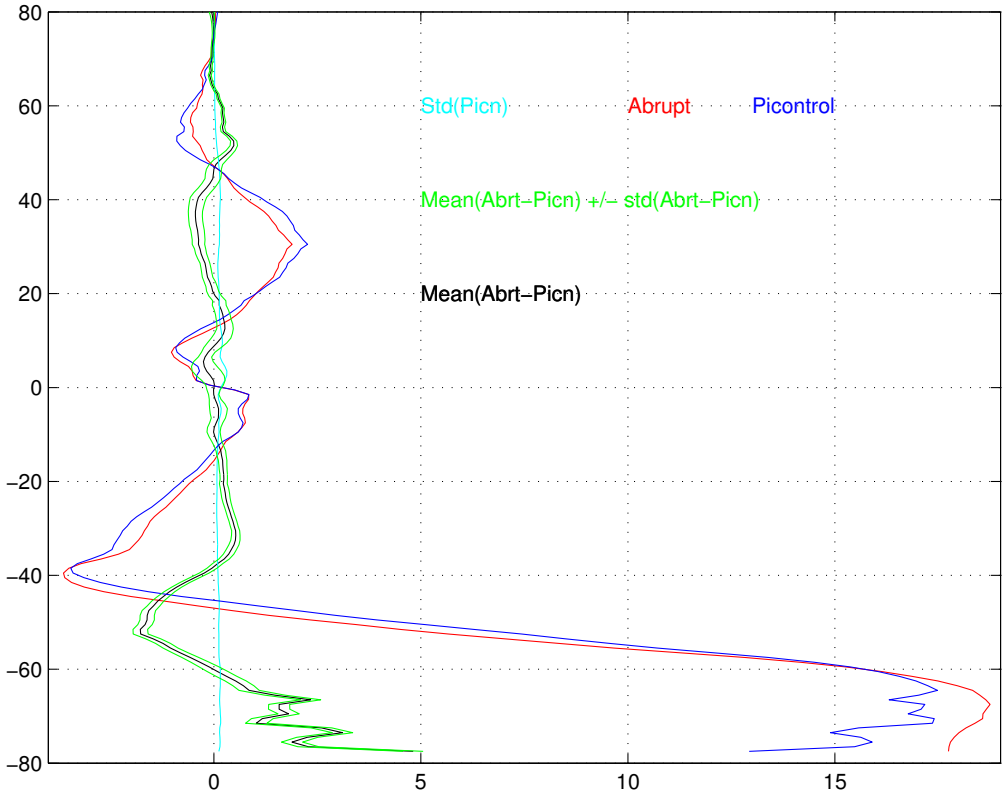

Figure 1.13: Zonal averaged barotropic streamfuntion abrupt and control average and the difference between them in the CESM-CMIP picontrol and $4XCO_2$ experiments

yrs and at depths shallower than that of the MOC?

- Why does heat uptake reach deeper in the Atlantic than in other basins?
- What are the timescales associated with different transport processes? How are these timescales changed by redistribution?
- How are the passive and redistributive terms of ocean heat uptake distributed among the basins
- How are the passive and redistributive components of ocean heat uptake changed by different surface perturbations

Chapter 2: Methodology

2.1 Model

The Parallel Ocean Program model, POP, is used in a stand alone ocean run to test mechanisms of ocean heat uptake. POP is a z - coordinate model developed at the Los Alamos National Laboratory, LANL (Smith and Gent (2002)). The 3-D primitive equations in general orthogonal coordinates in the horizontal are solved with the hydrostatic and Boussinesq approximations. A linearized, implicit free-surface formulation is used for the barotropic equation for surface pressure (surface height). The global integral of the ocean volume remains constant because the freshwater fluxes are treated as virtual salt fluxes, using a constant reference salinity. POP uses a dipole or tripole displaced - pole grid for better resolution of the Arctic. Tracer and momentum advection are computed on a B grid. We use horizontal grid with resolution varying from 0.95^o to 1.25^o and a displaced north pole of the model coordinates to Greenland, and 60 vertical levels of thickness varying from 10m in the top to 250m in the bottom layer.

CESM4 (Community Climate System Model 4, Gent et al. (2011)), uses a slightly later version of POP as its ocean component. Hence, the effectiveness of POP in representing the mechanisms of ocean heat uptake can be measured by the CESM-CMIP5 results shown in Figure 2.1 and Figure 2.2. Figure 2.1 compare very well with the observed temperature trend pattern shown in Figure 1.4. Both figures show the Southern ocean intense warming around latitudes 35^oS to 50^oS, the cooling in the high latitude Atlantic 50^oN to 60^oN, subsurface cooling around the equator and surface cooling southward of latitude 60^oS in the Pacific and Indian oceans. The 500m depth temperature anomaly pattern (Figure 2.2), also compare well the AR4 models ensemble average heat uptake, Figure 1.5. They both show the Atlantic has gained more heat than the other basins and the band of intense warming

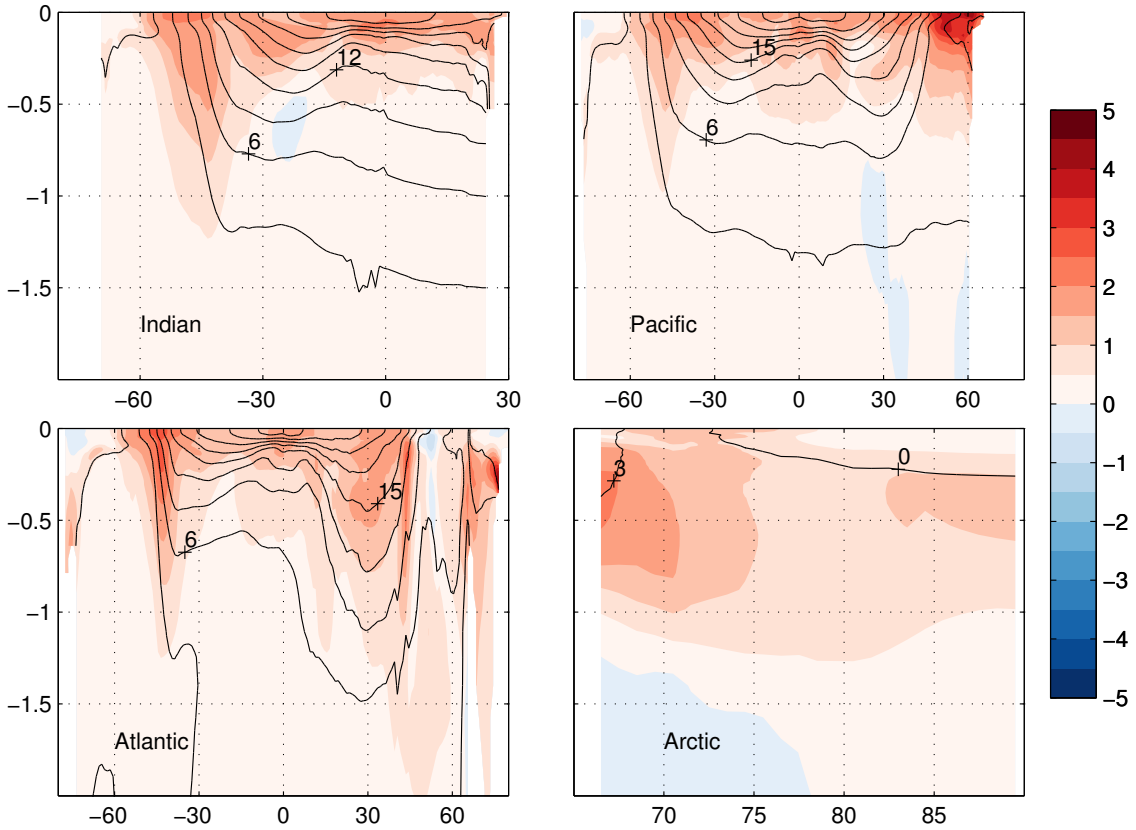

Figure 2.1: 100th year snapshot of zonal average temperature anomalies in 1*pct* CO_2 increase perturbation experiment CESM-CMIP5 run (Shaded: 1pct run temperature anomalies, Contours: Control run temperature)

around between 35^oS to 50^oS, from the Argentine basin to the Australian continent. Hence, to a large extent POP is a good tool for understanding the pattern or distribution of ocean heat uptake.

2.2 Experimental Design and Data

The response of a global-domain ocean model to a surface warming perturbation is examined using surface fluxes and wind based on simulations from CESM-CMIP5 (Climate Model Intercomparison Project 5, Taylor et al. (2012)). All forcing variables are monthly climatological values from the century long CESM run output. The POP control forcing

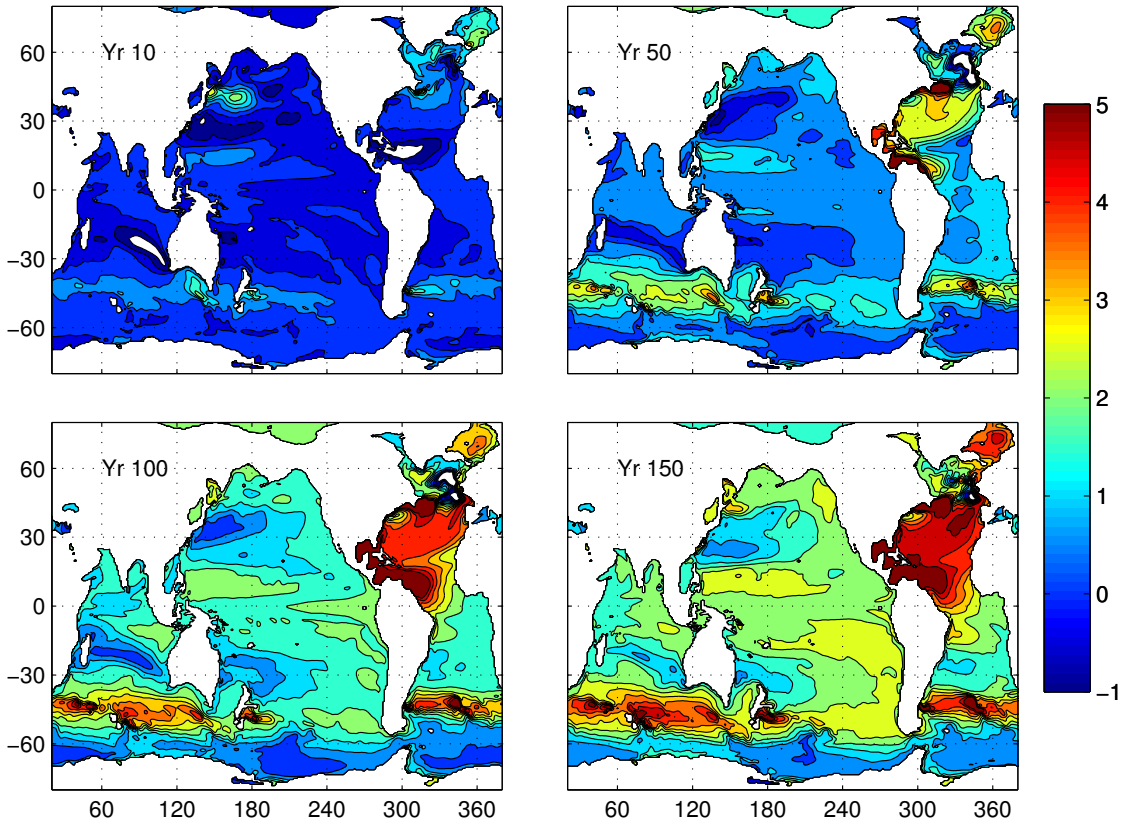

Figure 2.2: Snapshots of temperature anomalies at 500m depth in $4xCO_2$ increase perturbation CESM - CMIP5 run

is derived from a CESM - CMIP5 pre-industrial control (piControl) run, and the perturbation experiment forcing is derived from the CESM-CMIP5 $4xCO_2$ abrupt experiment. CESM-CMIP5 piControl run has non-evolving, pre-industrial conditions imposed, which includes prescribed atmospheric concentrations of all well-mixed gases (including CO2), some short-lived (reactive) species, prescribed non-evolving emissions or concentrations of natural aerosols or their precursors some short-lived (reactive) species and unperturbed land use, . The CESM CMIP5 abrupt $4xCO_2$ experiment is initialised from piControl run at year 1850, but has atmospheric CO_2 instantaneously quadrupled.

Wind stress is applied directly from the coupled model output, while a restoring boundary formulation, shown in Equation 2.1, is used to compute temperature and salinity surface

fluxes.

$$Q = \alpha(T_\star - T_s), \quad Q_S = \frac{\alpha}{C_p}(S_\star - S_s) \tag{2.1}$$

The model surface temperatures and salinity, T_s and S_s, are continually restored to the target temperature and salinity, $T_\star$ and $S_\star$, this produces surface heat and salinity fluxes, Q and Q_S, into the ocean. The temperature restoring strength, $\alpha = 40\text{W m}^{-2}\text{ K}^{-1}$, equivalent to restoring cofficient of 12 days in time units, determines how quickly the ocean surface approaches the target values and specific heat capacity of water, $C_p = 3,992$ J kg^{-1} K^{-1} is used, as in Xie and Vallis. (2012). The target temperature, $T_\star$ and target salinity, $S_\star$, are derived analogously from the coupled model surface heat flux, temperature, surface salinity fluxes and salinity, using the same 2.1, and target salinity is derived analogously from virtual salt flux and sea surface salinity. The target values are then used to compute surface fluxes in the POP ocean run, also following 2.1

Ocean-only experiments, forced with monthly climatological surface conditions, improves the signal-to-noise ratio for the forced perturbations by removing interannual and higher-frequency atmospheric weather noise associated with a coupled model, at the same time, ensures the model does not drift away from realistic climatological surface conditions and retains the annual cycle which is an inherent part of the heat uptake process. Quadrupled CO_2 level gives large temperature anomalies to facilitate observations of propagation and evolution.

2.3 Experiments

2.3.1 Control

The ocean control run is initialized from the January month average of year 1850 of CESM - CMIP5 piControl run. The control surface forcing is derived using the formulation described in the previous section, from the monthly averages of the last 250-year period starting with the initialization time. Surface wind and surface heat and salinity fluxes are computed every

time step, by interpolating the monthly climatology time target values to current model time. Surface forcing conditions are shown in Figure 2.3.

The control initial conditions and forcing are very close in time, thus reducing spin off time. The ocean control run is spun-up for 500 years using the tracer acceleration method (Bryan (1984)) followed by another 300 years with conventional time stepping. Eddies are represented by the Gent McWilliam parametrization Gent et al. (1995)), with a diffusion coefficient of 1.25×10^3 m^2/s used both for the bolus and Redi parts. Vertical turbulent mixing is represented with the KPP parametrization (Large et al. (1994)) with a background diffusion of 1×10^5 m^2/s applied everywhere, and convection is represented by strong vertical diffusion. Figures 2.4 and 2.5 show the control state.

2.3.2 Forced Experiments

Perturbation experiments are initialized from the near equilibrium (Year 901, see Figure 2.5) POP control run state and continued for 100 years. Surface forcings are the monthly climatology values computed from the last 50 years of the CESM-CMIP5 abrupt 4xCO_2 run (years 100 -150), using the same surface forcing formulation for the control run (Equation 2.1). The surface forcing anomaly from the control forcing is shown in Figure 2.6. The same model parameters used in the control run (see Section 2.3.1) were also used.

In contrast to our forced experiments, the CESM abrupt run surface conditions changed more gradually in the first 100 years due to the quadrupled CO_2 level, and was close to its final equilibrium values within the last 50 years. For our forced experiments, using the last 50 year climatology forcing from CESM abrupt gives somewhat like a step forcing to the CESM final state, as a result, initial surface fluxes and temperature anomalies are much higher compared to the CESM results. This way the CESM and our POP forced experiments have the same final state but different evolution to the final state. This monthly climatological step forcing, serves the purpose of this study, to isolate ocean only mechanisms and associated time scales. It almost completely removes the interannual variability in the surface heat flux, hence, atmospheric noise, while higher temperature gradients allows

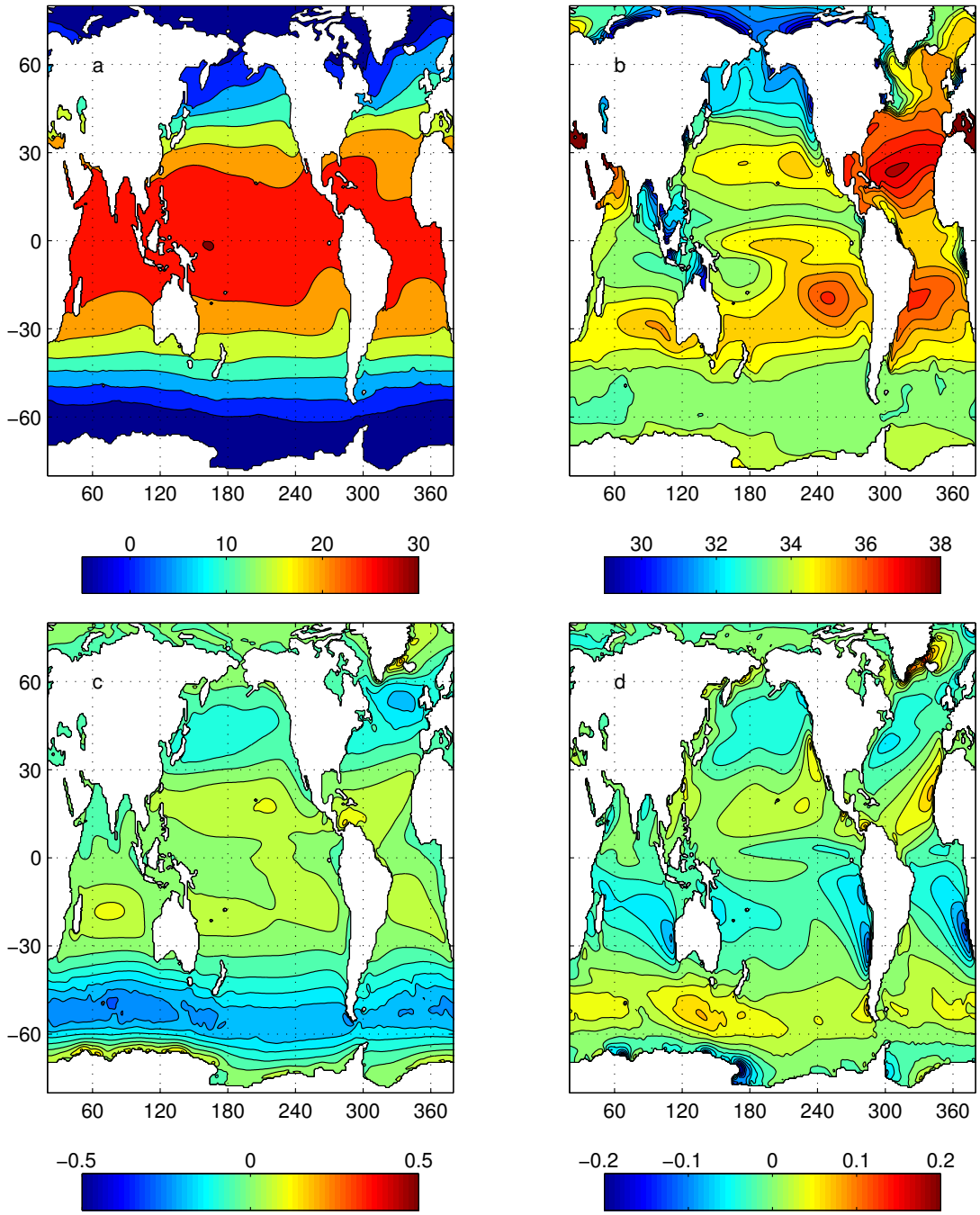

Figure 2.3: Control run surface forcing (a) Restoring temperature c.i.=5^oC (b) Restoring Salinity c.i.=.5psu (c) Zonal wind stress c.i.=.05Nm^2 (d) Meridional wind stress c.i.=.02Nm^2

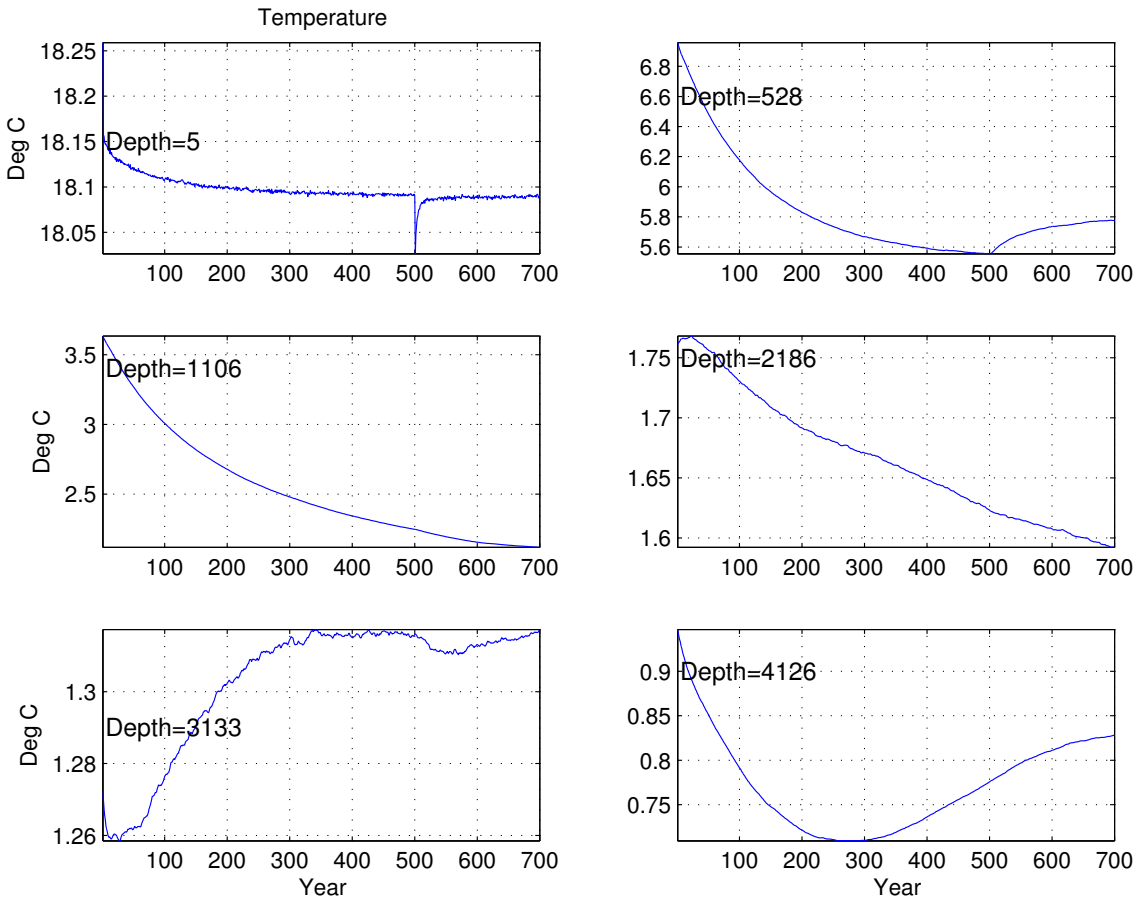

Figure 2.4: Control run global average temperature at different depths

us to see propagation path more clearly. This also allows us to isolate timescales associated only with ocean processes rather than timescales affected by the gradual change in forcing. Assuming linearity, the step forcing case can be used to reproduce the time varying forcing.

A set of three forced experiments is performed (see Table 2.1), all are initialized from the POP ocean control run. However, combination of surface forcings from the CESM piControl and abrupt experiment data are used in each forced experiment, all three experiments though, use surface temperature forcing from the CESM 4xCO_2 abrupt experiment. The Abrupt changed (AC) experiment has all surface forcings (Wind, salinity and temperature) changed, that is, derived from the CESM - $4xCO_2$ coupled output. The Wind Unchanged experiment (WU) uses the CESM piControl wind forcing, while the salinity and temperature

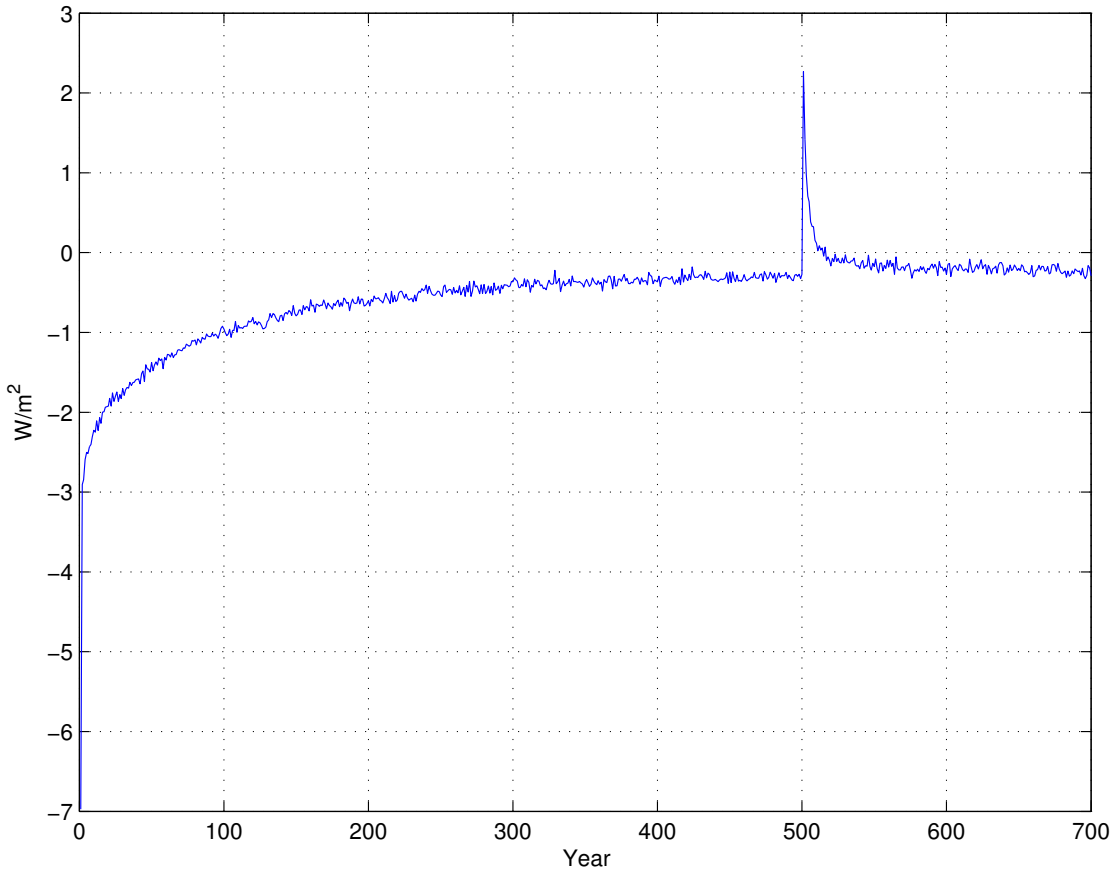

Figure 2.5: Control run global average surface heat flux

surface forcings are changed to that from the CESM - $4xCO_2$ coupled output. The Wind - Salinity Unchnaged (WSU) experiment, has wind and salinity forcing from the CESM piControl, while only the temperature forcing is changed to that of the CESM - $4xCO_2$ coupled output. This allows us to isolate and quantify the effects of wind stress perturbation and temperature and salinity perturbation on the circulation strength and the resulting effect on ocean heat uptake. The curl of wind stress in the CMIP5 picontrol and abrupt experiments are shown in Figure 2.7.

In order to study effects of passsive advection and redistribution on amount of heat uptake and surface anomaly propagation, two passive tracers are introduced in the forced experiments: "redistribution heat flux" passive tracer P_r, which is forced by the heat flux

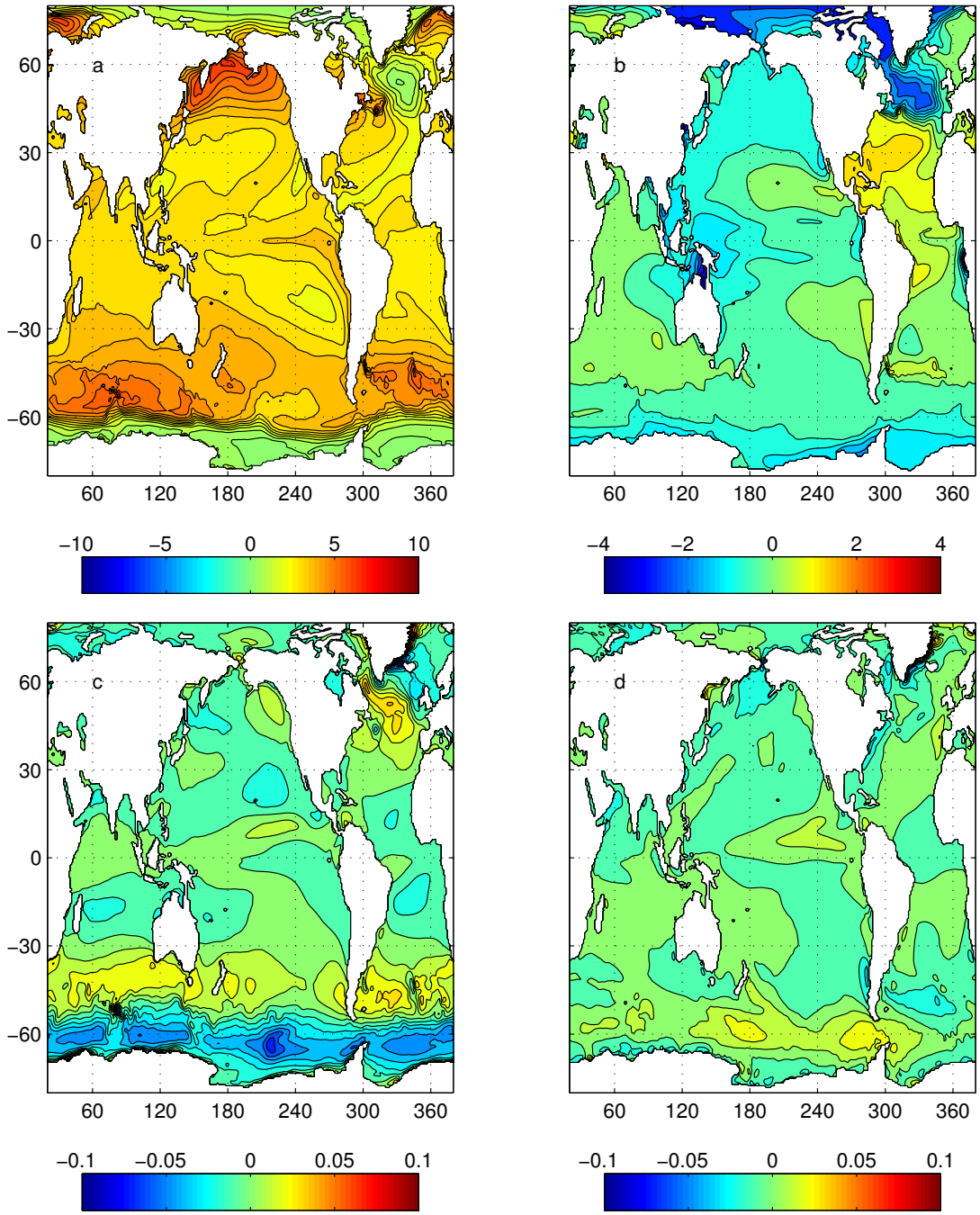

Figure 2.6: Abrupt surface forcing anomaly (a) Restoring temperature c.i.=.5^oC (b) Restoring Salinity c.i.=.4psu (c) Zonal wind stress c.i.=.01Nm^2 (d) Meridional wind stress c.i.=.01Nm^2

Table 2.1: Experiments: piCtrl- piControl experiment; Ctrl - Control; Abrt - $4xCO_2$ abrupt increase experimet

Experiment name	Initial.	Wind forcing	Salinity forcing	Temp. forcing
Control	CESM piCtrl	CESM piCtrl	CESM piCtrl	CESM piCtrl
Abrupt Changed (AC)	POP Ctrl	CESM Abrt	CESM Abrt	CESM Abrt
Wind Unchanged (WU)	POP Ctrl	CESM piCtrl	CESM Abrt	CESM Abrt
Wind-Salinity - Unchanged (WSU)	POP Ctrl	CESM piCtrl	CESM piCtrl	CESM Abrt

perturbation (2.6), and a "no-redistribution heat flux" tracer P_{nr} which is forced by the heat flux expression (2.8). The formulation for these tracers are discussed in Section 2.4.

2.4 Advection-Diffusion and Redistribution Effects

The conduct and analysis of the experiments is based in large part on the comparison of the evolution of temperature anomalies with that of passive tracers. The division of temperature anomaly T' (as a function of position (x; y; z) and time t) into components is based on the temperature advection-diffusion equation 2.2, which for generalized velocity v(x; y; z; t) (including a bolus component parameterizing eddy effects) and normalized surface heat flux, Q, can be written as:

$$\frac{\partial T}{\partial t} = Q - \nabla.(vT) \tag{2.2}$$

Note that what we refer to here as the "surface heat flux" is the surface heat flux into seawater; an additional flux Q_I is associated with melting or freezing ice. Given Q_A, the heat flux from the atmosphere, we have $Q = Q_A - Q_I$. For a perturbation experiment, writing variables in terms of an initial equilibrium value and an anomaly (denoted by an overline and prime, respectively), that is, $T = \bar{T} + T'$, the difference between (2.2) for perturbation and equilibrium experiments gives (2.3).

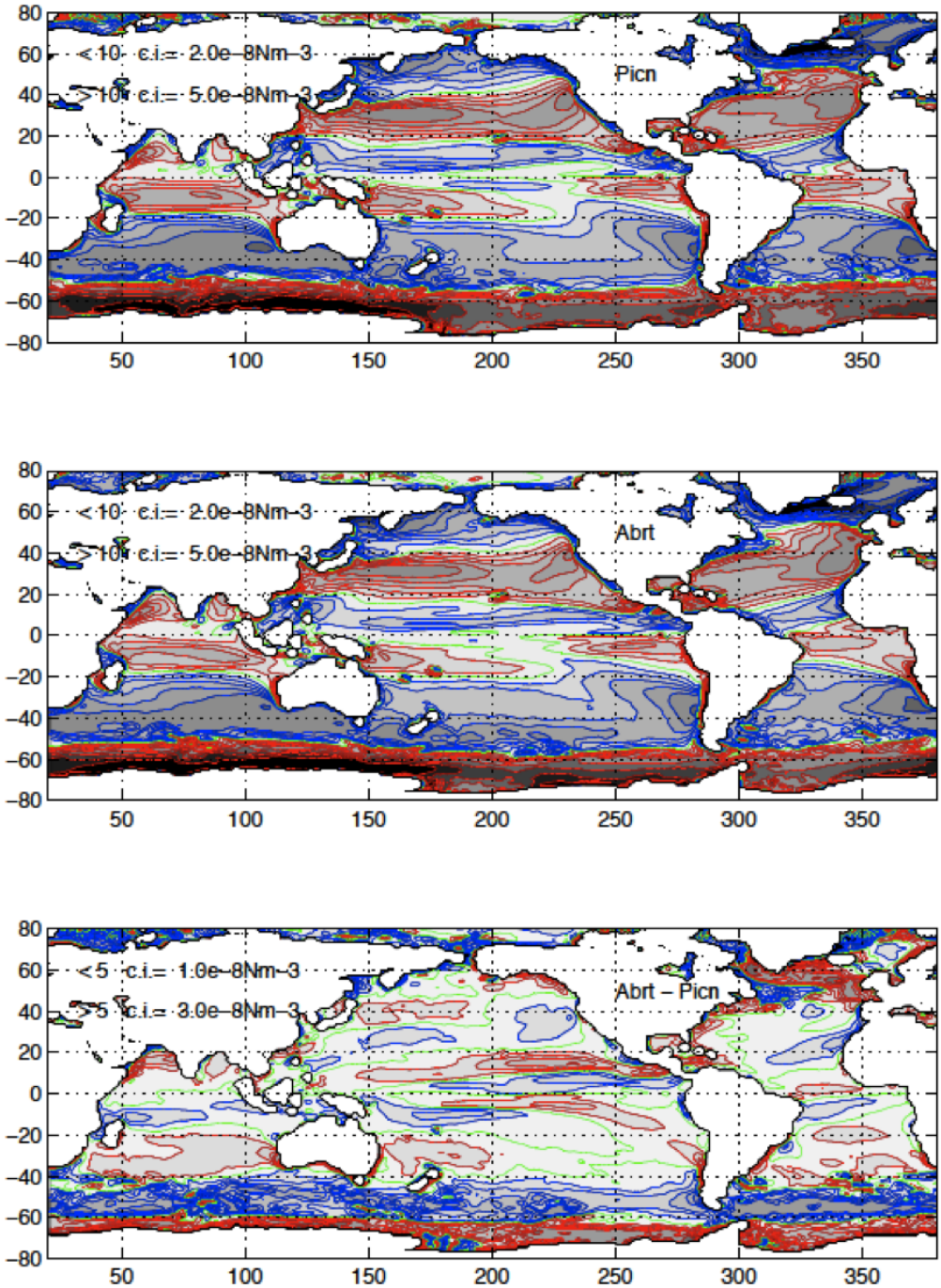

Figure 2.7: Wind stress in the CMIP5 Picontrol and Abrupt $4xCO_2$ increase experiment. Top Panel - Picontrol; Middle panel - Abrupt experiment; Bottom panel - Abrupt minus Picontrol

$$\frac{\partial T'}{\partial t} = Q' - \nabla.(vT' + v'\bar{T}) \tag{2.3}$$

Redistribution heat flux tracer, P_r

As in Banks and Gregory (2006) and Xie and Vallis. (2012), the perturbation temperature anomaly is further partitioned between a passive-advective component P and a redistributive component T'_r, that is, $T' = T'_r + P$. Both P and T'_r are zero at the beginning of the perturbation experiment. The passive component is defined as a tracer which is forced by the same surface flux anomaly, Q' and advected by the same velocity field as T' in (2.3).

$$\frac{\partial P}{\partial t} = Q' - \nabla.(vP) \tag{2.4}$$

The difference between (2.3) and (2.4) yields an equation for the evolution of T'_r:

$$\frac{\partial T'_r}{\partial t} = \nabla.(v'\bar{T} + vT'_r) \tag{2.5}$$

The redistributive temperature anomaly, T'_r, is due to ocean circulation change v'. The only "forcing" term for T'_r (i.e, a term that can be nonzero even if $T'_r = 0$) is the $v'\bar{T}$ term, which represents advection of the original equilibrium temperature gradients by the perturbation velocity. In that case, the integrals of 2.3, 2.4 and 2.5 give $\int dT'dV = \int PdV$, therefore, $\int dT'_r dV = 0$. Thus redistribution, as defined above, moves heat within the ocean but does not change the total heat content. This conservation implies that redistributive warming in any volume must be compensated by cooling elsewhere.

P and T'_r defined this way can be evaluated in two ways using passive tracers in the perturbation experiment. One way used in Banks and Gregory (2006), is to introduce a passive tracer, P, initialised at zero but forced with the same flux as T', which is the perturbation heat flux anomaly, Q'. The tracer evolution thus follows equation 2.4, T'_r can

thus be evaluated using $T'_r = T' - P$. The other method, used in Xie and Vallis. (2012), is to introduce a tracer, $\bar{P}$, in the perturbation experiment, but initialised at the control equilibrium temperature $\bar{T}$ and forced with equilibrium heat flux, $\bar{Q}$. Since it is introduced in the perturbation experiment, $\bar{P}$ is advected by the perturbation velocity $\bar{v} + v'$, so $\bar{P}$, with time is different from $\bar{T}$ but they both have the same content. T'_r is thus $\bar{P} - \bar{T}$. T'_r evolution thus follows Equation 2.5, so at the initial time, T'_r is zero, T'_r grows due to $v'\bar{T}$. P can also be evaluated from T'_r using T'. Both methods yield the same result for T'_r and P. For our experiment, we use the former method and we refer to P driven by this form and its surface flux as P_r and Q_r respectively (where $Q_r = Q'$), because the surface flux is by definition identical for P_r and T', this tracer cannot tell us how much redistribution alters the heat uptake by the ocean, thus, the subscript r denotes the effect redistribution included in the surface heat flux.

No-Redistribution heat flux tracer, P_{nr}

In order to isolate the perturbation heat flux anomaly originating in the atmosphere due to anthropogenic greenhouse forcing, from that originating in the ocean due to ocean circulation changes, we need a new tracer formulation which excludes the ocean redistributive effect rom the tracer surface flux. The use of restoring boundary conditions allows us to do this. For surface heat flux, the surface temperature $T_s(x, y, t)$ is restored to a target distribution $T_\star(x, y, t)$ on a time scale controlled by a parameter as in Equation 2.1. This forcing allows both heat flux and (to a smaller extent) temperature at the surface to change in response to ocean circulation changes. In the perturbation experiment, using the same notation as above, we can write the perturbation heat flux anomaly as equation 2.6.

$$Q' = \alpha(T'_\star - T'_s) \tag{2.6}$$

$T'_\star$ to a large extent captures the atmospheric heat flux anomaly into the ocean, due to GHG changes. However, Q' depends on $T'_\star$ and also on T'_s, which includes both the

atmospheric and oceanic perturbation influence, that is, P_{r_s} and T_{r_s}, in the tracer notation used earlier. In these terms we can rewrite the tracer flux, Q_r as:

$$Q_r = Q' = \alpha(T'_\star - T'_{r_s} - P_{r_s}) \tag{2.7}$$

Hence, (2.7) is equivalent to restoring the surface tracer value, P_{r_s}, to $T'_\star - T'_{r_s}$, rather than $T'_\star$. In order to force a tracer only with the atmospheric forcing anomaly and exclude oceanic influence, T_{r_s} must be zero. This will yield a different tracer flux and tracer, denoted as Q_{nr} and P_{nr}, the subscript "nr" denotes the non-redistributive effect in the tracer flux:

$$Q_{nr} = \alpha(T'_\star - P_{nr_s}) \tag{2.8}$$

The redistributive heat flux, which quantifies how much the surface heat flux is changed by redistribution temperature anomaly, T'_{r_s} altering the surface temperature, is thus Q_r - Q_{nr}, that is:

$$Q_r - Q_{nr} = \alpha(-T'_{r_s} + P_{nr_s} - P_{r_s}) \tag{2.9}$$

Using $P_r = T' - T'_r$

$$Q_r - Q_{nr} = \alpha(P_{nr_s} - T'_s) \tag{2.10}$$

Hence, the redistributive heat flux depends on the difference between P_{nr_s} and T'_s. Since P_{nr_s} and T'_s in (2.1) and (2.8), are restored to the same $T'_\star$, they both approach the same value eventually, but at a different rate because of the T'_{rs} in T'_s. A negative T'_{rs} means positive redistributive heat input and a longer time to equilibrium depending on how negative T'_{rs}, a positive T'_{r_s}, means negative redistributive heat input and a faster approach to equilibirum.

The net redistributive temperature anomaly $T'_{r_{net}}$, in the whole ocean column is thus $T' - P_{nr}$. Unlike T'_r, the $T'_{r_{net}}$ content, $\int T_{r_{net}} dV$ is not zero, it represents the total heat

content and distribution changes occuring as a result of ocean circulation changing. Since it is forced by the redistributive heat flux, it is positive when T_{rs} is negative and vice versa. Note that this content change can occur through any atmospheric perturbation causing ocean circulation changes, not necessarily through green house forcing (For example: surface wind changes)

2.5 Heat transports

In each of these experiments, the model output of advective, vertical diffusion and horizontal diffusion heat divergence terms will used to get to compare the relative importance of these heat exchange mechanisms for the tracers and temperature anomaly. The advective heat and tracer transport output from the model is also computed across basin boundaries in the control and perturbation experiment, in order to quantify passive and redistributive heat exchange among the basins.

Chapter 3: Passive Advection - diffusion of surface heat anomalies

3.1 Introduction

The analysis in this chapter looks at ocean heat uptake under passive advection - diffusion component. Ocean transport mechanisms, include advection, horizontal and vertical diffusion and convection, these mechanisms are have different time scales associated with them and are more important in different regions and different latitudes of the ocean. The strength and depth of Ocean circulation advecting tracers also vary at different latitudes and depths. We connect tracer propagation path to ocean transport mechanisms in these regions and the time scales associated with them.

The passive tracer P_r is used for the analysis here, because P_r includes the advection-diffusion of the total heat uptake by the ocean, hence, it gives larger anomalies and gradient compared to the P_{nr}, the uptake pattern or propagation path for both tracers are, however, similar. Among the three forced experiments, the heat uptake in the WU experiment is the greatest, hence P_r in the WU experiment is used for the analysis here. P_r's propagation pattern is similar in all three experiments. The comparisons between temperature anomaly T', and tracers P_r and P_{nr} in the WU experiment are discussed in the Chapter 4, and the differences in their uptake in the three perturbed experiments are discussed in Chapter 5. P_r is further partitioned into two; P_{rN} and P_{rS}; P_{rN} is forced in the northern hemisphere alone and P_{rS} is forced only in the southern hemisphere. This is done to know the origin of the tracers in a location. It also shows propagation along the surface more clearly.

3.2 Meridional Propagation

Atmospheric surface forcings; wind and temperature are largely zonally symmetric, hence, zonally averaged tracer values gives a quick overview of tracer advection in all basins. Tracer advection at the same latitude band, have common features in all the basins. The meridional - depth gradient in tracer propagation, that is, high latitude deep penetrating regions and low latitude shallow penetrating regions (Figure 3.1), suggest the shallow Ekman overturning cells, as well as the deep overturning circulation play important roles in passive heat uptake. Ekman pumping causes upwelling at equator and downwelling at the poleward edges of the subtropical cells and subpolar cell. The shallow regions transport the tracer only as deep as 500m, by the end of the century long run, and in the deep regions, tracers penetrate as deep as 1500m in the Southern ocean and as deep as 2500m in the Northern Atlantic.

In the southern hemisphere, evidence of the shallow and deep circulation path of propagation can be seen in the two tongues of tracer penetration forming a bowl shaped meridional-depth profile around 40^oS in Figure 3.1. A deeper southernmost vertical tongue at 50^oS and a shallow equatorward tongue around 30^oS. Comparing with the overturning circulation in each basin and globally, around this latitude (compare Figure 3.2), shows the anomaly tongue turned equatorward is due to the shallow downwelling branch of the subtropical cell, around 30^oS, which returns equatorward around 250 - 500m depth and upwells at the equator, in all the basins. The subtropical cell and the associated downwelling branch is less prominent in the Indian and Atlantic basins, this explains why the bowl shaped tracer penetration is narrower in both basins than in the Pacific. The southernmost vertical tongue coincides with the location of the downwelling branch of the deep Southern ocean circulation (Deacon cell), tracer penetration reduces poleward of the maximum due to the upwelling south of 60^oS. The vertical tongue does not reach as deep as the downwelling branch here, even after 100 years.

A somewhat similar pattern is seen in the Northern hemisphere in the Atlantic and Pacific, but more prominent in the Atlantic than in the Pacific. At 30^oN, the downwelling

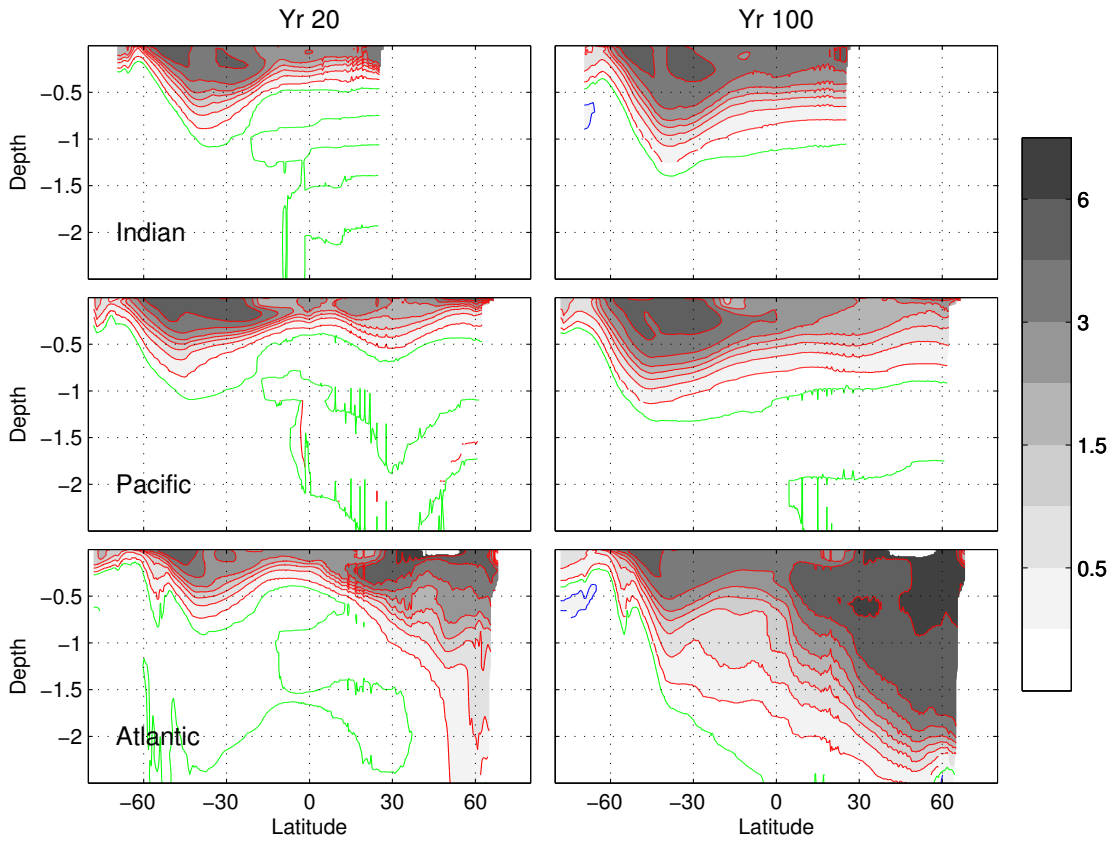

Figure 3.1: Zonal averaged tracer P_r in the ocean basins. Top panel: Indian; Middle panel: Pacific; Bottom panel: Atlantic. Left column: Year 20; Right column: Year 100. Contours: Red=positive, blue=negative. Units: Deg^oC.

tongue returning equatorward at the northern edge of the sutropical cell is also present in the Pacific and Atlantic. In the Pacific, this northern downwelling region forms a small bowl shaped profile of heat penetration around this latitude, but it is much smaller than that of the southern hemisphere. There is also no deep vertical tongue in the Northern Pacific, hence the tracer only goes as deep as the depth of the subtropical gyre here. In the northern Atlantic, the subtropical tracer tongue turned equatorward is much more prominent than its southern conterpart. A northernmost vertical tongue poleward of 50^oN, comparable to the vertical tongue in the Southern ocean is seen here, but it goes much deeper than that in the southern hemisphere. Comparing also with the circulation in this region (Figure 3.2), the inflow branch of the AMOC is connected through the subtropical

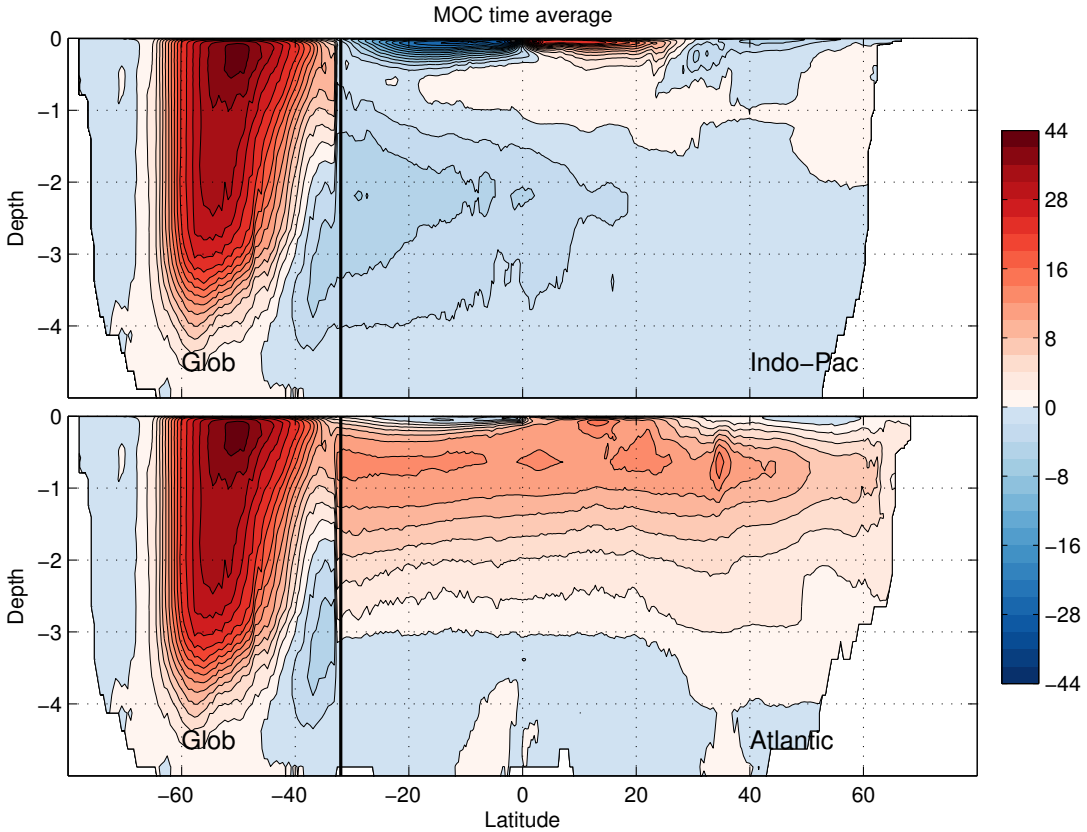

Figure 3.2: WU experiment's meridional overturning streamfunction in the basins, for the 100 year time average. Top panel: Indo-Pacific; Bottom panel: Atlantic. Contours: Red - positive, blue - negative. c.i.=2 Sv.

cell and its downwelling branch in the northern hemisphere. Hence, some of the tracer sinking through the subtropical cell is transported northward into the deep sinking region of AMOC where it is further transported into the deep ocean, a considerable amount also recirculates within the gyre returning equatorward.

3.3 Regional Propagation Mechanisms and Timescales

This section looks at regional propagation of the tracers in closer detail. Tracer propagation along horizontal and longitudinal and isopycnal cross sections are examined. Propagation

on horizontal surfaces show zonal propagation along gyres. Zonal propagation is important because it shows known circulation properties, for example, it has been shown that the AMOC flows along western boundary current. Kostov Y. and Marshall (2014) suggest this as evidence, among others, that the AMOC depth and strength among models determines ocean heat uptake. Tracers P_{r_N} and P_{r_S} are used where necessary to describe surface propagation path of the tracers. P_{r_S}, shows propagation path at the surface in the northern hemisphere, because it is forced only at the southern hemisphere surface, similarly, P_{r_N} shows surface propagation in the Southern hemisphere. The sum of the two tracers, P_r, shows propagation in the deep layers more clearly. Propagation on isopycnal surfaces also allows us to verify the conceptual model of Church et al. (1991), in which heat uptake is modelled as the passive advection of the temperature anomalies along isopycnals outcropping within the subtropical gyre.

The relative strength of heat or tracer divergence components in these regions, at different depth ranges and latitude bands are also analyzed to verify dominant heat uptake mechanisms. Latitudes 40^oS and 40^oN are chosen as the boundaries of these latitude bands because it is around the edge of the subtropical cell in the ocean basins, and hence marks the divide between the shallow cell meridional flow and the deep circulation in the Southern Ocean and the Atlantic, as well as the divide between the short timescale propagation and the long time scale propagation. The model output of the divergence terms from the heat equation at each grid point is used to compute these terms. The advective convergence term includes the horizontal and vertical advection components, while the vertical diffusive term includes the vertical diffusion along temperature gradient and convective term, which is parametrized using strong diffusion in these experiments.

3.3.1 North Pacific

Horizontal and Isopycnal Propagation

The horizontal cross sections at different depths and time in the northern Pacific are shown Figure 3.3. At the surface, the tracer P_{r_S} propagates from the southern hemisphere, northwestward between equator and 30^oN along the anticyclonic subtropical gyre and northeastward between 30^oN and 60^oN along the cyclonic subpolar gyre. (Figure 3.3, top panel)

At 250 and 500m depths, the tracer sum, P_r (Figure 3.3, bottom panel), sinks to these depths, only from the western boundary around 30^oN. This sinking reaches only as deep as 500m depth (compare Meridional propagation Figure 3.1). The sinking tracer then propagates eastward away from western boundary. The western boundary sinking appears quickly at the 250m depth within two years, while it takes about ten years for the tracer to reach the 500m depth. P_r does not reach the 1000m depth even after 100 years of the run.

The eastward propagation of the sinking on the western boundary at 30^oN seem curious because the propagation on the isopycnal surface outcropping within the subtropical gyre for which $\sigma = 24$, shows no propagation from the western boundary at this latitude, rather, tracer propagation starts poleward of 30^oN around 40^oN, in the middle of the basin and the propagates southwestward along the eastern boundary, around the 30^oN sinking region (Figure 3.4). On the western boundary up to the middle of the basin, there seem to be sinking, because the temperature continue to cool here. The same is true for the deeper density surfaces; $\sigma = 24.5$ and 25. This isopycnal propagation is consistent with propagation along the subtropical gyre, with sinking in the middle of the gyre. The eastward propagation on the horizontal surface at 250m and 500m depths can be explained by the sloping isopycnal surface, which is deeper on the western boundary than on the eastern boundary. Tracer sinking in the middle of the gyre at 30^oN or diffusing across the slope of an isopycnal surface, will reach a given depth first on the western boundary, and will appear later on the eastern boundary because the isopycnal layer is shallower there, hence it appears and like an eastward propagation of the tracer at this sinking latitude. Propagation is slower

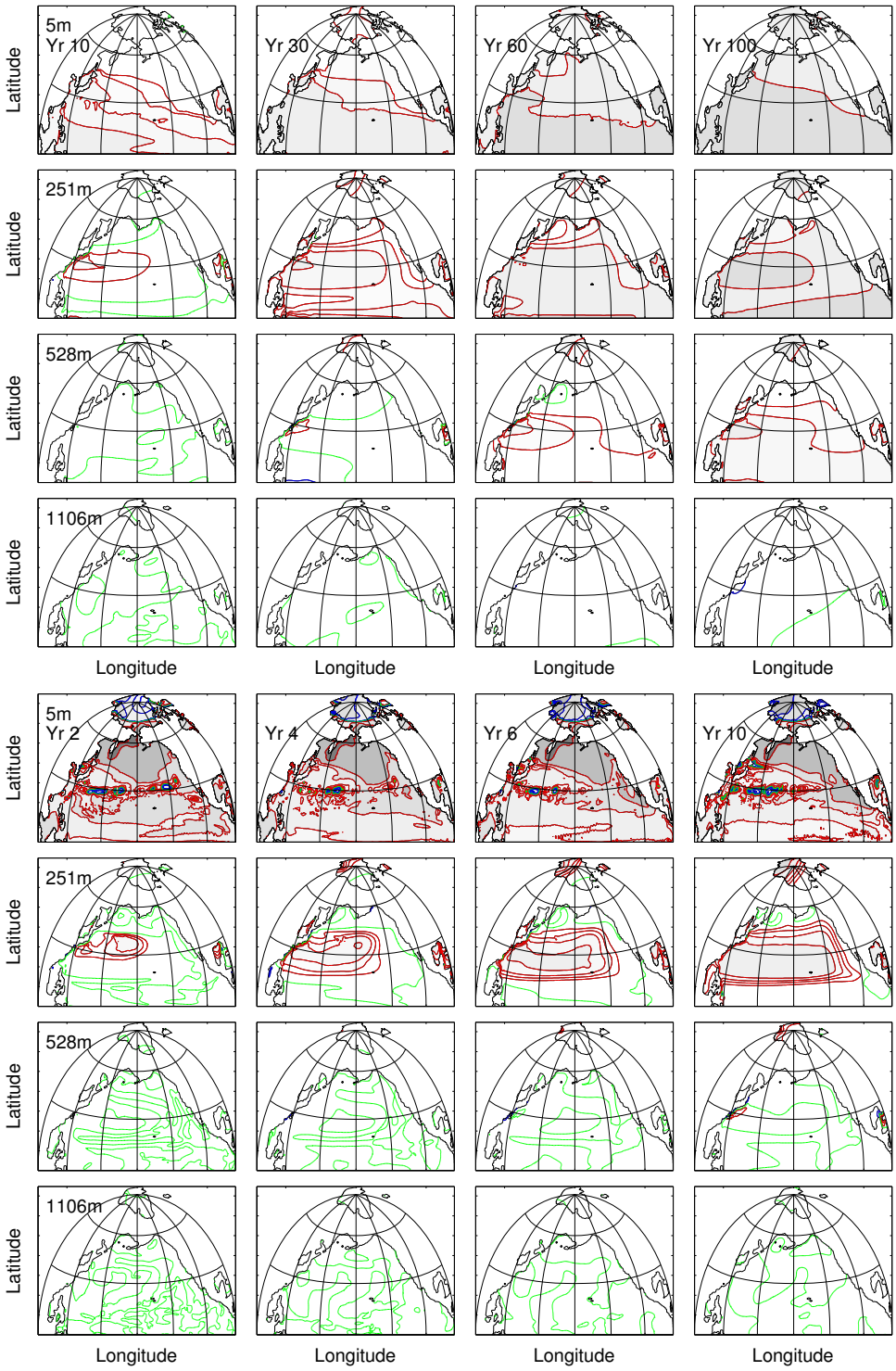

Figure 3.3: Tracer P_r on horizontal surface at different depths and times in the northern Pacific ocean. Top panel: P_{r_S}, forced only in the southern hemisphere surface; Bottom panel: Tracer sum $P_r = P_{r_S} + P_{r_N}$; 30° grid lines, Contours: Red-positive, blue-negative. c.i.= $[.1\ .25\ .5\ 1\ 2\ 4\ 8\ 12\ 16]^oC$.

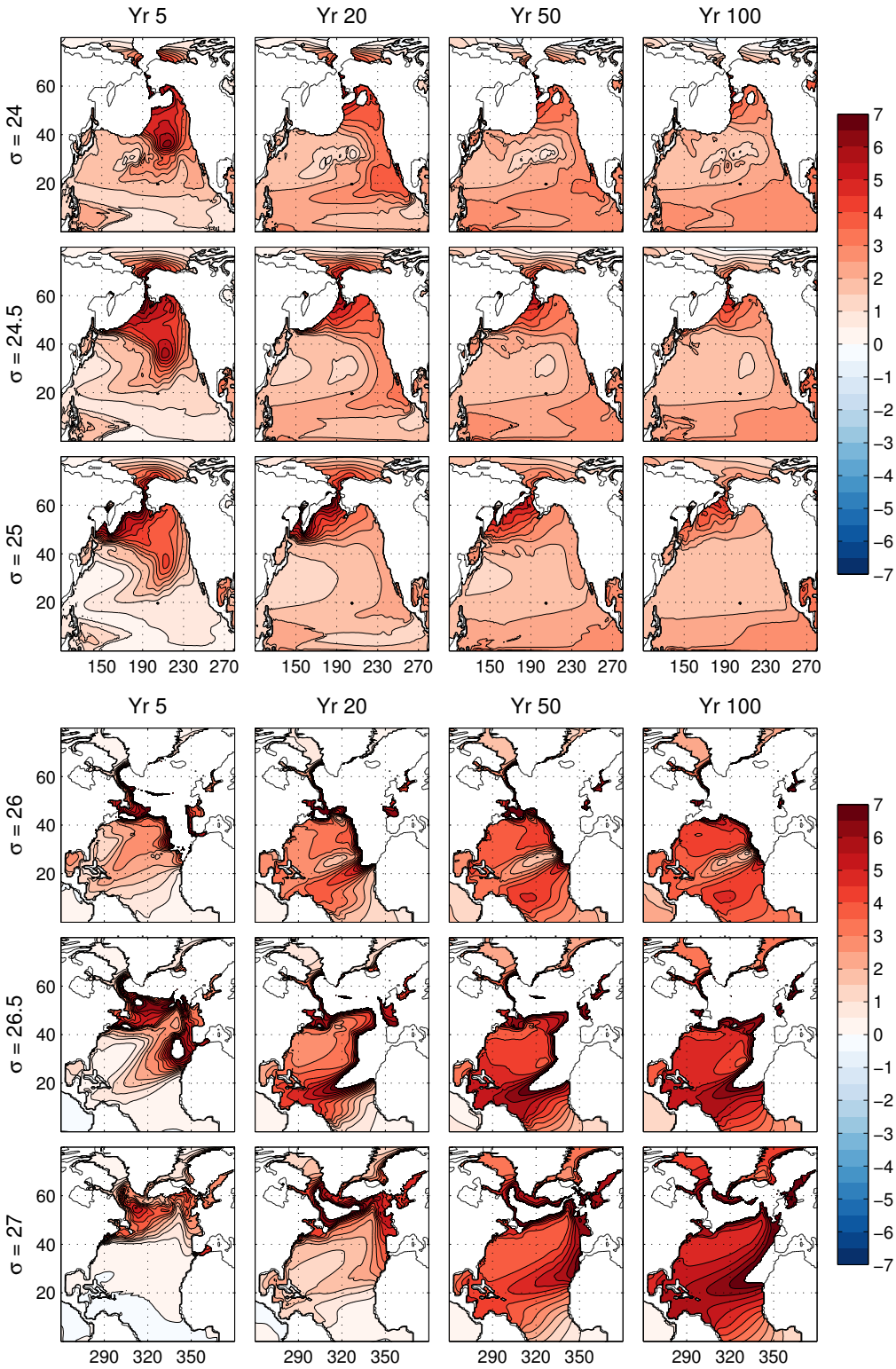

Figure 3.4: Tracer P_r on equal density surfaces, in the northern hemisphere. Top panel - Pacific, Bottom panel - Atlantic, c.i.=0.5^oC

on the isopycnal outcropping north of this latitude, tracer is still concentraed at the edge of the gyre even after 100 years because this isopyncal surface does not outcropp within the subtropical cell.

Transport Mechanisms

Figure 3.5, shows that the advective and vertical heat transport terms are dominant in the $40^oN - 90^oN$ latitude band, in the top 250m, while vertical and horizontal diffusion terms are more important in the 250m - 500m depth range, and very little propagation below 500m in the century long run in this latitude range. Vertical diffusion warms the top 250m while advection cools it. The $40^oN - 90^oN$ is outside the subtropical gyre and in the weak Pacific subpolar gyre hence, there is little isopycnal propagation. Tracer diffuses down from the surface in this region (Figure 3.6, left column), and some of it is propagated southward along the edge of the subtropical gyre as seen the isopycnal propagation described above, but most of the tracer remains in the subpolar region, where it diffuses across the isopycnal close to the surface

Below 250m, Vertical diffusion term warms the region after 20 years, largely from tracer diffusing across isopycnals. Horizontal diffusion cools this region, because it spreads out the tracer horizontally away from the vertical diffusion region. This explains the slower vertical propagation seen in the year 50 - 20 and 100 -50 time difference in Figure 3.6.

In the 40^oN to the equator (tropical) region, tracer propagates quickly horizontally around the subtropical gyre along isopycnals and through downwelling in the middle of the gyre, within the first 20 years. The tracer fills an average depth range 0-200m, (deepest at 30^oN and shallower away from this latitude) within the first 5 years, within 5 to 20 years, the top 200m cools (Figure 3.6), and warms the 250m - 500m depths. Advection is more dominant and warms 250m - 500m region (Figure 3.5), due to the equatorward advection along the subtropical gyre, of tracers sinking at 30^oN and 30^oS. Tracer propagates quickly down to the depth of isopycnal outcropping in the sutropical gyre. Below 500m, however, advection becomes smaller again and vertical diffusion becomes dominant and warms this

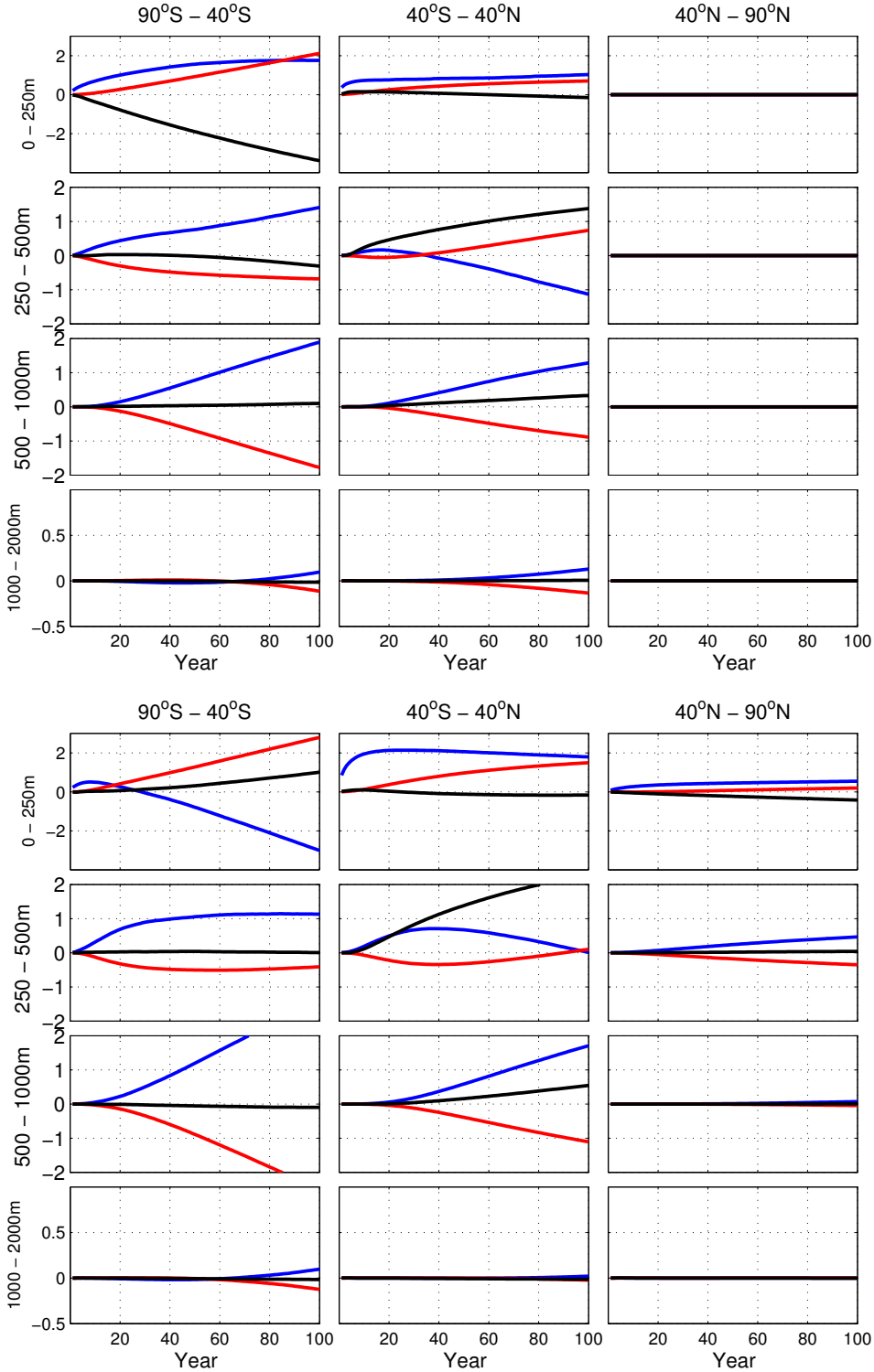

Figure 3.5: Volume integrated Heat convergence components in $10^9 degs^{-1}$, integrated over latitude bands and depth ranges. Vertical diffusion-Blue line; Horizontal diffusion-Red line; Advection-black line. Indian-top panel; Pacific-bottom panel

region because it diffuses the tracer across the outcropping isopycnal layers, and propagation becomes slower below these depth. The year 50 - 20 and 100 -50 time difference in Figure 3.6, shows the tracer diffuses down to an average depth of 500m, in the 20 - 50 year time period, within the following 50 years it diffuses to an average depth of 700m.

3.3.2 North Atlantic

Horizontal and Isopycnal propagation

The Atlantic surface propagation is also along the subtropical and subpolar gyres like in the northern Pacific (Figure 3.7). Below the surface, the Northern Atlantic has three sources of sinking, unlike in the northern Pacific. These sinking regions occur around 60^oN around the Greenland coast, around 40^oN on the eastern boundary from the mediteranean, the western boundary sinking around 30^oN is not so clear here, probably overshadowed by the other sinking sources. The other two sources are faster and stronger than the subtropical cell sinking at 30^oN. However, P_{r_S} propagation shows there is sinking in the middle of the subtropical gyre at least down to 250m (Figure 3.7, top panel). This sinking is clear from P_{r_S} because the tracer reaches the subtropical region before the subpolar region at the surface, because it is propagating from the southern hemisphere, and as a result the sinking in the middle of the subtropical gyre is not overshadowed by the Greenland sinking.

Greenland sinking is faster and deeper than anywhere else in the basin reaching down to 2000m (2000m not shown). This northernmost tracer sinking then follows the cyclonic subpolar gyre flow at all depths. The mediterranean outflow at 40^oN is only evident at 500m, this is because the subolar gyre cyclonic flow is eastward, against the Mediterranean outflow sinking, hence, the tracer sinking from the Mediteranean outflow is not able to spread out horizontally, it is pushed even deeper down to 500m where this eastward flow is not so strong.

At 500m depth, the tracer first appears (within the first 10years) in the north (60^oN) around Greenland coast and Iceland and also from the mediterranean outflow around 40^oN (Figure ptrcnatlprop, bottom). The mediterranean outflow is stronger at this depth is able

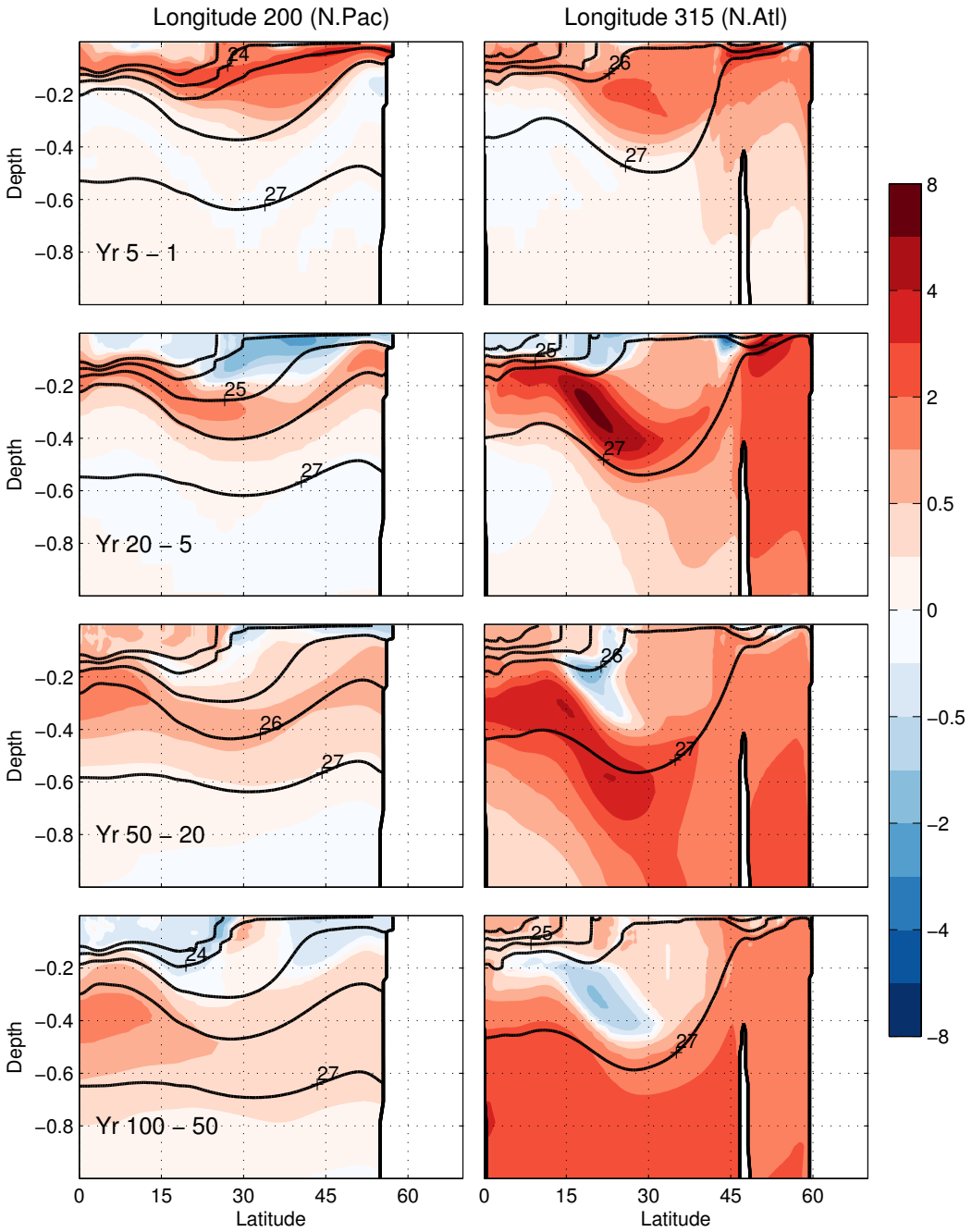

Figure 3.6: Passive Tracer P_r and Potential density cross sections in the northern Pacific and Atlantic, at longitudes 200 and 315. Tracer values (Shaded contours; Red=positive, blue=negative. c.i.= [0.1 0.5 1 2 3 4 5]^oC). Potential density (line contours c.i.= 2).

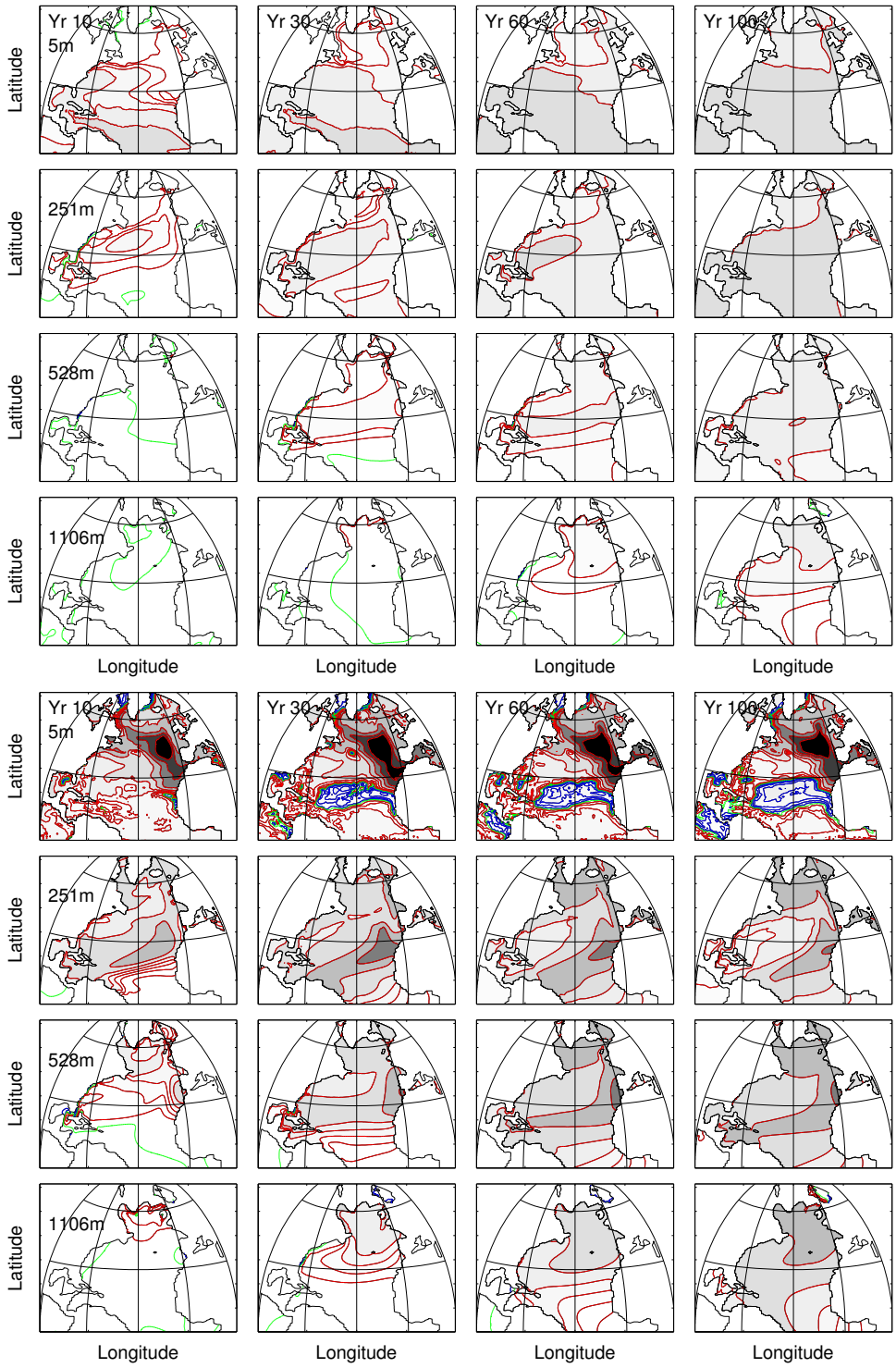

Figure 3.7: Horizontal propagation of P_r at different depths and time, in the northern Atlantic ocean. Top panel: P_{r_S}, forced at the surface in southern hemisphere; Bottom Panel: $P_r = P_{r_N} + P_{r_S}$; 30° grid lines, Contours- Red-positive, blue-negative. c.i.= [.1 .25 .5 1 2 4 8 12 16]^oC)

to spread westward at this depth. The northern tracer anomalies follow the cyclonic supolar gyre flow, which connects to the mediterranean outflow in the northeastern flowing branch around at 40^oN and then propagates southwestward around the subtropical gyre towards the equator.

At 1000m, the northernmost sinking region around 60^oN is the only source of tracer anomalies at this depth. Tracer anomalies appear in this region within the first 10 years and first circulates around the subpolar gyre, (Figure 3.7, bottom panel), and propagates southwestward and reaches all the way to the Southern ocean in about 50 years where it spread to other basins. The tracer propagating from the north Atlantic at this depth reaches the southern hemisphere at about the same time the tracer sinking from the surface at this southern latitude (45^oS) (Compare Figure 3.10, top panel). This southward propagating tracer at this depth in largely on the western boundary, especially in the outflow seen at year 50 in the southern hemisphere, but spreads out to the entire basin later by year 100

Transport mechanisms

In the top 250m, in the northern Atlantic ($40^oN - 90^oN$ region), advection and vertical diffusion are important (Figure 3.8). Advection warms this region and vertical diffusion cools it. The time difference along at longitude 315° (Figure 3.6), shows there is little isopycnal propagation in this region, rather there is fast sinking, a uniform band of tracer down to 800m, is seen within the first 20 years, which cools off in the next 30 and 50 years, while the depths below it get warmer. This may explain why vertical diffusion is cooling the top 250m and warming the 250 - 500m depth range, in this region. The vertical diffusion term includes convection, and convection can explain the uniformity of the tracer sinking in top 500m in this region, while horizontal diffusion spreads the tracer away from this region.

In the 250m - 500m depth range at the same latitude band, advection is neglibible. This is not consistent with horizontal propagation of the sinking around the the subpolar gyres at these depths, described in the previous section. A reason for this, might be that advection into and out of the region cancels out each other. It has been discussed earlier that the

main source of tracer in this region is from the Greeland coast, which sinks down to about 2000m within 10 years which quickly propagates southward. The sinking here is not only due to convection but is also advective, which is evident from the AMOC streamlines here (Figure 3.2). Hence, advection removes heat from this region as quickly as it adds it.

Unlike in the other basins, below 500m and down to about 2000m, the advective divergence term becomes dominant, while the diffusive terms are negligible, in the $40^oN - 90^oN$ region, in the Atlantic (Figure 3.8). The only explanation for this is the downwelling branch of the AMOC present here (Compare Figure 3.2), not even convection because the vertical diffusion term is close to zero. The time scale associated with the AMOC transport, however, is surprisingly short, it gets the tracer to the deep high latitude (below 1000m) within 20 years. This short time scale may be aided by convection mixing tracer down quickly to depths where AMOC sinking branch is able to transfer it even deeper. The AMOC deep outflow branch aslo explains the $40^oS{-}40^oN$ advective term being stronger below 1000m after 50 years, thus tracers sinking from the surface reach the deep tropics in about 50 years. This is consistent with the fast horizontal propagation of P_{r_N} seen at 500m and 1000m depths as quickly as 50 years, in the southern hemisphere (Figure 3.7, top panel).

In the $40^oS - 40^oN$ region, Figure 3.6 shows, propagation along isopycnal in top 500m, in the first 20 years and propagation across the isopycnals below 500m, in the next 30 and 50 years. Again this explains why advection is warming the 250 - 500m depth range due to isopycnal propagation around the subtropical gyre, and vertical diffusion warms the 500m - 1000m depth range due to diapycnal diffusion, while horizontal diffusion smooths out the the vertically diffused tracer gradient horizontally. Advection also warms the depth below 500m in this region, because this depth range includes some the deep ouflow branch of the AMOC. Below 1000m, which covers completely the AMOC deep ouflow branch, transport is purely advective, as explained before.

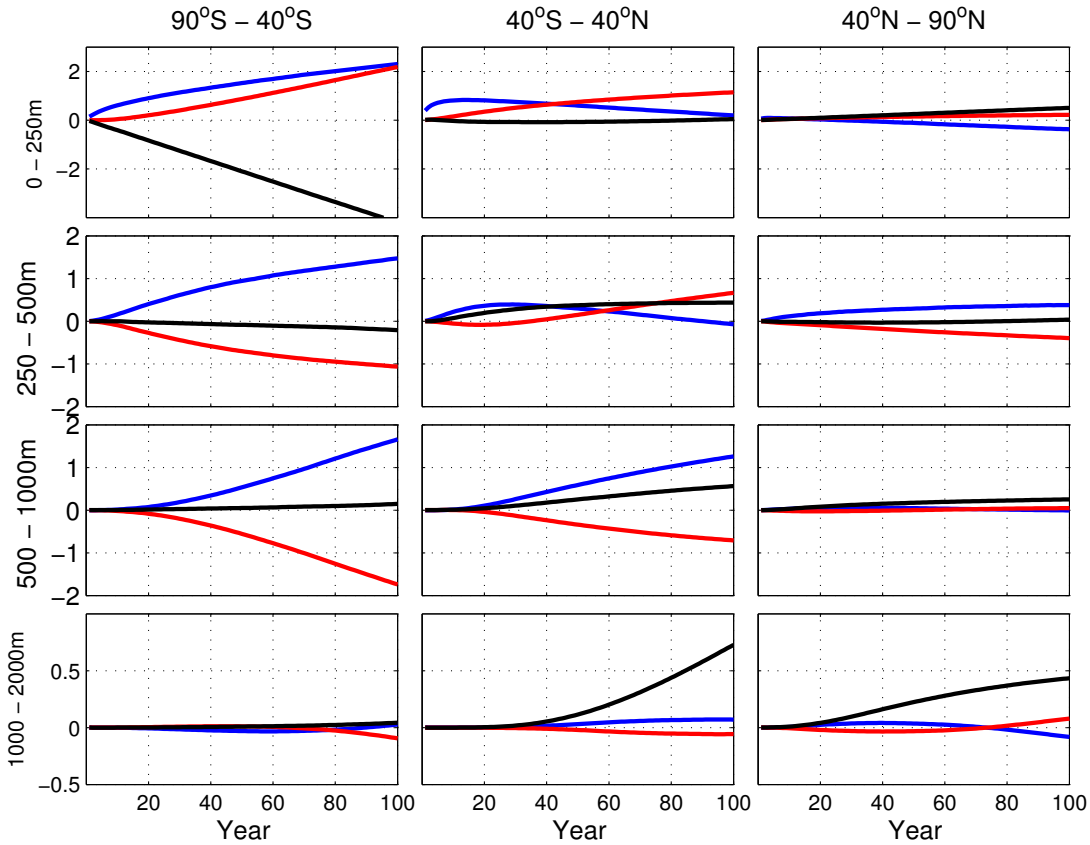

Figure 3.8: Volume integrated heat convergence components in 10^9 $degs^{-1}$, integrated over latitude bands and depth ranges in the Atlantic. Vertical diffusion-Blue line; Horizontal diffusion-Red line; Advection-black line

3.3.3 Southern hemisphere

Horizontal and Isopycnal propagation

In the southern hemisphere, at the surface, P_{r_N} propagation is also along the gyres, southwesterward between 0 to 30^oS along the cyclonic subtropical gyre and southeastward along anticyclonic subpolar gyres between 30^oS to 60^oS (Figures 3.9 and 3.10, top panels). At 250m depths, two sinking regions are observed 30^oS and 50^oS (Compare also Figures 3.9 and 3.10, top and bottom panels). The 30^oS sinking is the sinking at the edge of the subtropical cell and it is seen more clear from the P_{r_N} propagation because the southward propagating tracer reaches 30^oS first. This 30^oS sinking also occurs on the western boundary of the

Pacific and Atlantic basins.

At 500m and 1000m depths, only the southernmost sinking region is seen (Figures 3.9 and 3.10, bottom panels), from where it spreads northward and eastward along the Southern ocean flow. At these depths, this southernmost sinking region is shifted northward, up to 30^oS in the southern Atlantic, at these depths. Comparing Figure 3.1, it is clear that it is not the same as the subtropical cell sinking at the surface. Sinking at this latitude reaches 500m by the 10th year but propagates more slowly below 500 m, it only gets to 1000m by the 80th year. Infact, tracer P_{r_N} sinks in the north Atlantic and propagates southward to reach the 1000m depth in th southern ocean faster than P_{r_S} sinking from the Southern ocean surface reaches 1000m here.

The Southern ocean, show the clearest isopycnal propagation. Propagation on isopycnal surface $\sigma = 25$, which outcrops within the subtropical gyre, shows the fastest propagation, the tracer fills up the gyre within 20 years. Propagation along isopyncals outcropping outside the gyre is much slower. The distribution along the isopycnal $\sigma = 26$ at year 20, outcropping around the southernmost sinking region, shows the tracer is still concentrated at the outcrop latitude, not evenly distributed across the gyre. Propagation on $\sigma = 27$ surface is even slower, it still doesn't cover the subtropical gyre after 100 years (Figure 3.11). Horizontal velocities along this isopycnal suggest another mechanism, a slower one, is responsible for tracer propagation on this isopycnal. These results confirms timescale calculated in the Church et al. (1991) study, where a renewal time of about 20 years for advection within the subtropical cell. (See Section 1.3).

Transport mechanisms

Time differences of the tracer explain the slow isopycnal propagation on $\sigma = 27$ surface, (Figure 3.12). This density layer does not outcrop in subtropical gyre or in the 50^oS sinking region. Tracer sinking at the outcrop latitudes propagates along the outcropping isopycnals within the first 20 years. In the next 30 years and 50 years, the tracer is seen propagating across isopycnals and cooling the top isopycnal layers. On the $\sigma = 27$ surface, propagation

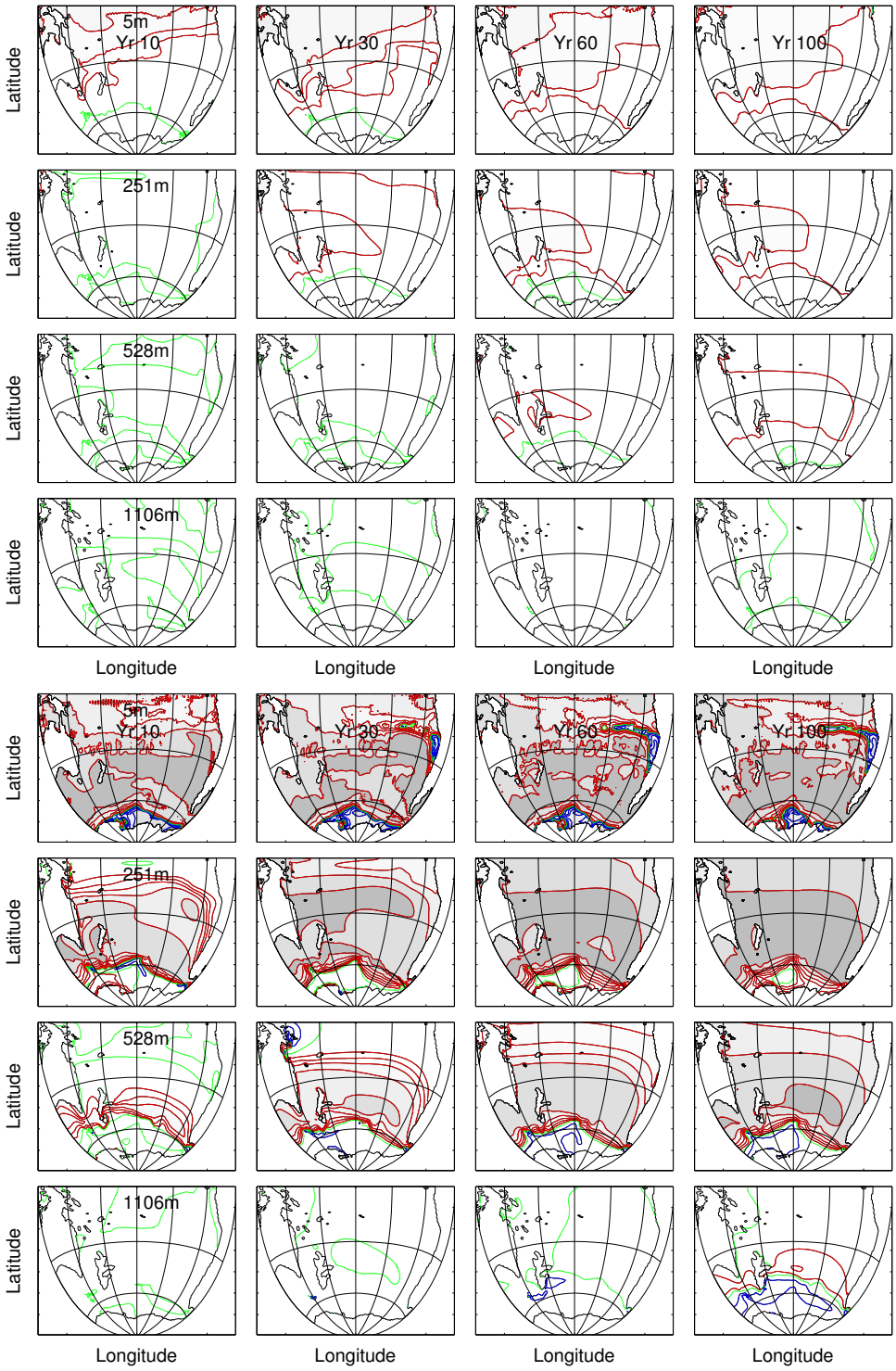

Figure 3.9: Horizontal propagation of P_r at different depths and time in the southern Pacific ocean. Top panel: P_{r_N}, forced at the surface in northern hemisphere; Bottom Panel: Tracer sum, $P_r = P_{r_N} + P_{r_S}$;30° grid lines, Contours: Red-positive, blue-negative. c.i.= [.1 .25 .5 1 2 4 8 12 16]^oC.

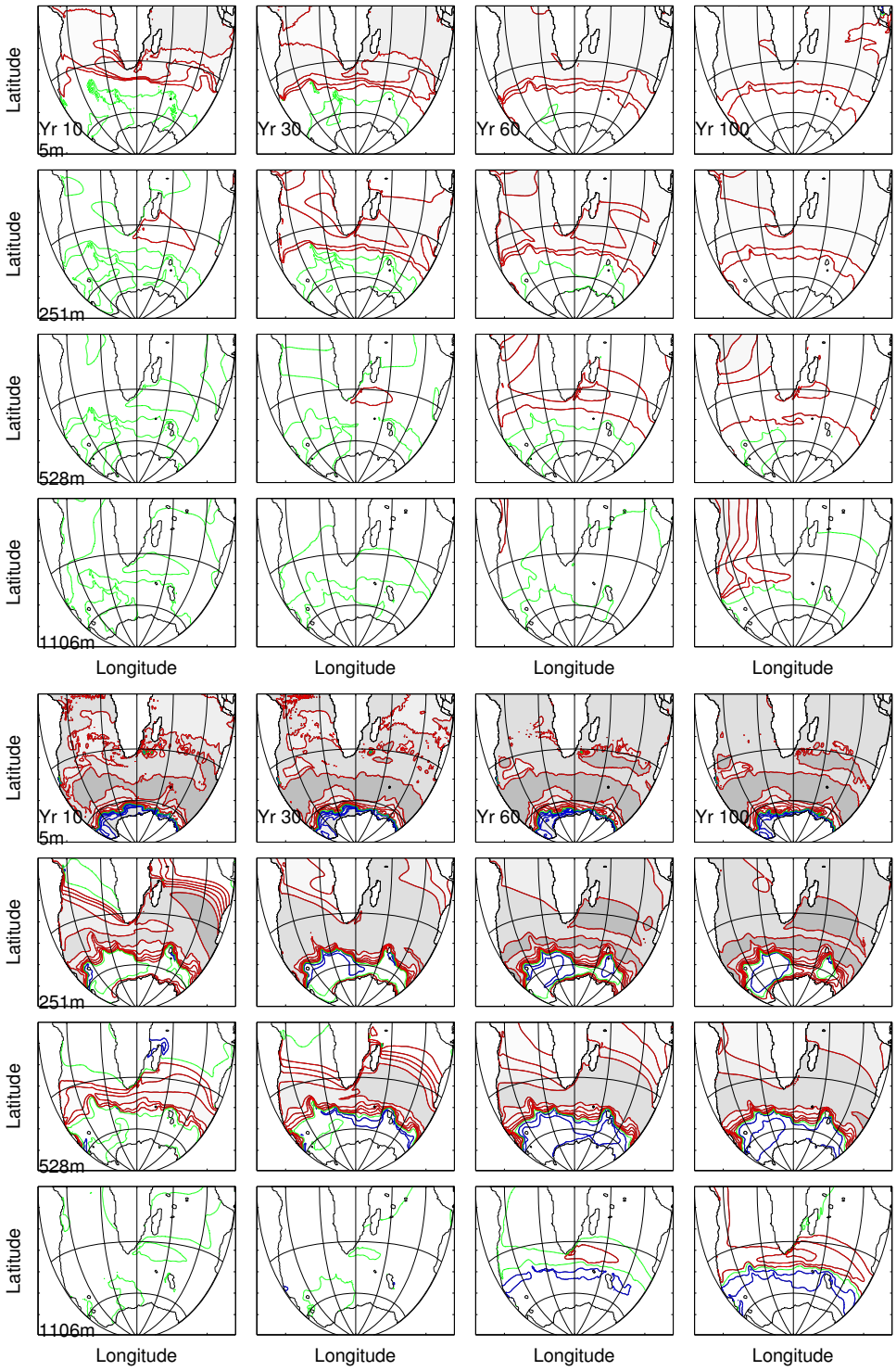

Figure 3.10: Horizontal propagation of P_r at different depths and time, in the Southern Atlantic and Indian oceans. Top panel: P_{r_N}, forced at the surface in northern hemisphere; Bottom Panel: Tracer sum, $P_r = P_{r_N} + P_{r_S}$;30° grid lines; Contours: Red-positive, blue-negative. c.i.= [.1 .25 .5 1 2 4 8 12 16]^oC.

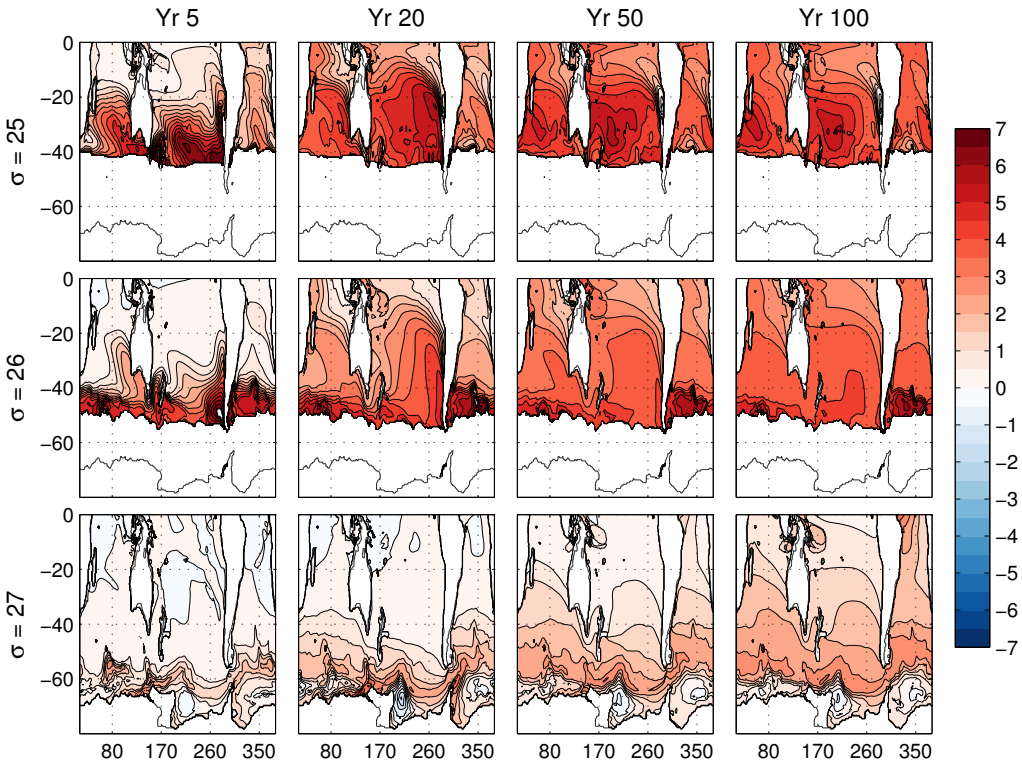

Figure 3.11: Tracer P_r on equal density surfaces, in the southern hemisphere. c.i.=0.5^oC.

only occurs by vertical diffusion across the isopycnal layer, hence tracer propagation along this isopycnal is very slow.

Given the slow timescale, it is not surprising then that vertical and horizontal diffusion are more important below 250m in the Southern ocean ($40^oS - 90^oS$) in all the basins (Figures 3.5 and 3.8, first columns). These diffusion terms by themselves are stronger than at other latitude bands in the ocean, even though they almost cancel out because they are opposite in sign. Tracer diffusing vertically across outcropping isopycnal warm the depths below 250m, while horizontal diffusion cools it, however, the vertical diffusive term is larger than the horizontal diffusive term, so that there is a net warming of the deep ocean. Horizontal diffusion cooling these depths is expected because isopycnals are sloped across the latitudes here, hence heat diffusing across isopycnals have meridional gradient, which horizontal diffusion smooths out. The result of horizontal diffusion smoothing out

meridional gradient is evident in the smaller meridional gradient at year 100 compared to year 20 in Figure 3.1.

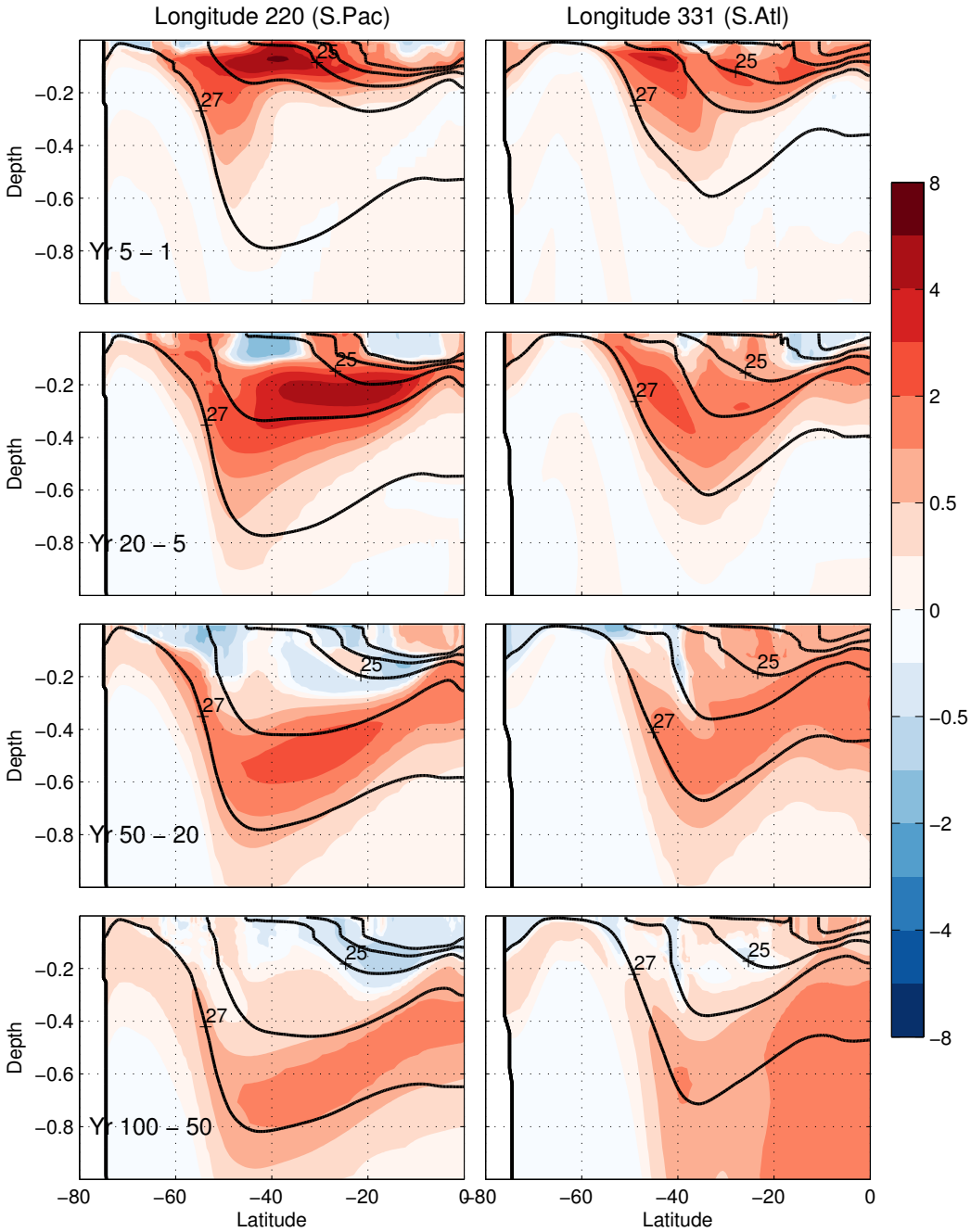

Figure 3.12: Passive Tracer P_r and Potential density cross sections in the Southern Pacific and Atlantic, at longitudes 200° and 331°. Tracer values (Shaded contours; Red=positive, blue=negative. c.i.= [0.1 0.5 1 2 3 4 5]^oC). Potential density (line contours c.i.= 2).

Chapter 4: Passive and Active Ocean Heat Uptake

4.1 Introduction

Ocean heat uptake includes the effects of redistribution of the pre-existing or reservoir ocean heat content due to circulation changes. As discussed in Section 1.3, previous studies have shown that changes in reservoir temperature distribution change the transient response of ocean and enhance the uptake surface heat flux anomalies from the atmosphere. The additional heat uptake resulting from changes in ocean's reservoir surface temperature, also changes the pattern of ocean's uptake of surface heat flux anomalies (Winton et al., 2012, 2010). This additional heat uptake can be referred to as the redistributive component of ocean heat uptake, while the passive component is the uptake of radiatively forced atmospheric surface heat flux anomalies by the Ocean. The passive uptake would be the heat uptake one would expect if ocean circulation was not allowed to change in response to atmopsheric heat flux anomalies such as in Winton et al. (2012).

Redistributive uptake on the other hand can occur, even when there are no heat flux anomalies in the atmosphere, for example, changes in surface wind or freshwater forcing change ocean circulation strength and as a result could increase or reduce heat flux into the ocean. When it occurs as a result surface heat flux anomalies, redistributive heat uptake can be viewed as a response to the passive component forcing. This is analogous to treatment of ocean heat uptake as forcing rather than a feedback in the climate transient response by Winton et al. (2012). The redistributive response to passive uptake changes the efficacy of the heat uptake among the models

Redistributive effects are studied by comparing the two tracers, P_{nr} and P_r, to the actual temperature anomaly, T' and their surface fluxes, Q_{nr} which excludes redistributive heat flux and Q_r which is the same surface flux for T' and includes redistributive heat flux.

The tracer formulations have been discussed in Section 2.4, while their propagation path and passive advection of surface heat anomalies have been discussed in Chapter 3, here, total ocean heat uptake including redistributive effects will be analysed. Because it has the largest redistributive heat input among the three forced experiments, the WU experiment, with perturbations only to surface salinity and temperature, is used to show redistributive effects. This experiment isolates the effect of thermohaline forcing peruturbation on deep circulation from wind driven shallow and deep circulation changes.

Effects of redistribution include changing geographical distribution of existing ocean heat content and the resulting change amount of ocean heat uptake. The geographical effect of redistribution have been shown in the study of Banks and Gregory (2006) and Xie and Vallis. (2012), hence it is not the focus here, rather, the influence of reservoir heat content redistribution on the net ocean heat uptake will discussed. The evolution and distribution of these heat uptake components in the basins are different because of the different circulation depth and strength within the basins, this, as well as, the influence of redistribution on the rate of global warming will be discussed in the following sections.

4.2 Temperature distribution

Over the century of the perturbation experiment, the temperature anomaly T' and tracers, P_r and P_{nr} fill roughly the top kilometer of all the ocean basins (Figure 4.1). As in observation and couple model, P_{nr}, P_r and T' reach deeper in the Atlantic than in other basins. The distribution in latitude and depth of the two passive tracers, P_r and P_{nr}, as discussed in chapter 3, have similar features to each other because they are advected by the same velocity field. However, the magnitudes are quite different in the high latitudes, especially in the North Atlantic, where P_r is much bigger than P_{nr}. The difference in P_{nr} and P_r content is due to redistributive effect on surface heat flux.

The passive tracer distributions are noticeablly different from the T' field in all the basins. (Figure 4.1). Though T' and P_r content are the same, their distributions are quite

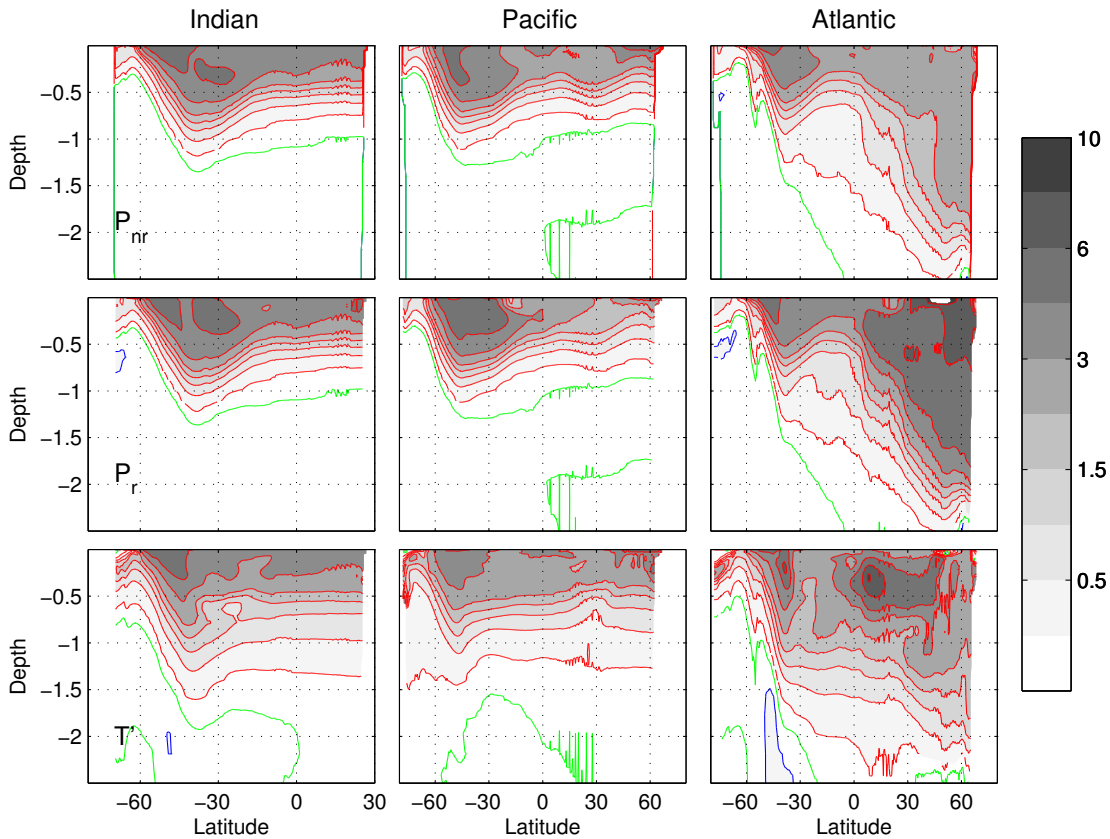

Figure 4.1: Meridional distribution of tracers, P_{nr} and P_r and temperature anomaly, T' among the bains. Basin zonal averages against depth of Tracers P_{nr}, *top row* and P_r, *middle row* and Temperature anomaly T', *bottom row*. Units: Deg^oC

different. One main difference between the T' and P_r field is the tropical deep warming, below 700m, in all the basins. Geographical redistributive temperature anomaly, $T'_r = T' - P_r$, warms the tropical deep layers (below 700m) and cools the Northern Atlantic and Southern ocean high latitudes (Figure 4.2), as a result, smooths out meridional - depth gradient of T' compared to that of the tracers. As suggested by Xie and Vallis. (2012), the difference in the content of P_r and P_{nr} occurs at high latitude regions of deep uptake (Figure 4.1), where redistribution temperature anomaly, T'_r, cools the surface and as a result, increases surface heat flux into the ocean. The overall redistributive effect is combination of the geographical and surface flux effects. Hence, the net redistributive temperature

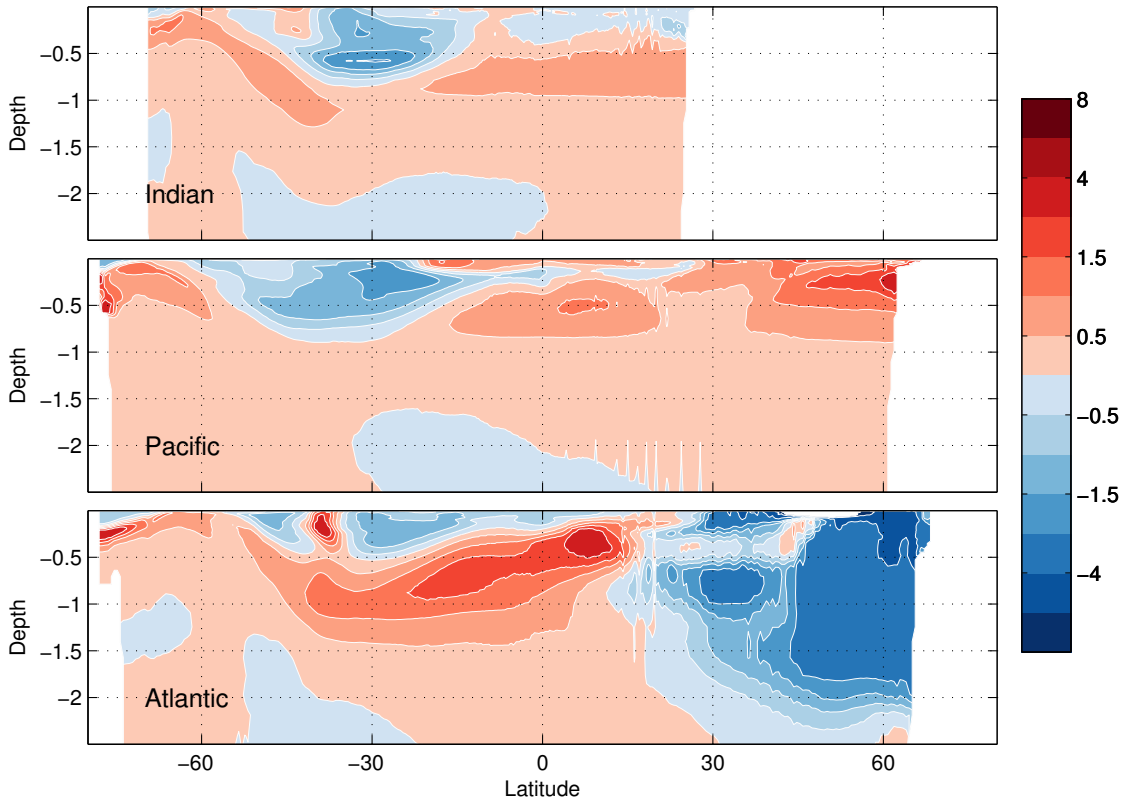

Figure 4.2: Basin zonal averaged geographical redistribution temperature anomaly, $T' - P_r$, for years 81 - 100 time avera.e, Units: Deg^oC

anomaly, $T'_{r_{net}} = T' - P_{nr}$, show that redistribution puts heat below the surface in all the basins (Figure 4.3). Additional heat from the surface compensates the net surface cooling in the Atlantic.

Despite the complex pattern of geographical redistributive warming and cooling shown in Figure 4.2, the global integral of T'_r is zero as shown in Section 2.4. If on average, redistribution cools the surface layer, it has to compensated by warming of the lower layer, as a result redistribution also smooths out vertical gradient in penetration, in this way ocean heat uptake warms the deep ocean more than the surface (compare black and red lines of Figure 4.4). The basin horizontally averaged profile of T' and P_r, shows a net redistributive surface cooling, occur only in the Atlantic (within the top 300m) and not in the Indian and

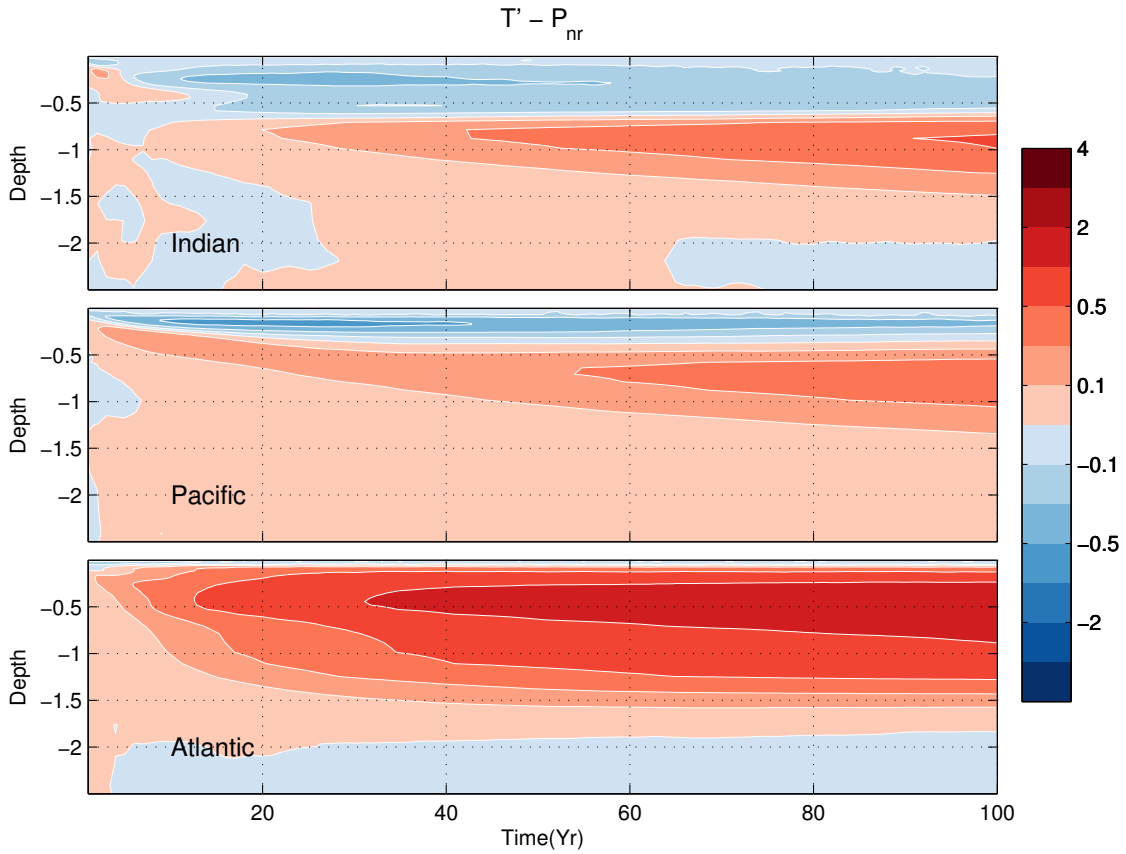

Figure 4.3: Horizontally averaged net redistributive temperature anomaly, T' - P_{nr}; Units: Deg^oC

Pacific oceans. The high latitude cooling dominates the warming in the Atlantic, giving a net surface cooling, while in the Indo-Pacific the warming and cooling balances out each other. Thus for horizontal averages P_r is greater P_{nr} in the Atlantic (Figure 4.4) and the difference continued to grow with time, while the tracer values remain very close, over the century, in the Indo-Pacific, because it has no geographical redistributive surface cooling.

Since positive values of T'_r need to be compensated by negative values elsewhere, the net redistributive cooling near the surface in the Atlantic is compensated by warming below 700m. In the Indo-Pacific, there is deep warming also but there isn't enough surface cooling compensating for it. Moreover, the small surface cooling in the Indian decrease in time while the deep warming increases. This imbalance suggests that the source of deep warming in

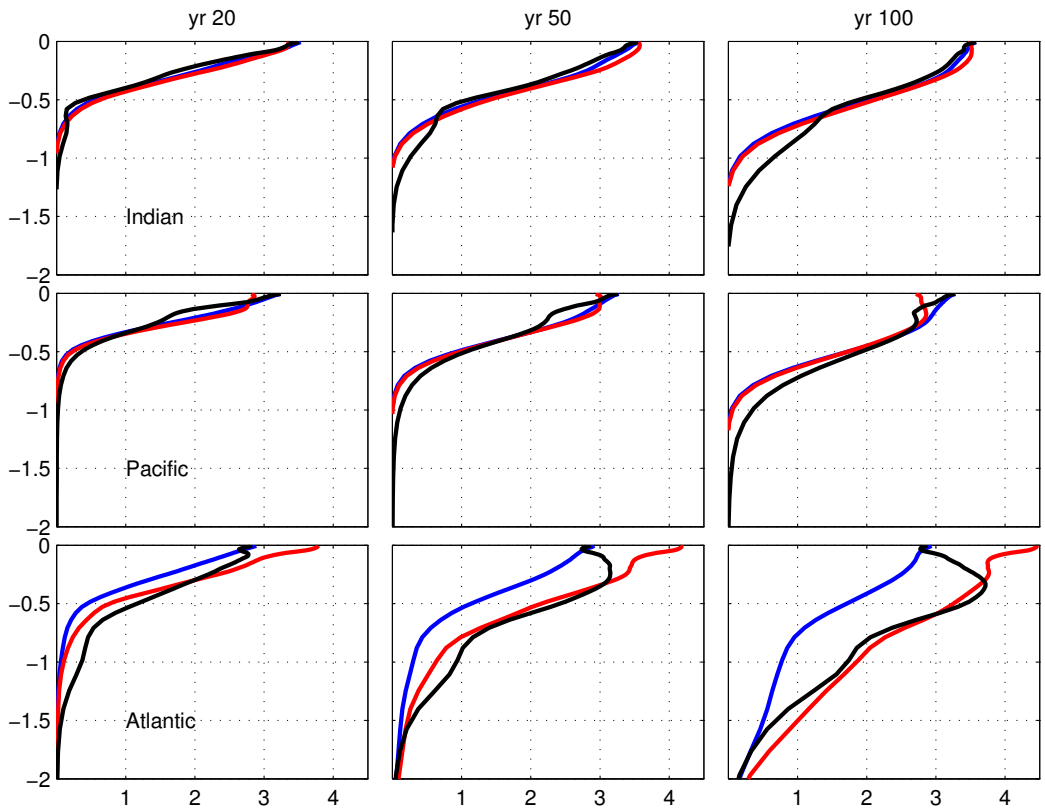

Figure 4.4: Horizontally averaged temperature anomaly and tracers - depth profile. Black line-Temperature anomaly, Red line-Redistribution passive tracer P_r, Blue line-No-Redistribution passive tracer P_{nr}; Units: Deg^oC

the Indo-Pacific is being imported from the Atlantic. This export of heat reduces the redistributive deep warming in the Atlantic between years 50 and 100 (Figure 4.4).

4.3 Redistribution and Effective depth

The effective depth measure has been used to quantify the average depth of ocean heat uptake, we use this measure to quantify the relative effects of passive advection and redistribution on speed of downward propagation of surface temperature anomalies in the basins and globally. Following Xie and Vallis. (2012), we measure the average penetration depth of any property θ (representing T', P_{nr} and P_r) over a volume with surface area A, with effective depth, H_e given by:

$$H_e(t) = \frac{\int T'(x,y,z,t)dV}{\int T'(x,y,0,t)dA} \tag{4.1}$$

We can apply this to the entire ocean or to individual basins. The H_e estimates both the content as well as the average depth of temperature anomalies, however, caution should be used in interpreting it as heat uptake. The heat content anomaly is $AC_p\rho H_e$ multiplied by the average surface value. For example, all three basins have roughly the same P_{nr} surface value, however, the Indian and Atlantic have about the same surface area (7.4 x $10^{11}m^2$ and 8.8 x $10^{11}m^2$ respectively), but the Atlantic's H_e is twice as deep as the Indian H_e (1200m and 650m by the 100th year, Figure 4.5), hence the Atlantic has almost twice the Indian's heat content. The Indian and the Pacific have about the same H_es, but the Pacific's surface area (18x$10^{11}m^2$) is more than twice that the Indian surface area, thus it has twice the heat content anomaly of the Indian.

The effects of the redistribution can be seen by comparing the H_es of P_r and P_{nr} to that of T'. For all three tracers, the H_e grows over time and is larger both for passive advection and redistribution for the Atlantic than for the Pacific or Indian (Figure 4.5). And passive advection gives the main contribution to depth of uptake even in the Atlantic where redistribution is more important. By the 100th year, the Atlantic H_e is almost twice as deep as the Indian and Pacific H_es, which are about the same. Redistribution greatly deepens H_e only in the Atlantic, with H_e for T' about 45% larger than for P_r and 65% larger than for P_{nr}. The values of global H_e is dominated by the Pacific and Indian basins. Thus the global penetration of warming is not strongly influenced by the redistribution term, despite its importance in the Atlantic.

The meridional profiles of the H_e of P_r and P_{nr} (Figure 4.6), illustrate the meridional gradient in heat penetration discussed in the previous section. Passive advection alone carries heat quite deep at high latitudes but shallow in the tropics. In the southern hemisphere, the latitudes of deep and fast uptake ($60^oS - 20^oS$) are centered and peak around 40^oS in all the basins. P_{nr} reaches as deep as 800m around 40^oS by the end of the century in all the

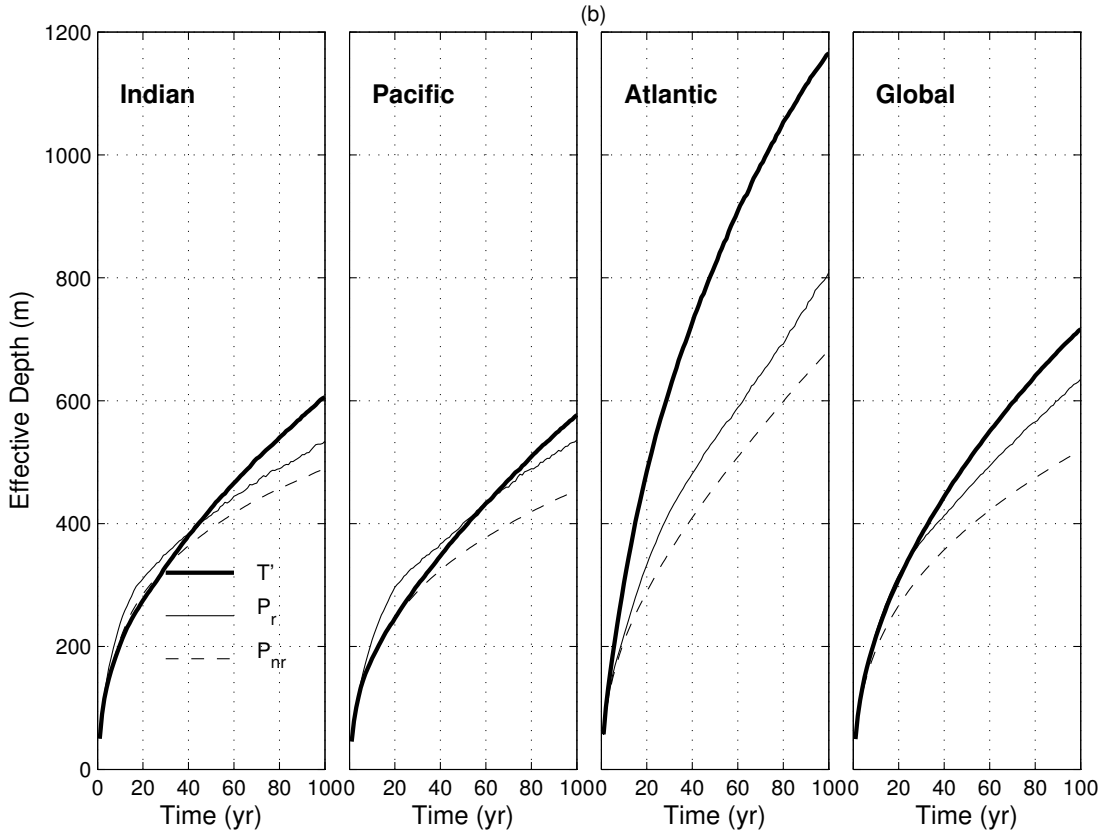

Figure 4.5: Global and basin effective depth time evolution in metres, in the WU experiment

basins. The depth of penetration reduces poleward of this latitude, up to 0m at 60^oS, and equatorward up to 20^oS. The tropical shallow region, between 20^oS to 20^oN, reaches only down to $400m$. In the northern hemisphere, only the north Atlantic shows deep uptake at the high latitudes, the H_e goes deeper poleward of the equator all the way up to the northern boundary of the Atlantic. Here H_e increases from $400m$ at the equator down to 1500m around 60^oN, by the 100th year (deepest region of heat uptake).

The two effects of redistribution both change meridional penetration in opposite ways. The heat flux effect of redistribution, increases the meridional gradients by concentrating more surface heat flux at high latitudes and less heat flux at low latitudes (Figure 4.6, compare P_{nr} and P_r). The geographical effect smooths out meridional gradients by moving heat from the regions of deep heat uptake regions of shallow uptake, (Figure 4.6, compare

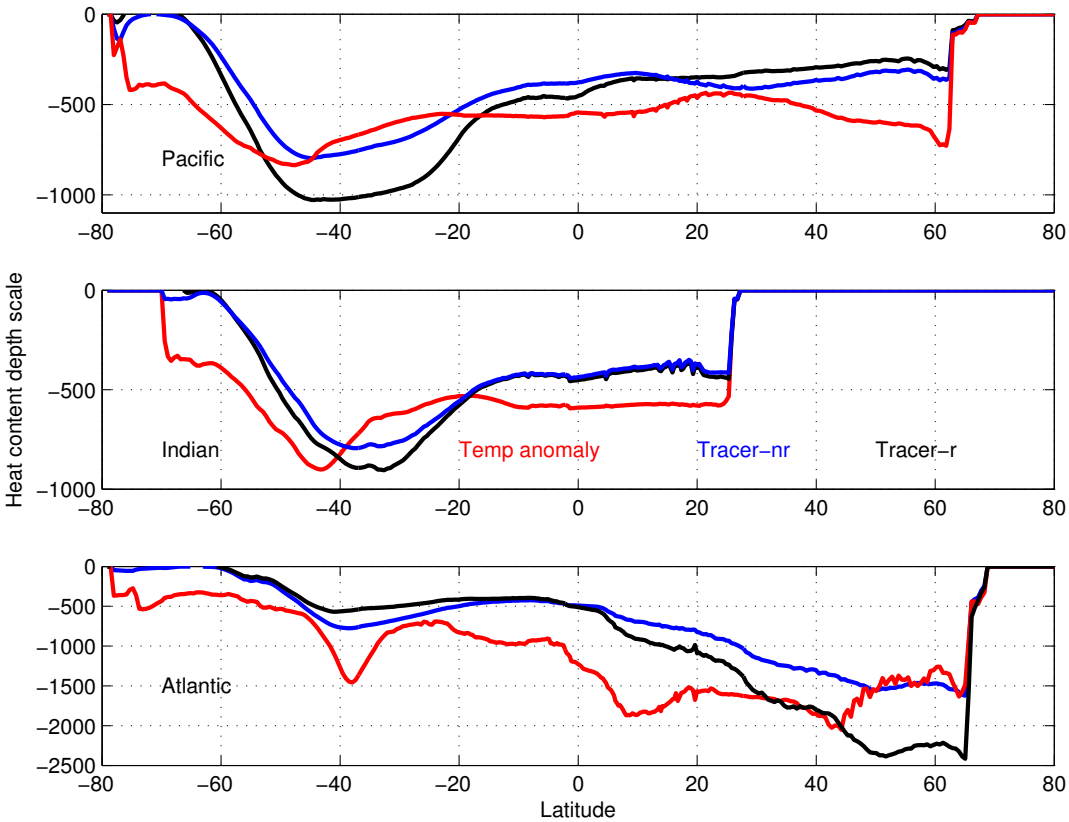

Figure 4.6: Zonal average effective depth in meters, at 100th year

T' to P_r). Redistribution moves heat to the regions of relatively shallow heat uptake in each basin. It moves heat to the tropics ($20^oS - 20^oN$) in all the basins, poleward of 20^oN in the Pacific and poleward of 45^oS in the Southern ocean. It also increases, heat uptake at 40^oS the in Atlantic, though this is a latitude of deep uptake in the Indo-Pacific, the heat uptake here is shallow compare to other deep regions of uptake in the Atlantic. It however, moves heat away from regions of deepest heat uptake around $45^oS - 20^oS$ in the Indo-Pacific and around $45^oN - 65^oN$ in the Atlantic.

Due to redistribution, temperature anomaly H_e increased by about 400m poleward of 60^oS in the southern ocean and about 200m in the Indo-Pacific tropics and about 500m in the tropical Atlantic and reduced by about 500m at 40^oN in the Atlantic and 300m between

$40^oS - 40^oS$ in the Indo-Pacific. Redistributive effect at the high latitude regions of deep uptake is different across the basins, while it reduces the H_e in the Indo-Pacific around 40^oS, it increases it in the Atlantic around these latitudes. In northern high latitude as well, redistribution effects on H_e in the Pacific and Atlantic are opposite, the temperature anomaly H_e, poleward of 40^oN is deeper in the Pacific, while in the Atlantic it is shallower compared to the tracer H_e. The circulation changes causing this is discussed in details in Section 4.6

We can relate the redistributive influence on H_e to surface properties by remembering that $T' = P + T'_r$ and that for the case of $P = P_r$, the global volume integral of T' and P_r are equal. In the individual basins, however, this is not completely true, due to lateral exchange among the basins. However, $\int T_r dv$ is still approximately zero, since P_r and T' have the same surface flux. Their respective lateral exchange is almost the same, the small difference in their lateral exchange occurs because of the difference in their respective distribution across the lateral exchange boundaries. Comparing the H_e for T' and P_r, we get

$$H_{T'} = \frac{\int P_r dV}{\int (P_r + T'_r) dA} \tag{4.2}$$

$$H_P = \frac{\int P_r dV}{\int P_r dA}. \tag{4.3}$$

We can see that $H_{T'} > H_P$ when the surface average of $T'_r < 0$, indicating surface cooling by redistribution.

The two effects of redistribution are measured by the difference between $H_{T'}$ and H_P for P_r and by the difference between H_P for P_r and H_P for P_{nr}. As shown in Figure 4.5, the growth in $H_{T'}$ due to the first effect is greater than the growth due to the second. This is because P_r and P_{nr} have similar surface distributions (though different magnitudes) and are advected by the same v field, while $H_{T'}$ is largely affected by the T'_r term in (4.2). The

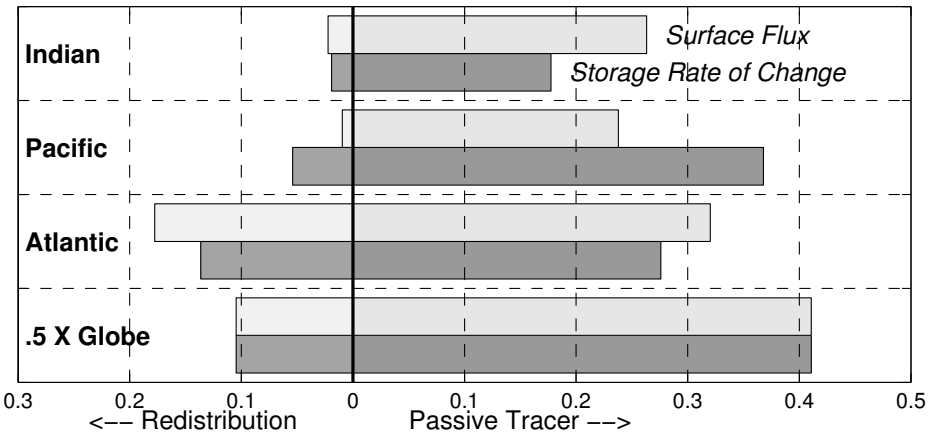

Figure 4.7: Heat transport anomaly through surface (light gray) and rate of change of heat content anomaly (dark gray) within individual ocean basins of the WU experiment based on passive tracer (above zero line) and temperature minus passive tracer (below zero line), in PW. Atlantic includes the Arctic and mediterranean

latter redistributive effect doesn't result in a large H_e growth because P_s also grows as the tracer content increase, hence the ratio of the content growth to surface value increase is about the same. Figure 4.3 shows the H_e for the P_{nr}, P_r and T', the difference between T' and P_r H_es indicates the contribution from the geographic redistributin while the difference between that of P_r and P_nr indicates the contribution from heat uptake redistribution. The plot shows H_e grows faster due to geographical effect and than due to heat uptake effect.

4.4 Heat uptake and lateral heat transport among basins

In the discussion below, "Heat" refers to $c_p\rho\theta$ (where θ is any of the tracers) and "surface heat transport" or "heat input" into an ocean basin is the integral of heat flux over the top surface. Here we do not consider P_r, because P_r and T' utpake are equal and their lateral fluxes between basins are almost equal as well. We refer to P_{nr} as the passive component and $T_{r_{net}} = T' - P_{nr}$ as the redistributive component. Averaging over the surface area of the ocean, the total heat transport into the ocean of about 1 PW is equivalent to an average heat flux of 3 W/m^2.

The 100-year average heat input of passive tracer P_{nr} is similar for all three basins (Figure 4.7), despite the different sizes and dynamics of the different basins. In the Atlantic, the faster downward propagation of heat compensates for the basin's small area. In contrast to the passive tracer input, the additional heat input associated with redistribution (Figure 4.7) is very different in each basin. In the Atlantic, it is more than 50% of the passive contribution, here, the division for the Atlantic basin includes the Arctic Ocean and Mediterranean Sea, excluding these basins, redistributive surface input into the Atlantic is about 80% of the passive contribution(Compare, Figure 4.7). In the Indian, it is about 15% of the passive, and in the Pacific it is negligible. Including both passive and redistributive parts, about 50% of total surface heat transport entering the three basins enters the Atlantic alone. For the globe as a whole, redistribution increases heat uptake by about 30%.

Rates of change of basin heat content (Figure 4.7) tell a somewhat different story than the surface fluxes. The Pacific gains more heat than the Atlantic which in turn gains more than the Indian. In the Pacific, T' content is 80% greater than the surface input, P_{nr} content is 50% greater the surface input, and T'_r content is 40% of the total T' input, though surface T'_r input is negligible. As a result the Atlantic and the Pacific have about the same heat uptake, each accounting for 40% of the global heat content, while the Indian ocean accounts for the remaining 20%. In summary, the Atlantic has the greatest gain in surface heat transport due to redistribution, while the Pacific has the greatest gain in heat content from lateral heat transport.

Differences between surface heat input and change in internal heat content indicate transport of heat between basins. For a given region, lateral heat transport L consists of the area integral along the side boundaries of the flux terms in (2.2) through eq2.5: $v_n\bar{T}$ for $\bar{T}$ transport, $L_{\bar{T}}$, $v_nT'+v'_n\bar{T}$ for T' transport $L_{T'}$, v_nP for P transport L_P, and $v_nT'_{r_{net}}+v'_n\bar{T}$ for $T'_{r_{net}}$ transport $L_{T_{r_{net}}} = L_T - L_P$, where v_n refers to the component of velocity normal to the boundary. POP outputs horizontal heat transport components at each grid point and we estimate the individual terms from annual-average velocity, temperature, and tracer fields.

Table 4.1: Lateral Heat transports integrated over the 100-year run, for the control temperature, $\bar{T}$, passive tracer, P_{nr}, temperature anomaly, T' and redistributive anomaly, $T' - P_{nr}$. Transports are given across the basins' northern and southern boundaries respectively. Northern boundary for the Indo-Pacific is the Indonesian throughflow and for the Atlantic is the Arctic boundary. The Bering strait heat transport (not shown) is neglible, hence it doesn't count as the Pacific northern boundary. The Southern ocean is the southern boundary for all basins

values in $10^{23} Joules$.

	$\bar{T}$			T'			P_{nr}			$T' - P_{nr}$		
	Ind	Pac	Atl	Ind	Pac	Atl	Ind	Pac	Atl	Ind	Pac	Atl
Ind.Thr	32.1	-32.1	0	-0.8	0.8	0	3.2	-3.2	0	-4.0	4.0	0
S.Ocn	-25.0	17.6	7.4	-1.8	5.5	-3.7	-5.6	7.8	-2.2	3.8	-2.3	-1.5
Net	7.1	-14.5	7.4	-2.6	6.3	-3.7	-2.4	4.6	-2.2	-0.2	1.7	-1.5

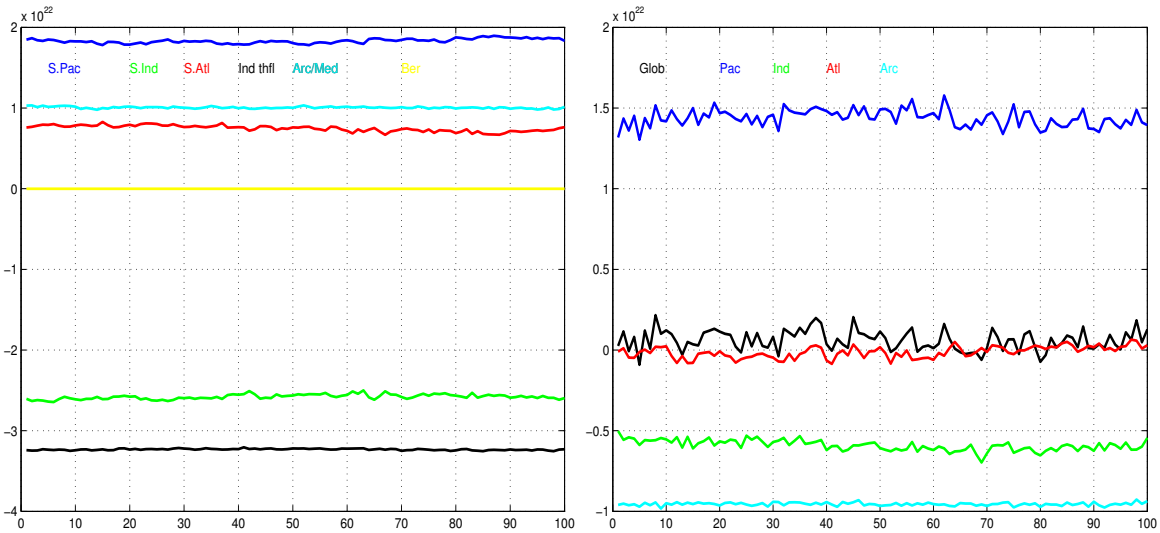

Figure 4.8: Lateral heat transport (left plot; Lateral boundaries the same as in Table 4.1), and surface heat flux among the basins(right plot), in Joules, for the control experiment

We consider the energy budget for individual basins. In the control climate, the equilibrium basin temperatures are maintained by lateral heat transports balanced by surface heat transports. The lateral transport is maintained by the conveyor belt, with 0.24 PW flowing out of the Indo-Pacific, through the Southern Ocean, and into the Atlantic (Figure 4.8 and Table 4.1, column 1), where it is augmented by tropical heating and exported to the Arctic (including Labrador and Nordic Seas). Bering Strait heat transport is negligible. In the

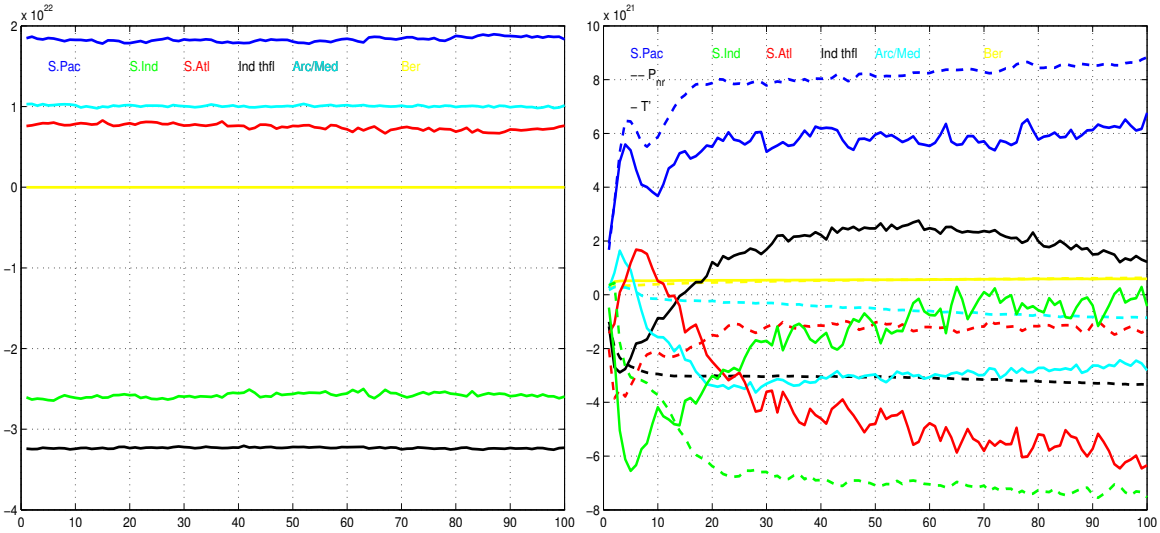

Figure 4.9: Heat exhchange in Joules through basin boundaries: Southern ocean and Indonesian throughflow, Bering strait, Arctic and mediteranean (Positive = heat gain, negative = heat loss). Negative values through indonesian through flow mean Pacific heat loss and Indian heat gain. Positive Bering and Arctic/Med values means Arctic heat gain and Pacific and Atlantic heat loss respectively (a) Control heat transports. (b) Temperature anomaly heat transport-solid line and P_{nr} heat transport - dashedline

Indo-Pacific, the 10 Sv of relatively warm (1.02 PW) Indonesian Throughflow water from the Pacific to the Indian is exchanged for relatively cold water (0.82 PW) leaving the Indian and entering the Pacific and Atlantic in the Southern Ocean. Hence in steady state the Pacific exports heat t(0.44 PW) to the Indian (0.2 PW) and Atlantic (0.24 PW) oceans via the Southern ocean and Indonesian Throughflow. This exchange transfers the surface heat input into the Pacific to the Indian and Atlantic (Also compare Figure 4.8, right and left plots).

In the warming climate, the direction of heat anomaly transport is opposite that of the control heat transport, with the Pacific importing heat anomaly from both the Indian and the Atlantic. The direction of heat transport reverses for two reasons, the distribution of heat anomaly (affecting the $v_n T'$ and $v_n P$ terms) and the weakening circulation (affecting the $v_n' \bar{T}$ term).

The velocity in the $v_n T'$ or $v_n P$ term is in the same direction in the perturbation

experiment as in the control equilibrium. However, the $v_n T'$ term integrated over all the boundaries of each basin has the opposite sign of integrated $v_n T$. A swath of relatively high T' water circling Antarctica in the Southern Ocean weakens near the Drake Passage where water flows into the Atlantic sector. This pattern comes from the T'_* forcing and ultimately from the coupled experiments, thus it is seen in the P_{nr} distribution too. It is a robust feature and can also be seen in CMIP3 models forced by A1B radiative forcing (Kuhlbrodt and Gregory (2012); see their Figure 4). Thus for the Atlantic and Indo-Pacific, the exchange reverses: high T' water leaves the Atlantic, low T' water enters, so that the Atlantic exports heat. For the Pacific, the same feature in the Southern Ocean of higher-T' water entering from the Indian sector and lower-T' exiting to the Atlantic implies heat import. Moreover, since low latitudes absorb less T' and P_{nr} than high latitudes, the combined effect of Indonesian Throughflow and exchange in the Southern Ocean is to import heat into the Pacific, subtantially from the Indian and some from the Atlantic (Figure 4.9 and Table 4.1 column 2).

The advection of tracer, $v_n P$, and temperature anomaly, $v_n T'$, are the same sign and similar in magnitude. Therefore, the contribution of redistribution to heat transport $L_T - L_P \approx v'_n \bar{T}$ term, and thus is dominated by advection of control temperature by circulation anomaly. At transport boundaries, the cause is the weakening of the circulation which gives v' the opposite sign to $\bar{v}$, hence the heat transport is opposite the control's. In the Southern Ocean, this term is exporting heat from the Atlantic and Pacific into the Indian (Table 4.1, column 4), while in the Indonesian throughflow it is exporting from Indian to Pacific. The net effect of all these transports is for the $v'_n \bar{T}$ term to export heat from the Atlantic to the Pacific, with little heat export also to the Indian. (Table 4.1, column 4). Thus the Pacific gains redistributive content, though with negligible redistributive surface input. The Pacific gains all of its redistributive import from the Atlantic and most of its tracer import from the Indian.

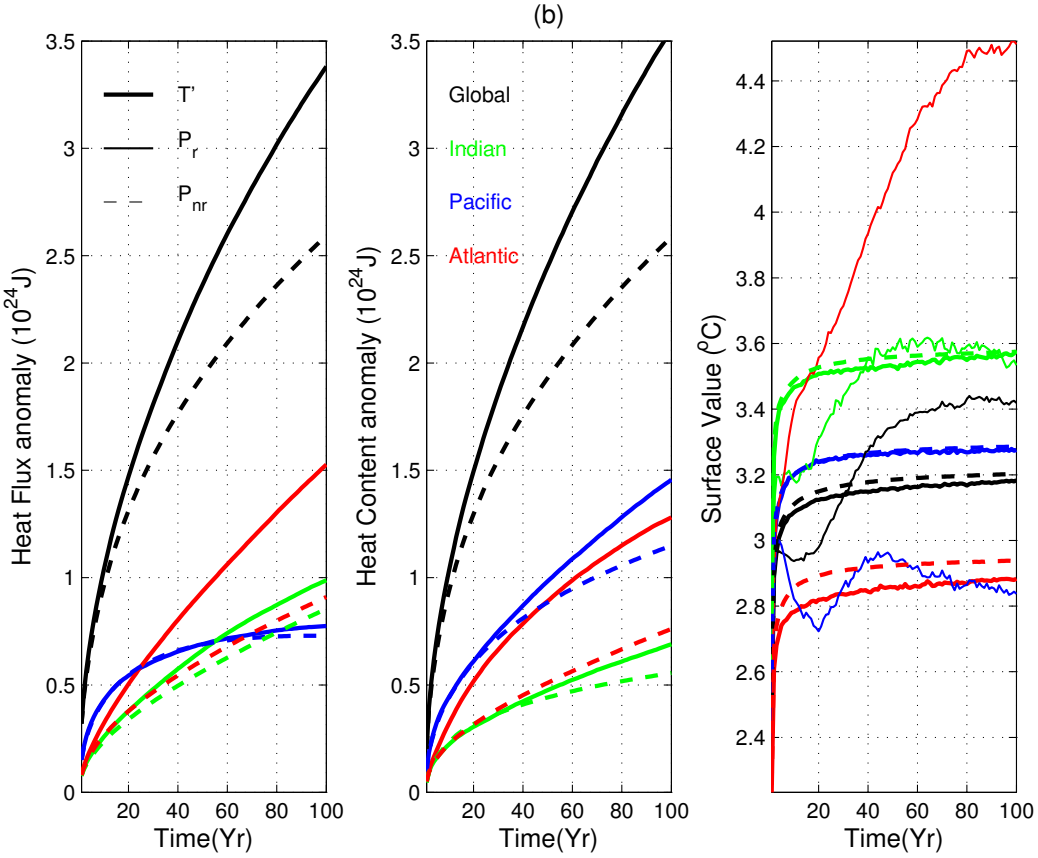

Figure 4.10: Content and Flux growth in time among the ocean basins (a) T' content and P_{nr} content. (b) T' and P_{nr} flux cumulative sum over time and integrated over entire global and basin surface.

4.4.1 Time evolution of heat uptake components

By design, the strong restoring and constant $T'_\star$ of the perturbation experiment ensures that most of the surface temperature increase occurs in the first few years (Figure 4.10, third panel), but the system is far from steady state even at the end of the experiment. This can be seen in time-integrated surface heat input anomaly into the ocean (Figure 4.10, first panel) and global heat content anomaly (Figure 4.10, middle panel). We expect such a long time scale based on AOGCM experiments which show millenial-scale adjustment after radiative forcing is changed (for instance Li and Marotzke (2012)).

Time evolution within different basins reflects the features discussed in Section 4.4. In

the Pacific, heat input anomaly (slope of curves in Figure 4.10, first panel) is small after about 50 years, but heat content continues to vigorously grow (Figure 4.10, middle panel). During the last 50 years of the experiment, the basin acquires about a third of its heat content increase but only about 10% of its surface heat input. The disparity is because of the heat import from other basins, which becomes the dominant source of warming in the Pacific after the first 50 years. In the last 50 years, the Atlantic, in contrast, receives about half of its surface heat input but only experiences about a third of its heat content growth. The changing composition of heat sources for the two basins reflects increasing lateral heat transport into the Pacific and out of the Atlantic in the last 50 years. The Indian Ocean exports heat at a more constant rate for the entire century.

4.5 Effect on global warming

The above results highlight how the redistributive mechansim increases ocean heat uptake efficiency. The ocean heat uptake balance is

$$\Delta N = \Delta F - \Lambda \Delta T = \kappa \Delta T \tag{4.4}$$

where ΔF is the TOA radiative forcing, ΔT is the surface temperature anomaly, ΔN is the ocean heat uptake and κ is the heat uptake efficiency coefficient. A comparison of surface values of the tracers and temperature anomaly with heat content anomaly change, indicates the change in uptake efficiency. P_r and T' have the same uptake but very different surface values. P_{nr} and T' have about the same value because they are restored to the same target temperature, but different uptake. (Figure 4.10, third panel) It is clear that the Atlantic uptake efficiency increases by about 50% (compare T' and P_r surface vlaue in Figure **??**b or T' and P_{nr} content) by the end of the century through redistribution. The increase in heat uptake efficiency also means slow approach to equilibrium, redistribution makes T' surface value approach the target value even more slowly than P_{nr} surface value. The Atlantic T' is very slowly approaching the P_{nr} value and has not reached this value by the end of the

run.

The Pacific uptake efficiency increased because the heat uptake almost doubled without significant change in surface temperature after 40 years. The Pacific surface temperature (Figure 4.10, third panel) approaches equilibrium value quite quickly compared to other basins. Despite this, the heat content of the Pacific continued to grow especially in the last five decades, when its surface heat flux is close to zero. (compare Figure 4.10, first and second panels). The Indian uptake efficiency doesn't increase so much. It's content anomaly and surface temperature increased a steady rate after the first 20 years. The Atlantic heat uptake efficiency increases via surface cooling, while that of the Pacific increases through changes in lateral heat transports.

4.6 Steady state circulation and circulation perturbation

So far, we've discussed ocean heat uptake and redistributive effects in the WU experiment without considering circulation and circulation perturbation causing them. The results shown earlier highlight the role of the deep and shallow circulation in each basins, in determining amount surface heat input into the basins and the role of the deep circulation and global conveyor belt in distributing heat uptake among the basins. It is necessary to connect the heat uptake redistributive pattern to the circulation strength in the basins.

4.6.1 Steady state circulation and heat transport

The control equilibrium overturning showin in Figure 4.11 has the familiar pattern of Atlantic inflow in the top kilometer, downwelling in the high latitudes and outflow in the abyss and some upwelling in the tropics; Indo-Pacific deep inflow, widespread upwelling in the tropics, and mid-depth outflow; Southern Ocean upwelling associated with surface Ekman divergence. About 4 Sv of the Indo-Pacific outflow connects to the shallow subtropical cell and upwells at the equator and returns southward at the surface via the sutropical gyre. The Atlantic inflow also connects to the northern subtropical cell

The circulation in the basins are connected via the global conveyor belt. Equilibrium

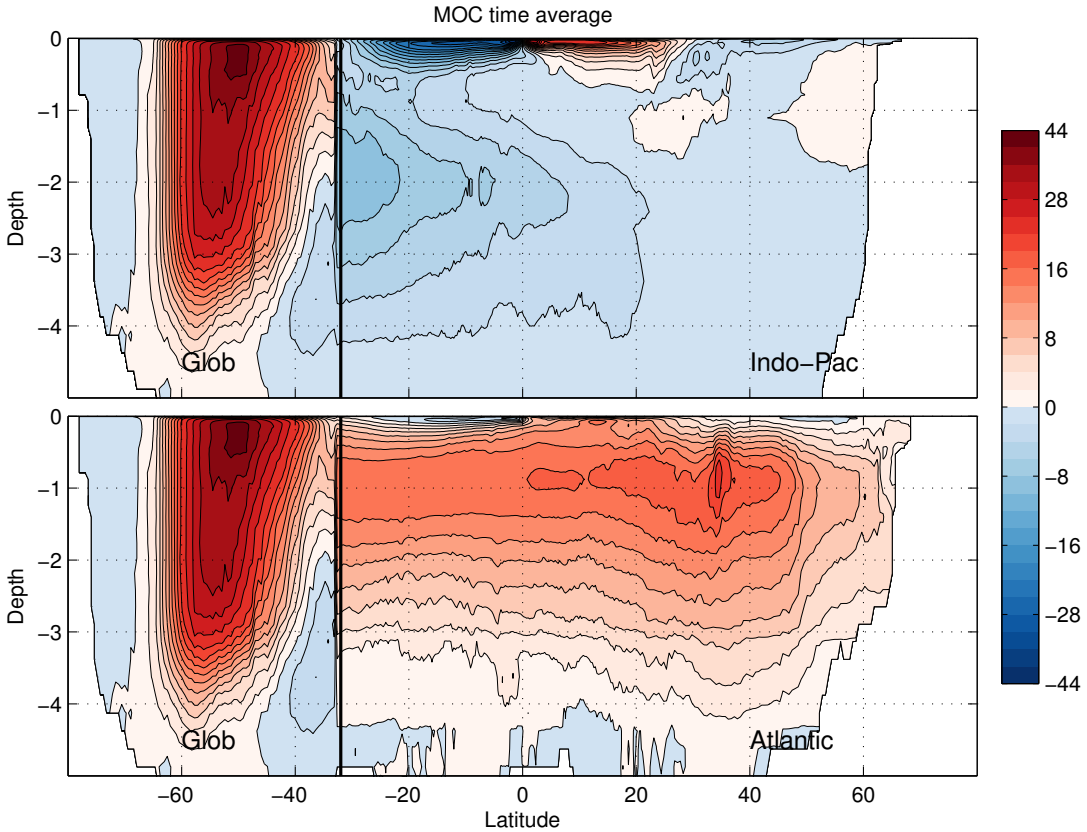

Figure 4.11: Control experiment Meridional Overturning circulation 100 year time average. (Contours Red=positive, blue=negative. c.i.=2 Sv.)

depth-integrated streamfunction Indo-Pacific circulation includes 10 Sv flowing from Pacific to Indian in the Indonesian Throughflow and returning to the Pacific from south of Australia. In the Southern ocean, the net volume transport is out of the Indian and into the Pacific in the Southern ocean which is balanced by the volume transport out of the Pacific into the Indian through the Indonesian Throughflow, so that the net volume in each basin is conserved. Most of the Southern ocean upwelling recirculates in Southern ocean and about 8Sv of it is drawn from the Atlantic abyss outflow. The Southern ocean net volume transport into the Atlantic is zero since what flows in the in the top Km is equal to the volume that flows out in the abyss. This circulation explains the steady state heat transport among the basins mentioned in Section 4.4.

Themohaline forcing circulation perturbation

The circulation changes caused by the perturbation in fresh water and temperature forcing in the WU experiment include changes to the meridional overturning and inter-ocean flow. The surface perturbation weakens the overturning, which is equivalent to adding a reverse AMOC of 10 Sv (Figure 4.12, top) and a decrease of Indo-Pacific upwelling of 4 Sv (Figure 4.12, middle). The weakened circulation is caused by warming and freshening of the North Atlantic deep water formation regions relative to other parts of the ocean. The Indonesian Throughflow flowing from the Pacific to the Indian ocean also weakens by about 4 Sv (Figure 4.12, bottom). Much of the circulation perturbation in the vicinity of the Indonesian Throughflow occurs in the top kilometer (Figure 4.12), with an Indian-to-Pacific flow. The reduction is curious because the depth-average circulation is usually associated with wind stress, which is not perturbed in the experiment. This looks to be a consequence of the weakening of the conveyer belt circulation associated with the decreases in overturning. The horizontal flow also shows signs of the decrease in the meridional overturning, with perturbation velocity flowing southward in the Atlantic and then flowing eastward out of the Atlantic and then northward from the Southern Ocean into the Indian and Pacific (the reverse of the equilibrium upper-limb flow out of the Indo-Pacific and into the Atlantic). The change in the Indian-Pacific exchange may be a consequence of this change in the overturning.

The connection between the deep circulation anomalies in the Atlantic and the Indo-Pacific anomalies can be explained by the mechanism setting deep circulation and global conveyor belt strength in the basins. The role of surface winds and bouyancy distribution in the basins in determining the deep circulation strength within the basins and the strength of the global conveyor belt connecting the circulation in the basins to one another have been studied in papers such as (Gnanadesikan (1999) and Schewe and Leverman (2009)). Southern ocean winds drive the deacon cell circulation, most of which recirculates in the Southern ocean, some of the Southern ocean upwelling, however, is drawn from the basins depending on their buoyancy distribution. The Atlantic meets the Southern ocean upwelling

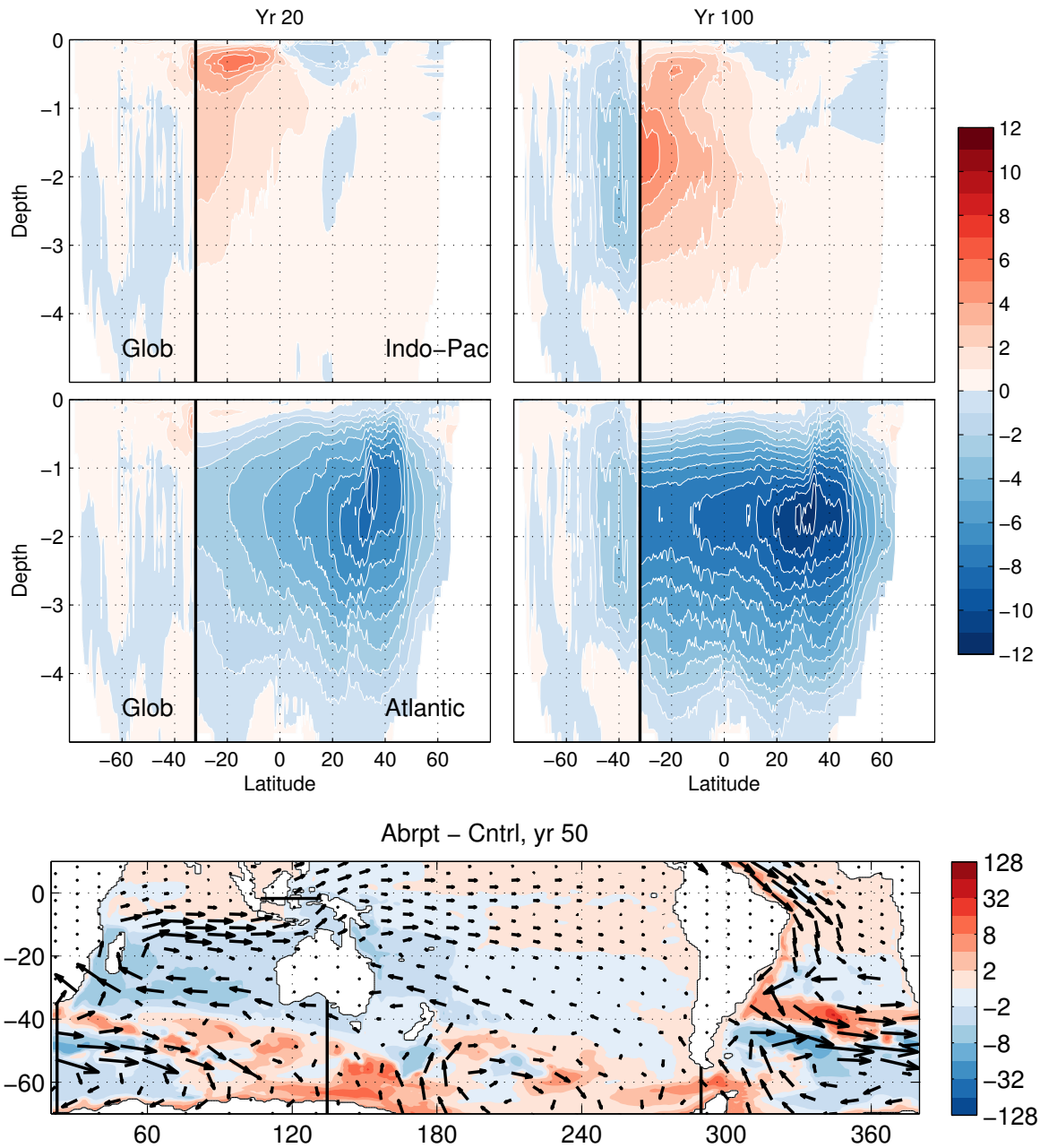

Figure 4.12: Circulation anomaly in the WU experiment as measured by (top 2 panels) meridional overturning streamfunction (contour interval 1 Sv) at years 20 and 100, and (bottom) horizontal velocity at year 50. Overturning is for zonally integrated velocity in (top) Indo-Pacific and (middle) Atlantic basins, and (both panels) globe south of approximately 35° S. Bottom panel includes stream function for full-depth integrated velocity (shading, units Sv) and horizontal velocity integrated over top 1041 m.

demand due to its larger buoyancy gradient. The NADW sinking in the northern Atlantic connects to the Southern ocean upwelling demand. Some of the Atlantic inflow also connects to the Indo-Pacific outflow through the Southern ocean, while the Indian and Pacific are connected through the Indonesian throughflow. The relative magnitudes of Southern ocean upwelling demand and the inflows and outflows from the basins, determine the amount of recirculation within the basins, thus setting the upwelling and as a consequence the thermocline depth in the Atlantic and the Indo-Pacific respectively.

The unchanging winds in the WU experiment mean the Southern ocean circulation is unchanged. However, NADW formation in the Atlantic is weakened, according to the study of Schewe and Leverman (2009), also implied in Klinger and Cruz (2009), this imbalance between Southern ocean upwelling demand and NADW formation is supplied from the Indo-Pacific. This is similar to their experiments with stronger Southern ocean winds while NADW formation is unchanged. The downwelling streamlines connected to the supply from the Atlantic is now connected in the Indo-Pacific. Circulation anomalies as a result of this gives an Indo-Pacific inflow at the surface and mid - depth, downwelling in the (a clockwise circulation in the latitude-depth plane). The circulation anomaly is very small and confined to the top 1km and south of the equator, that is in the subptropical gyre and the Indonesian Throughflow, in the first decade (not shown). It grows downward with time up to a depth of about 4km in 100years (Figure 4.12), as a result shrinking the Indo-Pacific AABW circulation over time.

Redistribution temperature anomalies in the WU experiment can be explained by the circulation anomaly pattern. This circulation anomaly pattern cools the northern high latitudes because less warm water are transported from the tropics to the northern high latitudes. The deep tropical Atlantic also warms as a result of less upwelling deep water pushing down the thermocline. The redistribution temperature anomalies due to this circulation anomaly pattern is shown in Figure 4.2. The Indo-Pacific circulation anomalies also give deep tropical warming and southern high latitude cooling. The difference between the Atlantic and Indo-Pacific circulation anomalies is that Atlantic anomalies are much deeper

and span the whole basin, allowing for deeper tropical warming than in the Indo-Pacific. The upwelling anomalies in the northern high latitude Atlantic is also much stronger, resulting in a lot more redistributive surface cooling that of the Indo-Pacific. The Indo-Pacific deep tropical warming anomalies also occur much later, in the last 50 years. This is because the circulation anomalies confined to the southern hemisphere subtropical gyre in the first few decades, but with time the circulation anomalies grow equatorward, the downwelling branch extends deeper into the tropics and hence more redistributive warming in later years.

4.7 Summary

The results described above, has shown the effects of passive and redistributive components ocean heat uptake, and how these components of ocean heat uptake grow and are distributed among the basin. Redistribution of existing ocean heat content due to circulation changes, increases ocean heat uptake by cooling the reservoir surface temperature and warming the tropical deep, and as a result increases heat flux into the ocean. Redistribution changes temperature anomaly gradients in the ocean, meridionally, by moving heat from high latitudes to low latitudes, and vertically by cooling the surface and warming the deep ocean. Vertical redistribution results in a deeper penetration of temperature anomalies and an increase in the effective depth of heat penetration.

Passive heat uptake contributes about 70% of the global ocean heat uptake, while redistribution contributes the remaining 30%. Of this global total, the Atlantic contributes all the surface redistributive heat uptake because redistributive surface cooling occurs mainly in the Atlantic due to AMOC weakening. The passive surface uptake is more evenly distributed among the basins. Lateral transport among the basins via the global conveyor belt connecting the basins via Indonesian throughflow and Southern ocean, allows more heat to accumulate in the Pacific through a greater net southern ocean heat anomaly import than the Indonesian through flow export. This is possible because the higher concentration of anomalies at the high latitudes than at the tropics, in contrast to steady state temperature

distribution. The global conveyor belt also weakens via AMOC weakening resulting in Indonesian through flow weakening. This allows more accumulation of heat in the Pacific by reducing its mean state heat export, to the Indian and Atlantic. This inter-basin exchange allows the Pacific and Atlantic to contribute almost equally, each about 40%, to the global heat uptake while the Indian contribute the remaining 20%

Chapter 5: Surface perturbations and Ocean heat uptake

5.1 Introduction

Ocean circulation strength is influenced by surface conditions, Southern ocean winds, temperature and fresh water forcing in the high latitudes determine the strength of the deep circulation and global conveyor belt. Surface winds in the tropics also determine the strength of the shallow Ekman cells. Perturbation to these surface forcings should influence ocean circulation changes in different ways. The different circulation change patterns from different surface forcing perturbations, should result in different redistributive pattern as well. It has been shown, in the study of Xie and Vallis. (2012) and from the results in the previous chapter, that weakening of the deep overturning circulation due to thermohaline forcing perturbation increases ocean heat uptake through redistributive surface cooling. This raises the question of how redistributive and passive components of ocean heat uptake will change given different perturbations to surface forcings other than atmospheric heat flux anomaly. Since we are able to separate the redistributive heat uptake from the passive one, the comparison of these heat uptake components among all three perturbation experiments helps us to understand how and surface perturbation change ocean heat uptake.

The differences between AC and the WU experiments allow us to isolate the effects of dynamical forcing perturbation from the thermohaline forcing perturbation, while the differences between the WU and WSU experiments allows us to isolate salinity forcing perturbation influence from the temperature forcing perturbation influence, for the thermohaline driven circulation. The experimental design and surface forcings of the WSU, WU and AC experiments are described in Section 2.3.2. Ocean heat uptake, redistribution and inter-basin transport in the WU experiment analyzed in Chapter 4 and will be constantly referred to here. The same analysis for the WU experiment in Chapter 4, will also

be shown for the AC and WSU experiments here, but results will be compared between the two experiments. Circulation changes resulting from surface forcing perturbations will also be compared among the experiments in order to understand the differences in the redistributive patterns.

5.2 Thermohaline forcing perturbation effects

Here we will compare results from the WU and WSU experiments, these experiments isolates the influence of thermohaline forcing perturbation from the wind forcing perturbation on ocean heat uptake. The WSU experiment has only the surface temperature forcing changed to that of the CESM abrupt experiment, while wind and salinity are kept the same as that of the CESM piControl run. Hence, it represents only the influence of surface temperature perturbation on ocean heat uptake. The WU experiment has both temperature and salinity changed to the CESM abrupt run, while the wind is kept the same as that of the CESM piControl run. Hence, the difference between the WU experiment and the WSU experiment isolates the influence of surface salinity perturbation on ocean heat uptake.

Surface temperature and salinity forcing perturbation are shown in Figure 2.6 a and b, as the restoring temperature and salinity anomalies. Surface temperature perturbation warms most of the ocean surface with the greatest warming in Southern subpolar regions and the northern Pacific subpolar region. The least warming occurs in the Atlantic subpolar region, in Arctic and the Southern ocean polar regions. Salinity perturbation freshens the north and south polar and subpolar regions but makes the tropics and the subtropics saltier, especially in the Atlantic. Thermohaline forcing perturbation, combines surface salinity and temperature perturbation, weakens mainly the AMOC and as a consequence, also the deep Indo-Pacific circulation via the connection to the global conveyor belt. This AMOC weakening nearly doubles heat uptake in the Atlantic due to redistributive surface cooling (see Chapter 4).

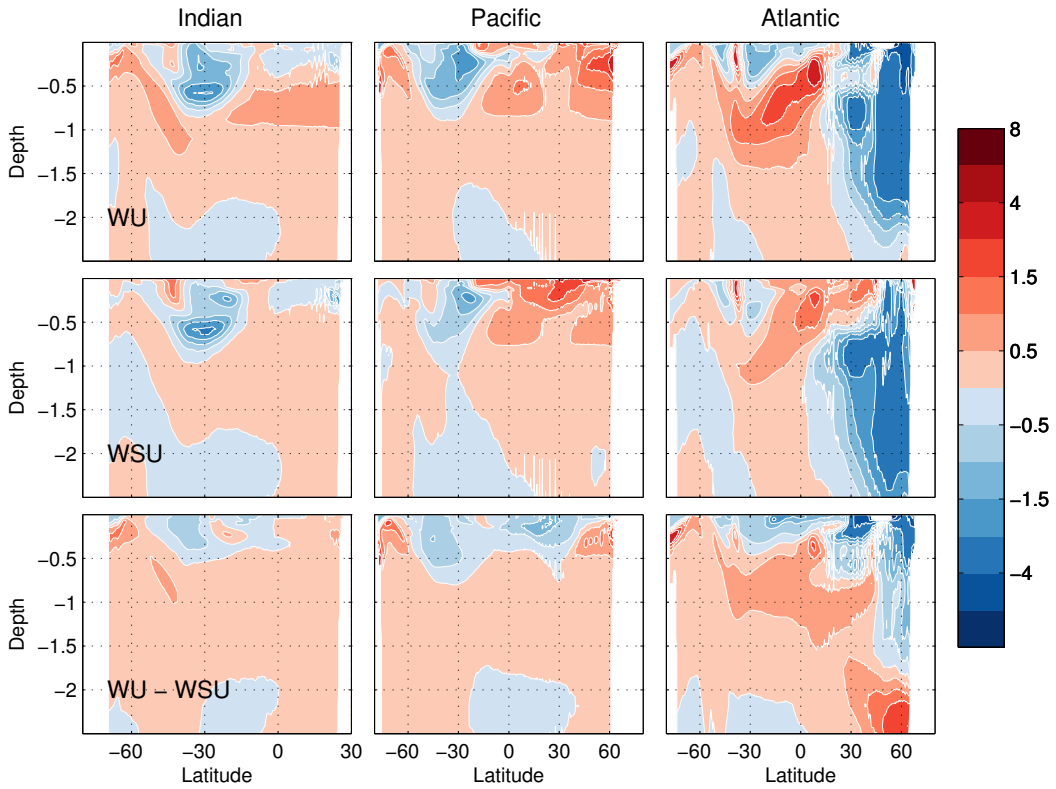

Figure 5.1: Geographical redistribtion temperature anomalies, $T' - P_r$ in the WSU and WU experiments, values are basin zonal averaged anomalies and time averaged over the last 20 years of the century long experiments. Contours:Red - Positve; Blue - negative. Units: Deg^oC

5.2.1 Temperature distribution

Temperature forcing perturbation alone, gives a very different redistributive temperature anomaly pattern ($T'_r = T' - P_r$). Redistributive temperature anomaly in the WSU experiment in all the basins, is generally warmer in top 500m and cooler below 500m than the one in the WU experiment, especially in the Atlantic (Figure 5.1). (Note: By definition of redistribution, this surface warming is not due to surface heat flux anomaly into the ocean. This is checked by the global integral of the redistributive temperature, which is zero). Though, surface high latitude cooling in the Atlantic and in the Southern ocean are present in both experiments, the magnitude of the surface cooling is smaller in the WSU experiments. The tropical surface is also generally warmer in all the basins. The Atlantic

tropical and northern subtropical surface warmed in the WSU experiment, in contrast to the cooling in the WU experiment. The Indo-Pacific tropical surface, though warm in both experiments, is warmer in the WSU experiment.

The warmer surface redistributive pattern in the WSU experiment suggest that redistributive cooling in the Atlantic surface, in the WU experiment is due salinity surface perturbation. The difference between the WU and WSU experiments (Figure 5.1, bottom panel), shows that salinity perturbation alone, gives redistributive cooling in the top 500m, not just in the Atlantic, but in all the basins, while it gives redistributive warming in the deep ocean. The surface redistributive cooling is especially more intense in the Atlantic subpolar region. The combined effect of these two redistributive patterns in the WU experiment, however warmed the Indo-Pacific surface and cooled the Atlantic surface.

Due to the different redistributive patterns, the vertical distributions of the tracer P_r and temperature anomaly (Figure 5.2), T' are very different between the two experiments, while the vertical distribution for the tracer P_{nr} remain the same in both experiments. The surface values of T' and P_{nr}, though, are the same between the two experiments because they are restored to the same surface target values (T'_*), in both experiments. In the Atlantic, the comparison between the P_r and T' indicates a net redistributive surface warming ($T' - P_r$), of about 0.5^oC in top 500m, compared to the cooling of about 1.5^oC in the WU experiment. The Indo-Pacific shows a net redistributive surface warming in the WSU, about twice that in the WU experiment, 1^oC in the Pacific and 0.4^oC in the Indian. The Atlantic deep also cooled by about 0.5^oC, opposite of the warming in the WU experiment.

5.2.2 Heat uptake

Given the redistributive pattern differences in the two experiments, described above, it is not suprising then, that the total heat uptake in the WSU experiment is a lot smaller than that of the WU experiment (Table 5.1, Figure 5.3), about 67% of WU's. The difference in total heat uptake occurs as a result of differences in surface redistributive heat uptake between the two experiments. Surface redistributive heat uptake in the WSU experiment

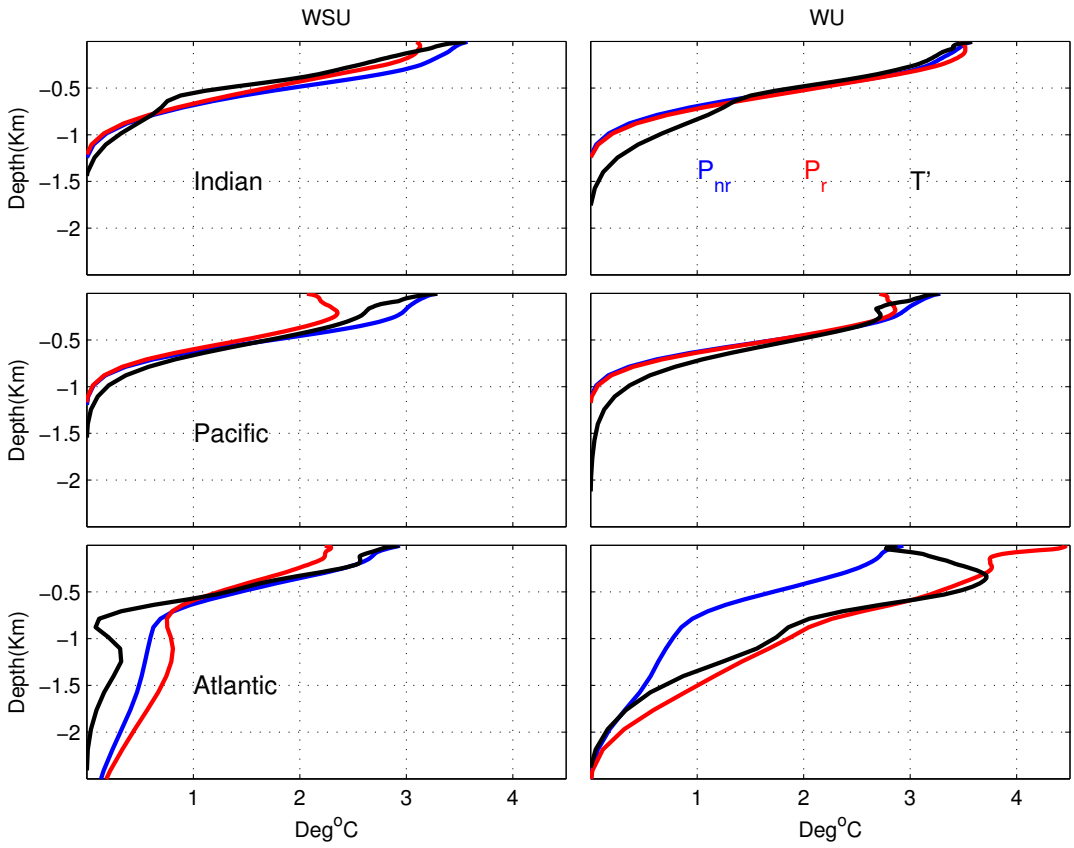

Figure 5.2: Horizontally averaged temperature anomaly, T' and passive tracers, P_{nr} and P_r - depth profile, in the WSU and WU experiments. Black line - T', Red line - P_r, Blue line - P_{nr}

is not only smaller in magnitude but it is also opposite in sign compared to that of the WU experiment. The passive heat uptake is about the same in both experiments. The difference in the redistributive surface heat input between the two experiments indicates surface salinity perturbation gives positive redistributive heat uptake, while surface temperature perturbation gives a negative redistributive heat uptake, in all the basins. The negative redistributive heat uptake, follows from the surface redistributive temperature anomaly warming ($T'_r > 0$), observed in the WSU experiment. As discussed in Section 2.4, redistributive surface warming give negative redistributive heat uptake, that is, cooling of reservoir heat content.

In the WSU experiment, negative redistributive surface heat uptake or redistributive

Table 5.1: Heat flux and content in Joules in the WU and WSU experiments, integrated over the 100- year run, for the passive tracer P_{nr} and temperature anomaly T' and redistributive anomaly (T' - P_{nr})

values in 10^{23} Joules.

	WU					WSU				
	Glob	Ind	Pac	Atl	Arc/Med	Glob	Ind	Pac	Atl	Arc/Med
Q'	32.5	9.0	7.8	14.2	1.3	21.8	9.6	4.9	6.9	0.4
Q_{nr}	25.9	8.3	7.5	9.1	1.0	25.4	8.5	7.6	8.4	0.9
$Q' - Qnr$	6.6	0.7	0.3	5.1	0.5	-3.6	1.1	-2.7	-1.2	-0.5
T' cont	32.5	6.2	13.3	11.8	1.2	21.8	4.6	11.6	4.7	0.9
P_{nr} cont	25.9	5.6	11.6	7.6	1.1	25.4	5.4	11.7	7.3	1.0
$T' - P_{nr}$	6.6	0.6	1.7	4.2	0.1	-3.6	-0.8	-0.1	-2.6	-0.1

surface heat loss occurs in the Pacific, Atlantic and the Arctic, while the Indian has some surface redistributive heat gain (Table 5.1). The Pacific contributes most of the redistributive surface heat loss more than twice that in that in the Atlantic because the Pacific has the largest redistributive surface temperature anomaly. Only the Indian ocean showed positive redistributive surface heat uptake in the WSU experiment, despite having surface redistributive temperature anomaly warming, though smaller than in other basins. This can be explained by lateral transport export of the Indian basin, which is larger in WSU experiment than in the WU experiment. The increase lateral export allows the surface absorb more heat than allowed by surface redistribution.

The passive uptake change between the two perturbed experiments is negligible compared to the redistributive uptake change. This is because passive surface flux only depends on the target temperature, T'_*, and the advection of the tracer away from the surface, (2.8). Since T'_* is the same between the two experiments, a change in the passive heat flux between the two experiments occurs only, as a result of the difference in the advection of passive tracer away surface between the two experiments ($v''P'_{nr}$), which is second order and hence negligible. In contrast, the redistributive surface heat flux depends on T_{r_s} (2.10). The difference between T_{r_s} in the two experiments depends on $v''\bar{T}$, which is not small because $\bar{T}$ is much bigger than P'_{nr}. Hence, only redistributive heat uptake changes between the two

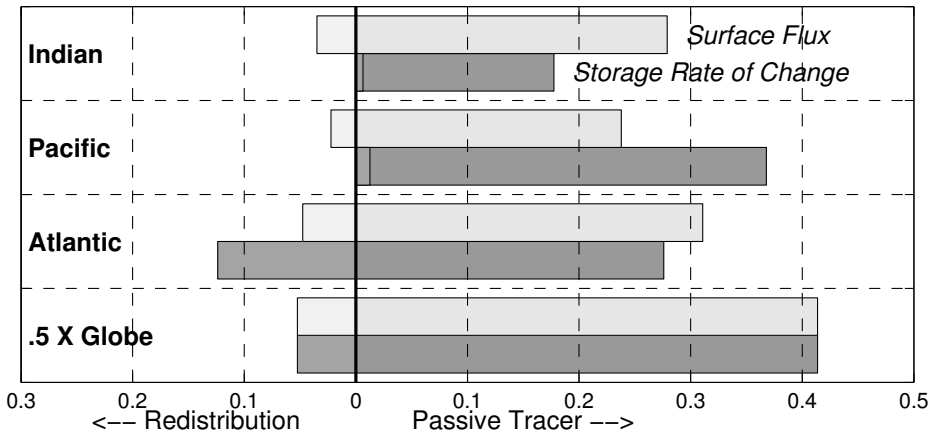

Figure 5.3: Heat transport anomaly through surface (light gray) and rate of change of heat content anomaly (dark gray) within individual ocean basins based on passive tracer (above zero line) and temperature minus passive tracer (below zero line), in PW, in the WSU experiment, Atlantic values include the Arctic/Mediterranean values

experiments. This also makes sense by definition of passive uptake, since the atmospheric heat flux anomaly is not changing, but only the oceanic component changes between the two experiments.

The effect of redistributive heat content loss on the speed of downward propagation of temperature anomaly can also be measured by comparing the effective depth for the tracers and temperature anomaly, shown in Figure 5.4. The plots shows redistributive heat content loss also reduces the speed of downward propagation of surface temperature anomalies. As the discussed in Section 2.4 and Chapter, the global integral of redistributive temperature anomaly, T_r' is zero, hence, a positive surface T_r', is compensated by a negative deep T_r' and vice versa. A negative T_r' in the deep is equivalent to a shallowing of the reservoir temperature distribution, which is comparable making the thermocline shallower (Compare T' between WSU and WU, Figure 5.2). This reduces the effective depth of heat penetration as seen in Figure 5.4

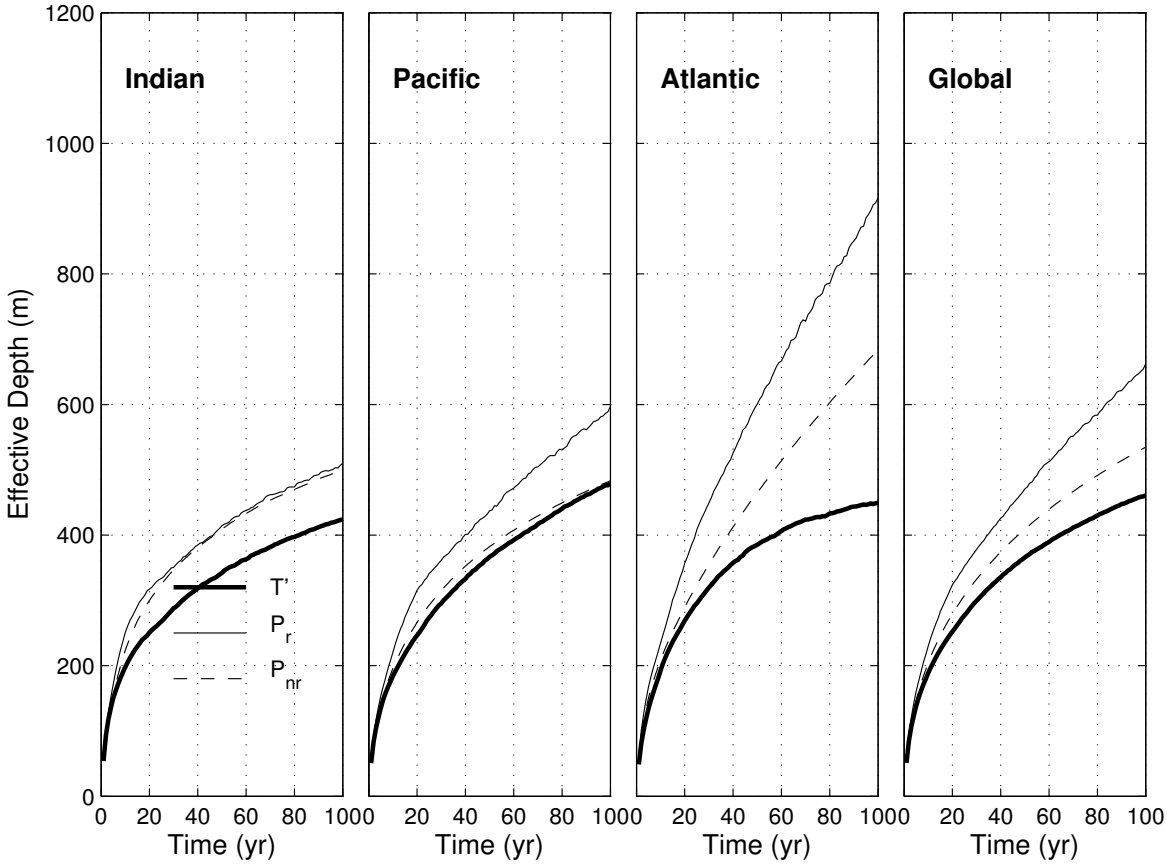

Figure 5.4: Global and basin effective depth H_e in the WSU experiment for tracers P_{nr}, P_r and and temperature anomaly T'

5.2.3 Salinity and Temperature forced Circulation perturbation

In order to understand the circulation changes causing the observed redistributive pattern, the circulation changes in WSU experiment can be compared the difference in the WU-WSU experiments (Figure 5.5). The differences in the two circulation anomaly patterns occur in the top 500 m, though, they both show a weakening of the deep circulation in the Atlantic, and the resulting Indo-Pacific AABW weakening, discussed in Chapter 4. Infact, the deep circulation weakening due to surface temperature perturbation is much larger (6 Sv) than that due to surface salinity perturbation (3 Sv). In shallow cells however, circulation changes are different. The deep circulation anomaly consists of an outflow in

the top kilometer and an inflow middepth and tropical downwelling in the Atlantic, and an inflow in the top kilometer and an outflow in the deep ocean and tropical downwelling in the Indo-Pacific. In the top 500 m, the WSU experiment shows a weakening of both subtropical cells in the Indo-Pacific, especially the southern hemisphere cell, shown by an anomalous equatorward flow at the surface and downwelling at the equator, this flow also connects to the deep circulation downwelling anomaly at the equator. The Atlantic top 500 m, some of the equatorward AMOC anomaly flow connects through the surface thus, weakening the equilibrium poleward flow at the surface, in the northern subtropical cell. The Atlantic southern hemisphere cell doesn't weaken as much.

In contrast to the WSU circulation pattern, WU-WSU circulation anomaly shows the northern Atlantic subtropical cell strengthens, such that the equatorward AMOC anomaly goes below it and instead connects at the surface through the subpolar cell. The equatorward moving AMOC anomaly connecting through the Atlantic subpolar cell, strengthens the existing equatorward flow of the subpolar cell. In the Indo-Pacific, there is a southward flow in the top 500m, this southward flow would also strengthen the Indo-Pacific southern subtropical cell. The strengthening of the shallow Ekman cell by salinity perturbation shown by the WU-WSU anomaly, explains the redistributive surface cooling pattern shown in Figure 5.1. Stronger subtropical cell increases upwelling at the equator, thus shallowing the thermocline and increases poleward transport of heat from the equator. As a result the tropical region is relatively cooler than the subtropical cells are weaker. By the same reasoning, weaker subtropical cells warm the tropics and cool the subtropics.

5.3 Wind forcing effects

Here we consider wind forcing perturbation effects. The wind forcing perturbation, shown in Figure 2.7, in the AC experiment changes the circulation strength by different amounts in different regions. The sutropical gyres weaken by different amounts in the basins; by 2 Sv in the Indo -Pacific, about 0.3 Sv in the Atlantic, the basins subtropical cell transport in the WU experiment, are about 47 Sv and 15 Sv respectively. Both the weakened volume

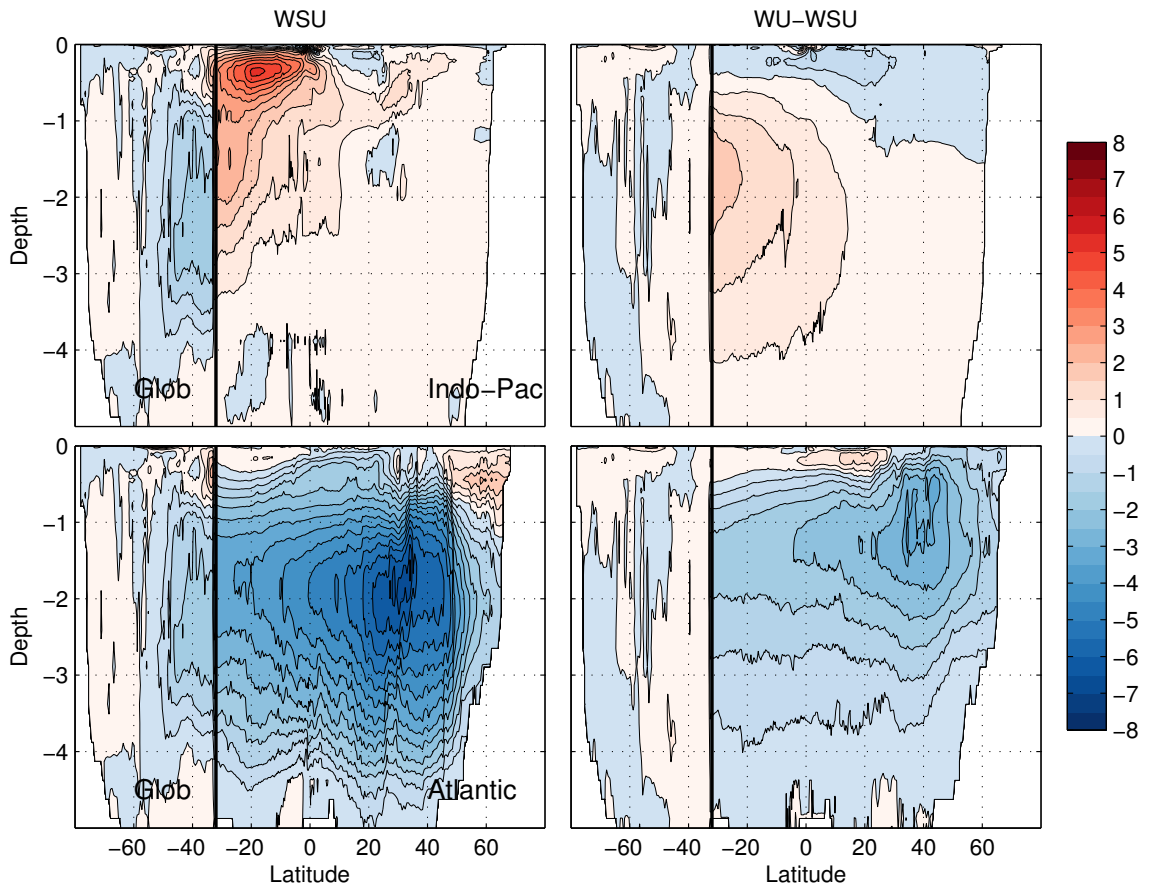

Figure 5.5: Meridional overturning streamfunction anomaly in the WSU experiment and for WU - WSU, for the 100 year time average. (Contours, Red=positive, blue=negative. c.i.=.5 Sv.)

transports are less than 5% of that in the WU experiment. The Southern ocean Deacon cell, weakened by 1 Sv in the WC experiment, this is about 2% of the Deacon cell circulation strength (41 Sv) in the WU experiment. There is also a southward shift of the southern hemisphere subtropical cells around 40^oS, in all the basins. We will consider how these changes in wind driven circulation, though small, change temperature anomaly distribution and heat uptake.

5.3.1 Temperature distribution

Similar to the WSU and WU experiment differences, the vertical distributions (Figures 5.6) in AC and WU experiments for P_r and T' are different, while that for P_{nr} are similar in both experiments. The surface values for T' and P_{nr} are likewise the same in the two experiments, due to the similar target values they are restored to. The difference in T' and P_r between the two experiments, occurs only in the top 500m only, unlike in the WSU and WU differences which extend to the deep ocean. The net geographical redistributive surface temperature anomaly, indicated by the difference between T' and P_r is generally warmer in all basins in top 500m in the AC experiment. Surface redistributive temperature anomaly warmed the Indo-Pacific surface more (about 1^oC in the Indian and 0.5^oC less in the Atlantic), while cooling the Atlantic surface less, as result of surface wind changes in the AC experiment.

Comparing the meridional pattern of redistribution temperature anomalies in both experiments (Figure 5.7), shows the top 500m warming occurs a and south of 40^oS which is around the edge of the southern subtropical gyre and poleward of 60^oS in all the basins. This warming is more intense in the vicinity of 40^oS in all the basins. Northern Indian in the top 500m warmed in the AC than in the WU, while the northern Pacific has cooler redistributive anomalies in the top 500m. Deep redistributive warming, however, appears to be smaller both in the Indian and Pacific basins. The location of warmer surface redistributive temperature anomaly in the tropics and at 40^oS is consistent with the wind perturbation pattern described above. Weakened of the subtropical cells will warm the equator since the causes upwelling around the equator and downwelling between $30^oS - 40^oS$. The southward shift of tropical cell explains the warming in the vicinity of the 40^oS, since it will brings downwelling to regions where it wasn't before. The differences inthe Indo-Pacific deep warming will considered in the discussion of the deep circulation perturbation. We consider now, how these changes in temperature distribution change heat input and lateral transport into the basins.

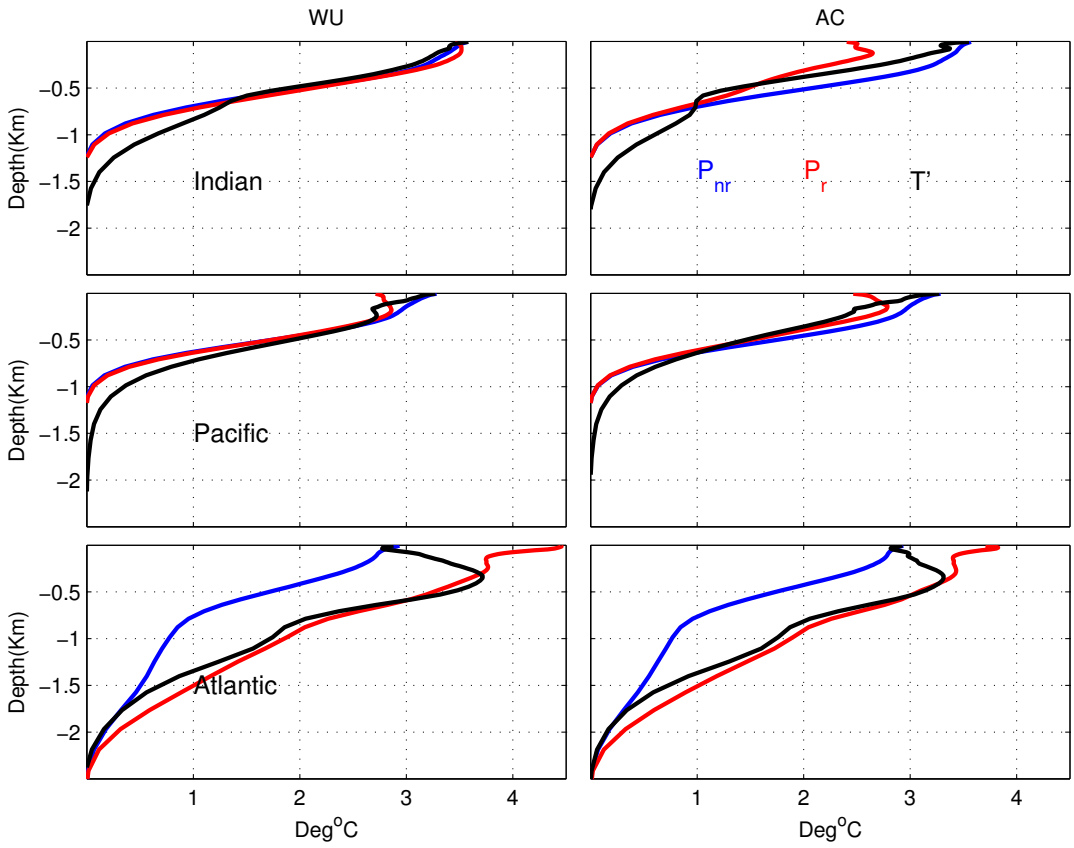

Figure 5.6: Horizontally averaged temperature anomaly, T' and tracers, P_{nr} and P_r - depth profile. Black line - T', Red line - P_r, Blue line - P_{nr}

5.3.2 Heat uptake and lateral transports

The surface heat input in the AC experiment reduces by 10% of that in the WU experiments. This difference occured mainly, as a result of reduction in the redistributive heat surface heat input. For the same reasons explained in the previous section, the passive surface heat input in the AC experiment is similar to that of the WU experiment (Table 5.2, also compare Figures 5.8 and 4.7). The global redistributive surface heat input, originally about 25% of the passive contribution in WU experiment, reduced by half the in the AC experiment. The Atlantic, the main source of the redistributive surface heat input in the WU experiment, has its redistributive heat input reduced to almost nothing in the AC experiment, while the redistributive heat input in the Indo-Pacific increased. This makes the Indo-Pacific

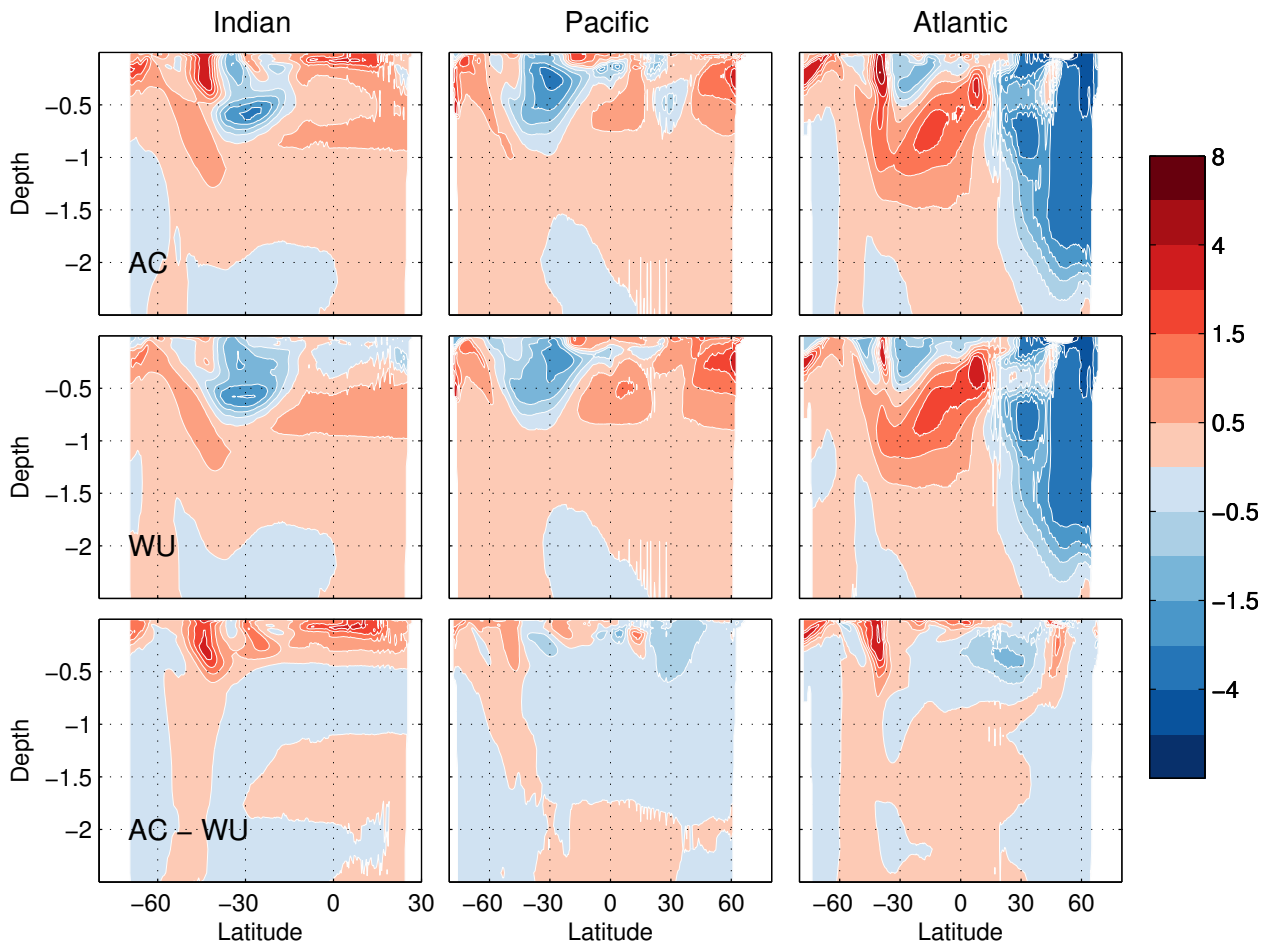

Figure 5.7: Geographical redistribtion temperature anomalies, $T' - P_r$, in the WU and AC experiments, anomalies are basin zonal averaged anomalies and time averaged over the last 20 years of the century long experiments. Contours:Red - Positve; Blue - negative; Units: Deg^oC

the main contributor of redistributive heat in the AC experiment. The redistributive heat input in the Indo-Pacific, is 15% of the global redistributive input in the WU experiment, while in the AC experiment contributes 50% of the global redistributive input in the WC experiment, (Also compare Figures 4.7 and 5.8).

The redistributive heat input change experiment is not very consistent with the redistributive surface temperature anomaly change between the two experiments. The Atlantic still has redistributive surface cooling in the WC experiment is only about two thirds that

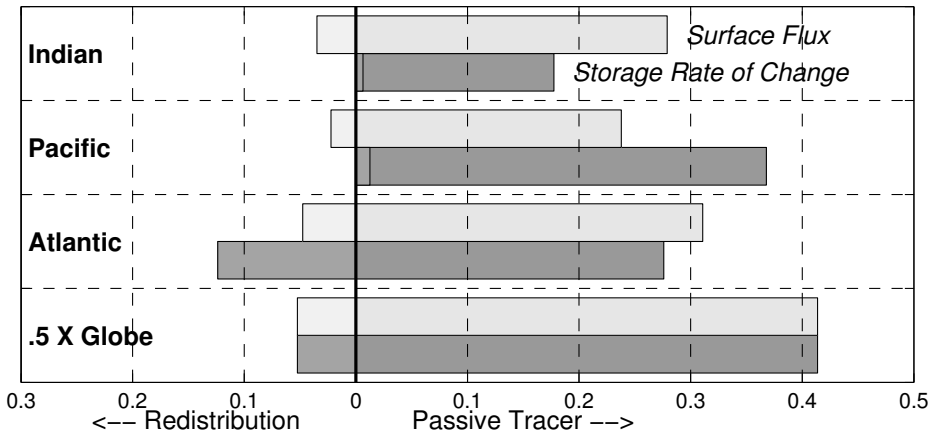

Figure 5.8: Heat transport anomaly through surface (light gray) and rate of change of heat content anomaly (dark gray) within individual ocean basins based on passive tracer (above zero line) and temperature minus passive tracer (below zero line), in PW, in the AC experiment, Atlantic values include the Arctic/Mediterranean values

of the WU experiment, it is expected that the Atlantic redistributive heat input will reduce as a result of less cooling, however, the redistributive heat input reduces almost to nothing. The Indo-Pacific has more redistributive warming yet, it gains redistributive heat. These inconsistencies can be explained by the heat transport among the basins. The passive heat input and transport are similar in both experiments (Table 5.2, also see Section 4.4), hence, heat transport differences in the experiments are due to the redisitributive transport change (Table 5.3). The Indian and Pacific both lose redistributive heat content to the Atlantic in the Southern ocean, compared with Atlantic redistributive content loss in the WU experiment. This heat exchange would reduce the effect of the Atlantic surface cooling for redistributive heat input, at same time increasing surface heat input in the Indian and Pacific, even though they have redistributive surface warming.

The main differences between redistributive transport in the two experiments are the increase in the Indonesian throughflow redistributive export from Indian to Pacific and the Atlantic redistributive heat import in the Southern ocean. The net export from the Indian increases as a result of the increase Indonesian through flow export in the WC experiment. In Southern ocean the Atlantic imports instead of the export in the WU experiment. The

Table 5.2: Heat flux and content in Joules in the WU and AC experiments, integrated over the 100- year run, for the passive tracer P_{nr} and temperature anomaly T' and redistributive anomaly (T' - P_{nr})

values in 10^{23} Joules.

	WU					AC				
	Glob	Ind	Pac	Atl	Arc/Med	Glob	Ind	Pac	Atl	Arc/Med
Q'	32.5	9.0	7.8	14.2	1.3	29.4	10.0	8.2	9.2	2
Q_{nr}	25.9	8.3	7.5	9.1	1.0	26.1	8.8	7.5	9.0	0.8
$Q' - Qnr$	6.6	0.7	0.3	5.1	0.5	3.3	1.1	0.7	0.2	1.3
T' cont	32.5	6.2	13.3	11.8	1.2	29.4	5.5	11.2	11.5	1.2
P_{nr} cont	25.9	5.6	11.6	7.6	1.1	26.1	5.6	11.6	7.6	1.1
$T' - P_{nr}$	6.6	0.6	1.7	4.2	0.1	3.3	-0.2	-0.4	3.8	0.1

Table 5.3: AC experiment's lateral Heat transports integrated over the 100-year run, for the control temperature, $\bar{T}$, passive tracer, P_{nr}, temperature anomaly, T' and redistributive anomaly, $T'-P_{nr}$. Transports are given across the basins' northern and southern boundaries respectively. Northern boundary for the Indo-Pacific is the Indonesian throughflow and for the Atlantic is the Arctic boundary. The Bering strait heat transport (not shown) is neglible, hence it doesn't count as the Pacific northern boundary. The Southern ocean is the southern boundary for all basins

values in 10^{23} Joules.

	$\bar{T}$			T'			P_{nr}			$T' - P_{nr}$		
	Ind	Pac	Atl	Ind	Pac	Atl	Ind	Pac	Atl	Ind	Pac	Atl
Ind.Thr	32.1	-32.1	0	-2.2	2.2	0	3.0	-3.0	0	-5.2	5.2	0
S.Ocn	-25.0	17.6	7.4	-2.0	1.4	0.6	-5.8	7.7	-1.9	3.8	-6.3	2.5
Net	7.1	-14.5	7.4	-4.2	3.6	0.6	-2.8	4.7	-1.9	-1.4	-1.1	2.5

Atlantic Southern ocean heat import is drawn from the Pacific, as a result, the Southern ocean Pacific export becomes bigger than its Indonesian throughflow import. Thus, giving a net redistributive heat export from the Pacific. This exchange mean the Atlantic imports redistributive content from the Indian and Pacific instead of the Pacific importing from the other two basins in the WU experiment.

As a result of the change in redistributive heat transport, the net heat transport for T', which includes the P_{nr} transport, also changed in the AC experiment. The Atlantic's redistributive heat import almost cancels out the Passive heat export in the Southern ocean Atlantic, reducing the net T' export of the Atlantic in the WC experiment compared the

WU's. Pacific's redistributive export in the AC reduces its net T' import compared to that of WU. The net T' export of the Indian ocean also increases in AC experiment compared to that of the WU experiment, because of the increased redistributive heat export in the WC experiment. As a result, the Pacific heat gain reduces to about 50% of that in the WU experiment and most of the Pacific's heat gain comes from the Indian alone. The Atlantic, however, loses very little in the Southern ocean but gains heat overall, mainly from the Arctic, it gains about 25% of the heat flux input into

Wind induced circulation perturbations

In the AC experiment, wind induce perturbation include changes to the shallow Ekman cells and the Southern ocean circulation. The winds weaken the subtropical gyres and there is a southward shift of the southern subtropical gyre in all the basins and a weaker subpolar gyre in the Atlantic. The mechanism of the global conveyor belt change described in Section 4.6, can be used to explain deep ocean changes, though small in this experiment. The Southern ocean MOC index suggest weakening of about 1 Sv, this reduces the imbalance between the already weakened NADW and the Southern ocean MOC, thus reducing the anomaly inflow into the Indo-Pacific AABW and the anomaly outflow out of the Atlantic to 3 Sv respectively (Figure 5.9). This means a 1 Sv decrease in the downwelling anomaly in the Indo-Pacific and an increase by the same amount in the downwelling anomaly recirculating in the Atlantic. The Indonesian througflow anomaly should also reduce by the same amount as a result of this, however the anomaly increases because of the weakening of the tropical gyre at the surface, adding to the Indonesian throughflow weakening anomaly

Redistributive anomalies difference between the WU and AC experiments can be explained by these circulation perturbation differences (Compare Figure 4.2). Weakened subtropical cells in all the basins produce relatively warmer redistributive anomalies in the tropical surface in the WC experiment in all the basins. The southward shift of the subtropical gyre gives much warmer redistribution anomaly at 40^oS the edge of the Southern

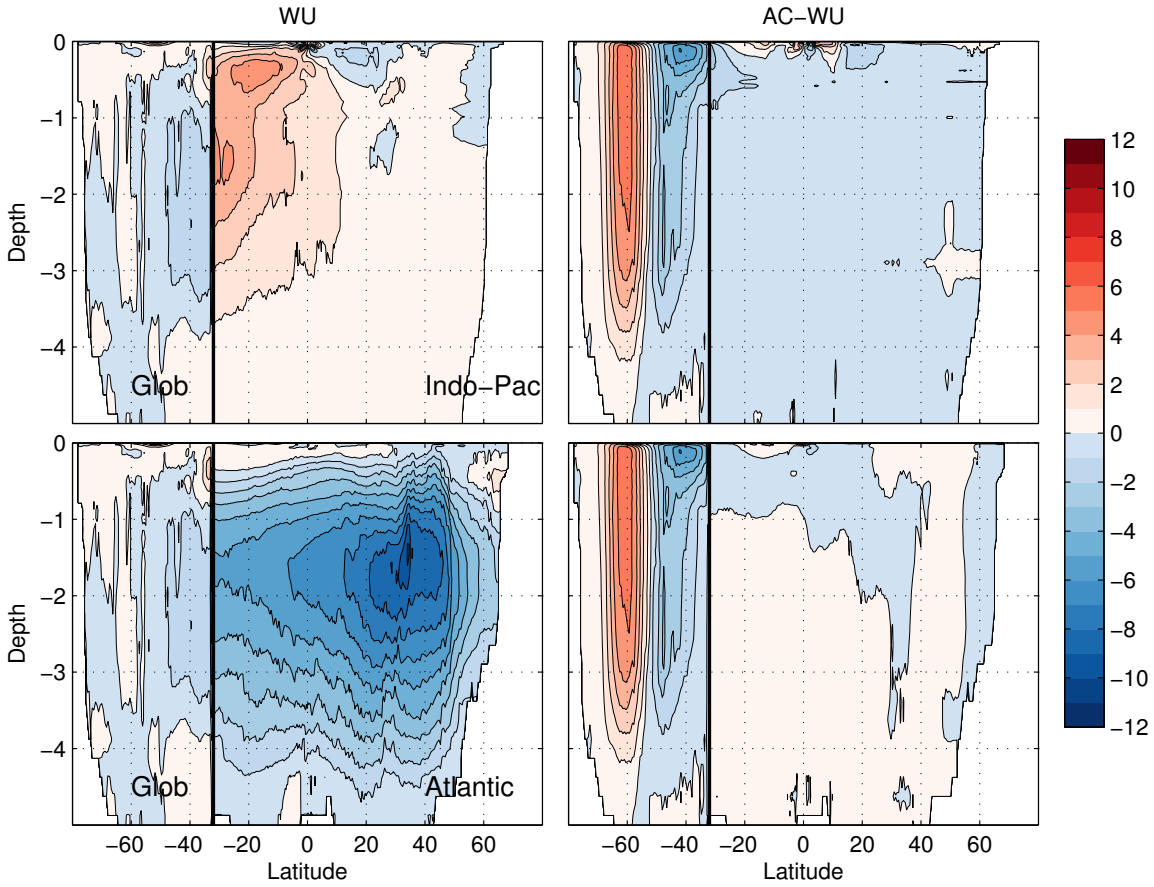

Figure 5.9: Meridional overturning streamfunction anomaly for AC -WU and WU experiment for the 100year time average. (Contours, Red=positive, blue=negative. c.i.=1 Sv.)

ocean zonal flow and subtropical gyre in the WC experiment. Weaker Indonesian Throughflow in the WC experiment explain the relatively cooler, top 500m north Pacific and the warmer, top 500m north Indian. The reduced downwelling anomaly in the Indo-Pacific mean relatively cooler redistributive temperature anomaly in the tropical deep Indo-Pacific (below 500 m) in the WC experiment, while the increased downwelling anomaly in the tropical deep Atlantic explains theWC's warmer redistributive temperature anomaly there.

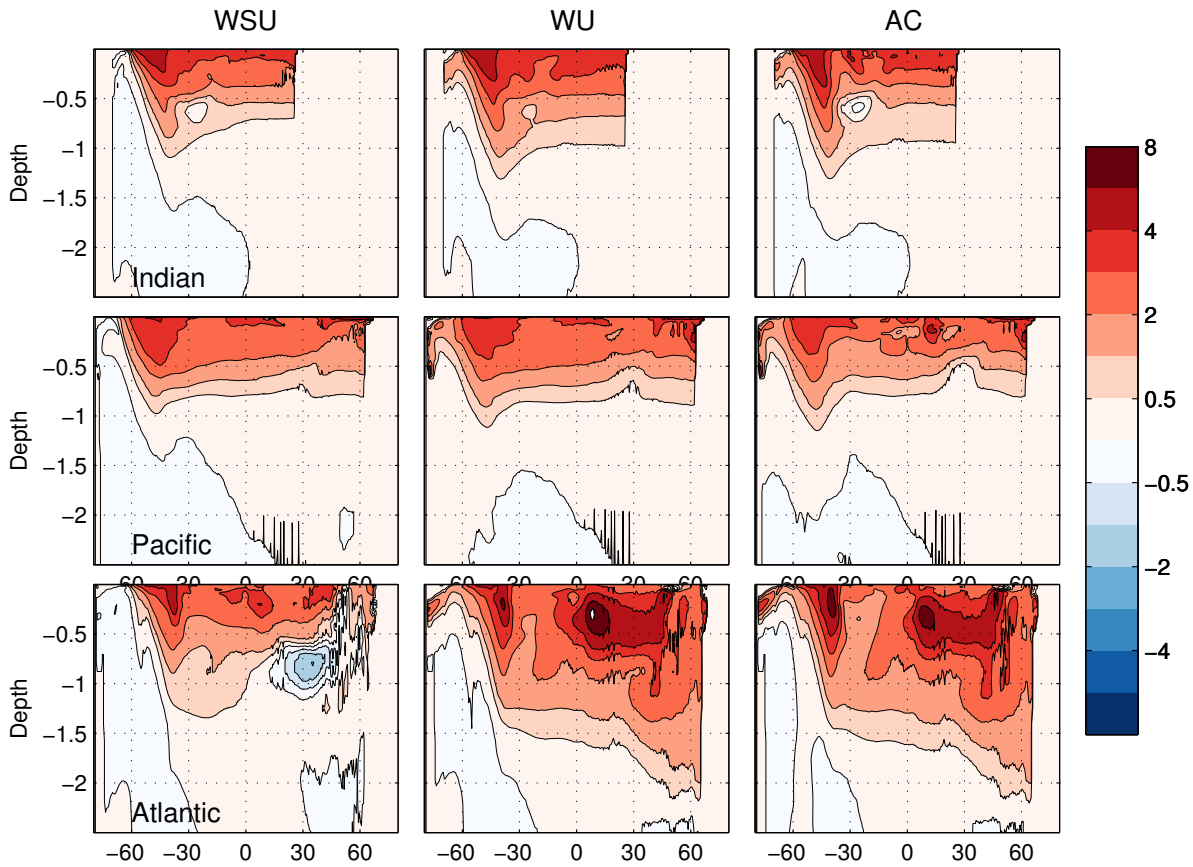

Figure 5.10: Zonally averaged temperature anomaly for the time average of years 81 - 100, among all three pertubation experiments. Units:^oC

5.4 Summary

From the above discussions, in all the three perturbation experiments, the WU experiment has the largest and deepest heat uptake, while WSU experiment has the smallest and shallowest heat uptake (Compare Figures 5.10 and 5.11). Only surface salinity perturbation gives positive redistributive uptake, temperature forcing perturbation and wind forcing perturbation both give about the same negative redistributive uptake. The positve redistributive uptake due to surface salinity perturbation is also much larger in magnitude enough to cancel out the negative redistributive heat uptake due to surface temperature perturbation in the WU experiment. This result is different from what was previously shown

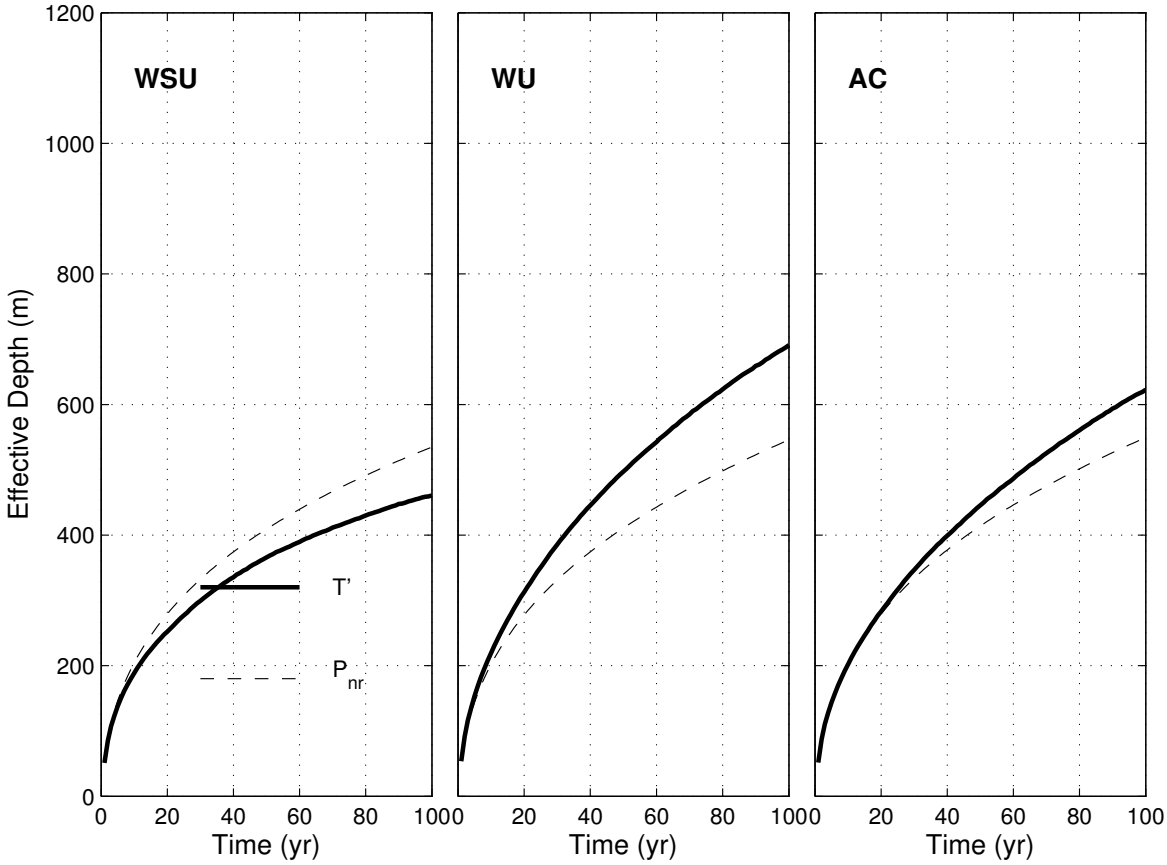

Figure 5.11: Global effective depth over time among the perturbation experiments

in other studies, that redistribution only increases heat uptake. The reason for this, may be due to the fact that total redistributive effect from all three surface perturbation still yields positive redistributive effect, as seen in AC experiment, because the salinity perturbation effect is dominant, but by themselves the different surface forcing perturbation can yield either a positive or negative redistributive effect.

The main differences in redistributive uptake occurs as a result of redistribution warming the tropics more in the experiments with negative redistributive effect, hence canceling out the high latitude redistributive cooling. Surface redistributive temperature anomalies is more sensitive to changes in the shallow sutropical cell circulation than to changes in the deep overturning circulation. This makes sense because the shallow cells are closer to the

surface and the equator and as a result, transport more heat than the deep circulation, suggesting shallow circulation changes in the tropics can be as effective in changing heat uptake as the deep overturning circulation. The passive component is the same among all three perturbation experiments (Figure 5.11), even though, the circulation changes are quite different, especially between the WSU and WU experiment. This suggest that effect of the weakening circulation in reducing heat uptake by slowing down the downward propagation of surface anomalies is negligible.

Chapter 6: Discussion and Conclusion

6.1 Discussion

The results described in the previous chapters compare very well with previous studies. Isopyncal propagation within the subtropical cells and the associated timescale agrees with the conceptual model of Church et al. (1991). Outside this region, tracer propagation is very slow on the isopycnal surfaces because tracer transport is mainly diffusive here. These timescales discussed here are not the same as the equilibrum time scales shown in the study of Yang and Zhu (2011). Though tracer propagates to these depth in a relatively short time, it takes a much longer time for transports to balance out one another in equilibrum. Southern ocean dominates tracer transport, in agreement with Gregory (2000), however, our results show diffusion is dominant here. His analysis, unlike ours, was done for total temperature anomaly, while the analysis here include only the passive component. Redistributive heat convergence is largely advective, thus can change the relative dominance of the advective term for tracer compared to temperature anomaly.

The novelty of this study is the separation and quantification of the passive and redistributive components of ocean heat uptake, and the analysis of the evolution and distribution of these of component of heat uptake among the basins. The difference between P_{nr} and T' content or surface flux is the redistributive uptake. The difference between their surface values and depth distribution confirms that redistributive uptake occurred due to redistribution cooling the reservoir surface temperatures and warming the tropical deep, and as a result increasing heat flux into the ocean, also suggested by Xie and Vallis. (2012). Surface cooling occurs mainly in the Atlantic due to the MOC in it, as a result, there is redistributive surface heat input into it, about 60% of the passive surface heat input into it, in the WU experiment, this effect is negligible in the other basins. The seperation of

the passive and redistributive heat content in this study is only possible due to the restoring boundary formulation used for this study. This may not be reproducible in a coupled ocean-atmosphere simulation, like the one used in Banks and Gregory (2006). However, as shown by Winton et al. (2010), the surface pattern of redistributive uptake is different from that of the passive uptake, this may enable the separation of the redistributive uptake from passive uptake in coupled simulation.

The no-redistribution passive tracer also allowed for easy comparison of ocean heat uptake efficiency increase due redistributive heat uptake. It shows redistributive heat uptake does not increase ocean surface temperature, at the same time, slows down the ocean's approach to equlibrium, unlike passive uptake. This is also comparable to the heat uptake efficiency increase shown in the study of Winton et al. (2012), for which he compared heat uptake efficiency increase for two experiments, one in which circulation is fixed and the other in which circulation is allowd to change. Our heat uptake efficiency increase of 1.5 in the Atlantic is comparable to the value they got for the circulation change experiment. The effect of redistribution increasing the speed of downward propagation of heat also agrees with the study of Xie and Vallis. (2012), only the effect of redistribution in deepening heat uptake in the Atlantic is much bigger in his study, probably due to the idealized single Atlantic basin used in their experiment. Their experiment does not allow for exchange with the other basins, like ours do.

The effect of different surface forcing perturbation on redistributive heat uptake also is also implied in other studies. Redistributive cooling of the existing reservoir heat content, due to temperature-increase perturbation, is implied in the cooling and warming experiments of Xie and Vallis. (2012), discussed in the introduction (Figure 1.9). For their warming experiments, they increased surface temperature by different amounts, and their results show that warmer surface temperature gives weaker MOCs, but yielded smaller effective depths while cooler surface temperature gives stronger MOCs, but deeper effective depth. This redistributive shallowing effect was also noted in the study of Marshall et al. (2015), their uniform surface warming experiment, leaves salinity and wind unchanged and

the found the passive tracer was deeper than the temperature anomalies

Like in our results, the salinity varying experiments in Xie and Vallis. (2012) showed the opposite effect, fresher high latitude surface yield weaker MOC, but deeper effective depth of heat penetration (Figure 1.8). Their wind varying experiments also shows that weaker southern ocean winds yield shallower effective depths. Though the results are similar it is not very comparable to our because they varied winds only in the southern ocean. The redistributive heat content loss seen here is due largely due tropical cells weakening, the southern ocean winds change is very small compared to their results. Their conclusion however, is that redistribution increases heat uptake only, but we have shown in this study that the effect of redistribution can either increase or reduce heat uptake. The net effect of all surface perturbation combined, however is the redistributive increase of heat uptake due to the dominance of Atlantic surface cooling, as a result of salinity freshening in high latitudes.

6.2 Summary and Conclusion

This study has highlighted the mechanisms of heat uptake in ocean basins by passive advection-diffusion and redistribution. Passive ocean heat uptake can be defined as an increase in ocean heat content resulting from surface heat flux anomalies from surface radiative forcing perturbation, while redistributive heat uptake is the ocean heat content increase resulting from the change ocean circulation, redistributive heat uptake can occur as a result of any surface forcing perturbation that could change ocean circulation strength, not necessarily, radiative forcing perturbation. Passive tracers are used to trace the propagation path of surface temperature anomalies into the deep ocean, among the basins, and a comparison among the tracers and the actual temperature anomaly are used to study the effects of the redistribution. Two tracer formulations are used for this study, the redistribution passive tracer, P_r, is initialised at zero and forced with the surface heat flux anomaly from the perturbation experiment which includes the effects of radiative forcing, as well as that of the changing ocean circulation. The No-redistribution passive tracer, P_{nr}, is also

initialised at zero but forced by restoring the tracer surface value to the target temperature anomaly ($T'_\star$). $T'_\star$ represents the equilibrium change in ocean surface temperature due to radiative forcing perturbation, hence P_{nr} flux excludes the effect of redistribution.

The propagation path of P_r shows advection is more important in the tropics, between $40^oS - 40^oN$, in the top 500m. The shallow subtropical cells advect heat anomalies, along the isopycnal surfaces, down to about 500m in the tropics in a short time scale of about 20 years. Below 500m, propagation becomes much slower, because propagation is mainly diffusive. Vertical diffusion and mixing and horizontal diffusion are more important in the Southern ocean, south of 40^oS, these propagate tracer down to about 1000m in all the basins in 100 years. In the northern high latitude, north of 40^oN, vertical diffusion and mixing and horizontal diffusion propagate tracers down to about 500m. In the Atlantic, advection becomes more important below 500m, the AMOC sinking branch transports tracers down to 2000m in a short time scale of about 20 years, then advecting tracers southward through the AMOC outflow branch to reach the deep tropics in about 50 years.

Redistribution, increases or reduces the speed of downward propagation of temperature anomalies, as well as the amount of heat uptake. Redistribution increases heat uptake through a net surface cooling, and net deep warming, thus allowing more heat to be absorbed by the ocean in addition to the passive transport of atmospheric heat flux anomaly. Redistributive surface cooling occurs especially in the northern high latitude Atlantic and southern high latitudes in the Southern ocean, as a result of AMOC weakening from thermohaline forcing perturbation. This net cooling occurs mainly in the Atlantic, and also increases the average effective depth of uptake there, due to deep warming also resulting from net surface cooling. The Atlantic from 800m to 1200m in 100 years. In the Indo-Pacific, tropical warming is not as deep as in the Atlantic and it occurs later, after 50 years, as a result, it only increases average effective depth of uptake of the Indo-Pacific by less than 100m.

Redistribution can also be negative, reducing the speed of downward propagation of heat, as well as the amount of heat uptake. It occurs through net redistributive surface warming,

and the resulting deep cooling. This redistributive pattern occurs mainly in the tropics, as a result of the weakening of the shallow subtropical cells. Subtropical cell weakening occurs as result of surface wind perturbation and as well as surface temperature increase perturbation. Salinity perturbation, on the other hand strengthens the subtropical cells. Ocean heat uptake is a lot more sensitive to subtropical cell weakening than the AMOC weakening. AMOC weakening of about by 35% due to thermohaline forcing perturbation yielded about the same fraction of redistributive input increase in the Atlantic. On the other hand, the subtropical cells weakened by an average of 3% due to wind forcing perturbation, and reduce the redistributive heat input into the Atlantic to nothing (about 35% the total heat input in the Atlantic). Though the change in gyre circulation strength is a lot weaker than than the change in AMOC circulation strength, it produced a bigger change in the ocean heat uptake. The same happened for surface temperature increase, though this perturbation resulted in a weakening of the AMOC as well, the subtropical celll weakening effect dominated the AMOC weakening effect and yield redistributive surface heat loss.

Another main conclusion of this study is the role of the global conveyor belt in redistributing ocean heat uptake among the basins, which allows redistributive effects to occur in other basins even without the deep MOC. In steady state, the Pacific exports heat to the Indian and Atlantic via the conveyor belt, balanced by surface heat input into the Pacific. The weakening circulation in the Atlantic causes the global conveyor belt also, to weaken, this allows more heat to accumulate in the Pacific by reducing its mean state heat export to the Indian and Atlantic. This inter-basin exchange doubles the heat uptake of the Pacific compared to its surface heat input, making its heat uptake greater than that of the Atlantic having the AMOC, while its surface temperature remained unchanged. The Indonesian throughflow and Southern ocean heat transport play a key role in this exchange. When Southern ocean winds weakened by 1 Sv, the direction of the redistributive transport also changed, allowing the Atlantic to gain heat from the other two basins and also from the Arctic. The Pacific imports less redistributive heat, while the Indian exports more. The implication of this, is that, the distribution of ocean heat uptake among the basins is largely

dependent on the accurate simulation of the global conveyor belt strength under climate change.

This study tries only to isolate mechanisms of increasing ocean heat uptake and its distribution among basins. It does not represent realistic transient radiative forcing and the influence of atmospheric changes (even excludes change in surface wind in the WU experiment) due to global warming. The heat convergence component used to describe transport are strongly dependent on the vertical and horizontal diffusivity constants used. The redistributive heat uptake estimate here is also model dependent. The restoring temperature anomaly used has some of the redistributive component imbeded in it, since it is calculated from the coupled model output which already has a weakened circulation. But it is largely due to surface temperature anomaly due to radiative forcing. Despite these caveats, our results show ocean heat uptake efficiency could result as ocean internal mechanism and it points to where to look, when diagnosing or tracing ocean heat uptake among models.

Bibliography

Banks, H. T. and J. M. Gregory, 2006: Mechanisms of ocean heat uptake in a coupled climate model and the implications for tracer based predictions of ocean heat uptake. *Geophysical Research Letters*, **33 (7)**, URL http://centaur.reading.ac.uk/5569/, l07608.

Bryan, K., 1984: Accelerating the convergence to equilibrium of ocean-climate models. *Journal of Physical Oceanography*, **14 (4)**, 666–673.

Bryan, K., S. Manabe, and M. Spelman, 1988: Interhemispheric asymmetry in transient response to co2 forcing. *Journal of Physical Oceanography*, **26**.

Church, J., J. Godfrey, D. Jackett, and T. McDougall, 1991: A model of sea level rise by caused by ocean thermal expansion. *Climate Dynamics*, **4**.

Gent, P. R., J. Willebrand, T. J. McDougall, and J. C. McWilliams, 1995: Parameterizing eddy-induced tracer transports in ocean circulation models. *Journal of Physical Oceanography*, **25 (4)**, 463–474.

Gent, P. R., et al., 2011: The community climate system model version 4. *Journal of Climate*, **24 (19)**, 4973–4991.

Gnanadesikan, A., 1999: A simple predictive model for the structure of the oceanic pycnocline. *Science*, **283 (5410)**, 2077–2079.

Gregory, J. M., 2000: Vertical heat transports in the ocean and their effect on time-dependent climate change. *Climate Dynamics*, **16 (7)**, 501–515, doi:10.1007/s003820000059, URL http://dx.doi.org/10.1007/s003820000059.

Huang, B., P. H. Stone, A. P. Sokolov, and I. V. Kamenkovich, 2003: The deep-ocean heat uptake in transient climate change. *Journal of climate*, **16 (9)**.

Klinger, B. and C. Cruz, 2009: Decadal response of global circulation to southern ocean wind stress perturbation. *Journal of Physical Oceanography*, **39**.

Kostov Y., K. C. A. and J. Marshall, 2014: Impact of the atlantic meridional overturning circulation on ocean heat storage and transient climate change. *Geophys. Res. Lett.*, **41**, 21082116, doi:10.1002/2013GL058998.

Kuhlbrodt, T. and J. Gregory, 2012: Ocean heat uptake and its consequences for the magnitude of sea level rise and climate change. *Geophysical research letters*, **39 (10)**.

Large, W. G., J. C. McWilliams, S. C. Doney, et al., 1994: Oceanic vertical mixing: A review and a model with a nonlocal boundary layer parameterization. *Reviews of Geophysics*, **32 (4)**, 363–404.

Lee, S.-K., W. Park, E. van Sebille, M. O. Baringer, C. Wang, D. B. Enfield, S. G. Yeager, and B. P. Kirtman, 2011: What caused the significant increase in atlantic ocean heat content since the mid 20th century. *Geophysical Research Letters*, **38**.

Levitus, S., et al., 2012: World ocean heat content and thermosteric sea level change (02000 m), 19552010. *Geophys. Res. Lett.*, **39**.

Li, J. V. S., C. and J. Marotzke, 2012: Deep-ocean heat uptake and equilibrium climate response. *Climate Dynamics*, **26 (10)**.

Lozier, M. S., S. Leadbetter, R. G. Williams, V. Roussenov, M. S. C. Reed, and N. J. Moore, 2008: The spatial pattern and mechanisms of heat-content change in the north atlantic. *Science*, **308**.

Manabe, S. and B. Spelman, 1991: Transient response to gradual changes in co2, part i. *Journal of climate*, **26 (10)**.

Marshall, J., J. R. Scott, K. C. Armour, J. M. Campin, M. Kelley, and A. Romanou, 2015: Ocean's role in the transient response of the climate to abrupt greenhouse gas forcing. *Climate Dynamics*, **44 (7-8)**, 2287–2299.

Nikurashin, M. and G. Vallis, 2012: A theory of the interhemispheric meridional overturning circulation and associated stratification. *Journal of Physical Oceanography*, **42 (10)**, 1652–1667, doi:10.1175/JPO-D-11-0189.1, URL http://dx.doi.org/10.1175/JPO-D-11-0189.1.

Schewe, J. and A. Leverman, 2009: The role of meridional difference for a wind driven overturning circulation. *Climate Dynamics*, **34**.

Smith, R. and P. Gent, 2002: Reference manual for the parallel ocean program (pop), ocean component of the community climate system model (ccsm2. 0 and 3.0). Tech. rep., Technical Report LA-UR-02-2484, Los Alamos National Laboratory, Los Alamos, NM, http://www. ccsm. ucar. edu/models/ccsm3. 0/pop.

Solomon, S., et al., 2007: *Climate Change 2007: The Physical Science Basis. Contribution of Working Group I to the Fourth Assessment Report of the Intergovernmental Panel on Climate Change*, chap. Observations: Oceanic Climate Change and Sea Level. Cambridge University Press, Cambridge, United Kingdom and New York, NY, USA.

Stouffer, R., 2004: Time scales of climate response. *Journal of climate*, **17 (10)**.

Taylor, K. E., R. J. Stouffer, and G. A. Meehl, 2012: An overview of cmip5 and the experiment design. *Bulletin of the American Meteorological Society*, **93 (4)**, 485–498.

Winton, M., S. M. Griffies, and B. L. Samuels, 2012: Connecting changing ocean circulation with changing climate. *Journal of climate*, **26 (10)**.

Winton, M., K. Takahashi, and I. M. Held, 2010: Importance of ocean heat uptake efficacy to transient climate change. *Journal of Climate*, **23 (9)**, 2333–2344.

Xie, P. and G. K. Vallis., 2012: The passive and active nature of ocean heat uptake in idealized climate change experiments. *Climate Dynamics*, **38 (3-4)**, 667–684, doi:10.1007/s00382-011-1063-8, URL http://dx.doi.org/10.1007/s00382-011-1063-8.

Yang, H. and J. Zhu, 2011: Equilibrum thermal response timescale of global oceans. *Geophysical Research Letters*, **38 (10)**.

Zanna, L. and D. Marshall, 2013: A conceptual model of ocean heat uptake under anthropogenic climate change. *AGU Fall Meeting Abstracts*, Vol. 1, 04.

Curriculum Vitae

Oluwayemi Garuba grew up in Akure Nigeria, where she got her Bachelor of Technology in Physics Electronics in 2007, from the Federal University of Technology Akure, (FUTA). In 2008 she got a scholarship to continue her studies in Physics at the International centre for Theoretical Physics, (ICTP), Trieste Italy, where she got the Pre-Ph.D diploma in Earth System Physics. She joined the Climate Dynamics Doctoral program at George Mason University in 2010.

Her research work has focused on ocean's influence on climate and more particularly on ocean heat uptake under climate change. In the future, she is interested in understanding the influence of changing ocean circulation and variability on the atmospheric weather patterns under global warming